HYDROLOGY OF THERMOKARST PONDS

NEAR COUNCIL, ALASKA

By

Matthew R. Fraver

RECOMMENDED:

_____

_____

_____

_____
Chair, Advisory Committee

_____
Chair, Department of Civil and
Environmental Engineering

APPROVED: _____
Dean, College of Science, Engineering and Mathematics

_____
Dean of the Graduate School

_____
Date

HYDROLOGY OF THERMOKARST PONDS NEAR COUNCIL, ALASKA

A

THESIS

Presented to the Faculty

Of the University of Alaska Fairbanks

In Partial Fulfillment of the Requirements

For the Degree of

MASTER OF SCIENCE

By

Matthew R. Fraver, B.S.

Fairbanks, Alaska

December 2003

Abstract

Water balances were conducted on a wetland complex near Council, Alaska on the Seward Peninsula during the 2001 and 2002 summers in order to investigate the possibility of subsurface drainage through open taliks. Ponds formed by ground subsidence resulting from the melting of ice-rich permafrost (thermokarst) are common in the valley east of Council. The majority of these ponds are displaying a decreased surface area when compared with aerial photographs and satellite imagery from the 1950's and 1980's. Because the long-term temperature and precipitation data from Nome do not reveal any conclusive climate trends that might result in the drying of the ponds, the cause of this change is suspected to be linked to the local permafrost and thermokarst conditions. From geophysical surveys, the permafrost in the area is typically 20 to 60 meters thick, and underneath the shrinking thermokarst ponds are large thawed regions (taliks), most of which extend through the local permafrost (open taliks). Downward hydraulic gradients have been identified in nested wells drilled into the open taliks, indicating the downward migration of water from the ponds to the subpermafrost groundwater. It was hypothesized that this water loss mechanism has a considerable impact on the hydrologic dynamics of the ponds and is related to recent drying.

The results of this two-year study demonstrate that evapotranspiration and lateral drainage are capable of accounting for essentially all of the observed storage changes during rainy periods. During dry periods, the combined water lost via subsurface drainage through an open talik and lateral drainage into nearby wetlands is less than the water lost through evapotranspiration. The magnitude of the subsurface drainage component of the water balance is confounded by the inability to quantify the subtle but influential lateral fluxes into nearby wetlands.

Table of Contents

List of Figures

List of Tables

Acknowledgements

I would like to thank the members of my committee (Larry Hinzman, Kenji Yoshikawa, Doug Kane, and Bob Carlson) who helped me complete this project and deemed this work worthy of a Master's Degree. I would specifically like to thank Larry Hinzman for his guidance and encouragement throughout this trying process.

I would like to thank all of the people who helped me with fieldwork, specifically Crane Johnson, John Gallagher, Jeff Oatley, Byron Roys, Trevor White, Tom Douglas, Doug Goering, Larry Hinzman, and Kenji Yoshikawa. I would also like to thank Ken Irving and Rob Geick for their help at the Water and Environmental Research Center (WERC), as well as Marin Kuizenga with VECO logistics. I would also like to thank Jason Beringer, Matthew Sturm, and Andrea Lloyd for their supplemental data contributions and technical advice.

Special thanks goes to the people of Council, Alaska who helped us "scientists" however they could. I would especially like to thank the Stang family for their hospitality and good humor.

Finally, I would like to thank all of my friends and family who have helped me during these past two years. I would specifically like to thank Jeff Oatley for his continuous encouragement and ridiculous optimism. I would also like to thank those of the Brentwood clan, who have provided the continuous amusement that has saved my sanity during these past ten months.

Funding for this project was provided by the NSF Office of Polar Programs, Arctic System Science Program (OPP-9818066).

1. Introduction

This study is funded under the Arctic Transitions in the Land-Atmosphere System (ATLAS) initiative within the Land Atmosphere Ice Interactions (LAII) program of the National Science Foundation's Arctic Systems Sciences (ARCSS) program. The objective of ATLAS is to better understand the feedbacks within the land-atmosphere system in arctic regions and to predict reasonable scenarios resulting from future global climate change. Hydrology is a keystone process influencing the mass and energy fluxes within terrestrial ecosystems and is a large component of the ATLAS program. The objective of this study is to better understand the hydrologic dynamics of shrinking thermokarst ponds in the discontinuous permafrost regions near Council, Alaska on the Seward Peninsula. A clear understanding of the climatic and terrestrial controls over water level dynamics in these ponds is necessary to predict local ecosystem changes and to contribute to pan-arctic studies and global climate change predictions.

The thinner and warmer, discontinuous permafrost in sub-arctic regions is suspected to react sooner to climate changes than the permafrost in arctic regions (Osterkamp and Romanovsky 1999; Jorgenson et al. 2001; Romanovsky et al. 2002; Fitzgerald and Riordan 2003; Yoshikawa and Hinzman 2003). Unlike arctic soils, where climate is mainly responsible for maintaining thermal equilibrium, vegetation and other surface conditions play a larger role in the thermal balance of sub-arctic soils (Gallinger 1991). Slight changes in the surface conditions of sub-arctic soils will result in physical responses in the subsurface, often evident in the process of ice wedge melting and subsequent ground subsidence, otherwise known as thermokarsting (Yershov 1998). Thermokarst terrain is a frequent occurrence on the tundra slopes of the Seward Peninsula, Alaska where the continuous and discontinuous permafrost is

relatively warm and unstable (Osterkamp 1983). The hydrologic dynamics of thermokarst terrain near Council, located roughly 120 kilometers northeast of Nome on the Seward Peninsula, is the focus of this study.

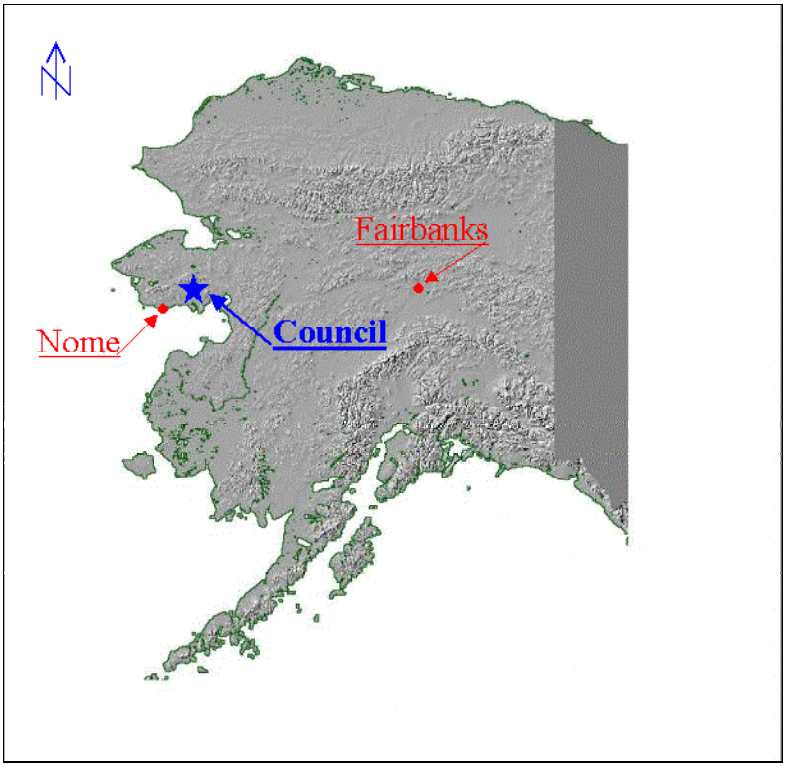

Figure 1. Study Location. Council, Alaska is located on the Seward Peninsula about 120 kilometers northeast of Nome.

Thermokarst terrain near Council can be identified as wetlands and ponds occupying surface depressions caused from ground subsidence in the upland tundra slopes, often clearly defined by steep banks of one to two meters. Thermokarst ponds in the area were examined to determine if recent changes in climate have impacted the dynamics of their development and degradation (Yoshikawa and Hinzman 2000 and 2003). These investigations included field studies through coring and thermal analyses, geophysical surveys, and historical analyses through archival photographs and satellite imagery. Twenty-six ponds

were identified on aerial photography collected in 1951 and 1981 and IKONOS imagery from 2000, and of the 24 ponds studied, 22 have decreased in surface area between 1951 and 2000. The two ponds that increased in size appear to be controlled by terrain while the others appear to be perched over permafrost and formed by thermokarsting.

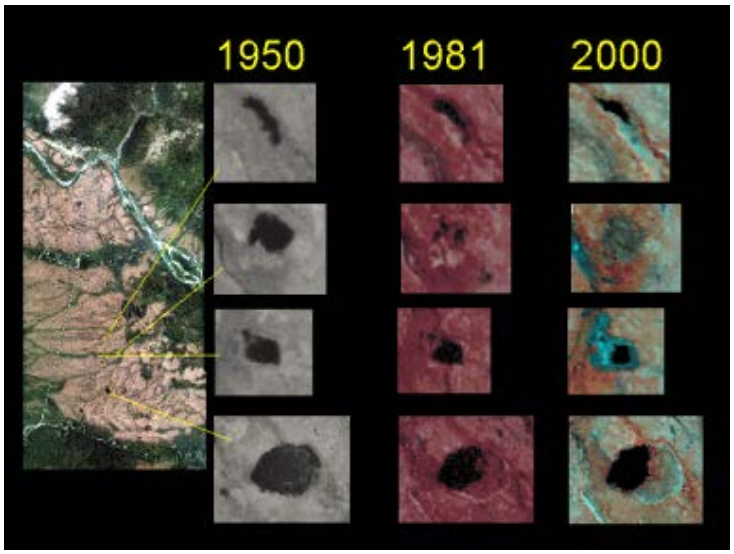

Figure 2. Shrinking Ponds. Ponds in the Council area are displaying a decreased surface area over the past half-century.

From DC electrical sounding and permafrost boring data, the discontinuous permafrost in the area is estimated to be 20 to 60 meters thick. Ground-penetrating radar (GPR) studies near ponds that have decreased in size indicate the presence of unfrozen ground below the ponds (taliks) extending to the bottom of the relatively thin permafrost (open taliks). Analysis of meteorological data from Nome indicates both short-term warming and cooling trends and increases and decreases in precipitation, but over the last fifty years, the long-term trends show little marked differences likely to cause drying of the ponds. Although recent warming has been correlated with thermokarst development, many areas have thermokarst features that show both aggradation and degradation of

permafrost simultaneously, suggesting that site-specific factors, as opposed to climatic factors, may be more influential in thermokarst dynamics (Burn and Smith 1990). While no obvious signs of permafrost aggradation are evident in the Council area, the importance of site-specific factors, such as surface disturbances, is recognized.

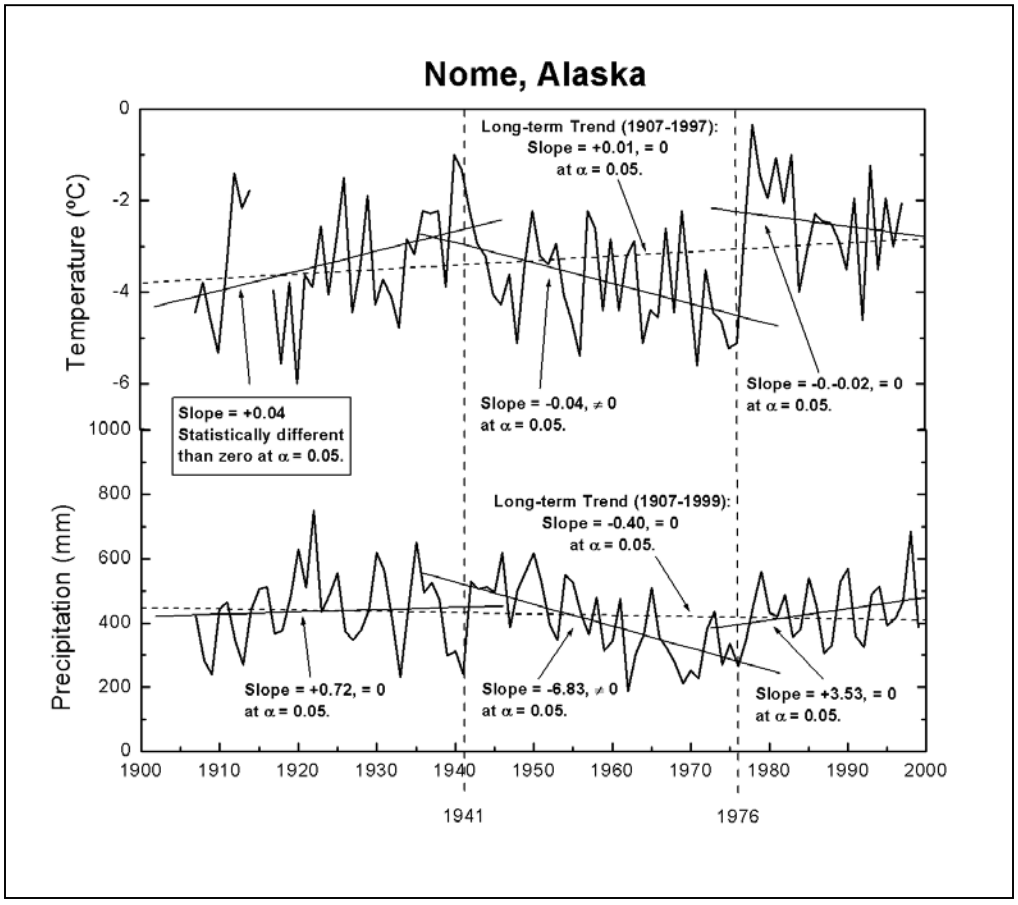

Figure 3. Long-term meteorological data at Nome. Long-term air temperature and precipitation data from the Nome Municipal Airport (National Climatic Data Center) show obvious trends but none that can be conclusively related to the drying of the ponds.

Hopkins (1949) described the drainage of lakes in the Imuruk Lake area on the Seward Peninsula as being either one of two processes: 1) slow lateral drainage

along thermokarsted channels formed directly above melting ice wedges, or 2) rapid drainage due to the intersection of the downward-migrating talik underneath the pond with coarse grained soils or bedrock, leaving what he defined as “thaw sinks”. This study investigates the possibility of drainage through the talik without the intersection of a coarse-grained soil layer necessary to facilitate rapid drainage. The effect of a recently formed open talik through the silty soils underneath the ponds could potentially increase the total water loss rate and result in lower pond water levels. Lower water levels may enhance peat growth around the perimeter of the ponds, which is necessary for the succession from pond to marsh (Mitsch 1993). Peat growth also contributes to the appearance of pond shrinkage as seen in aerial photography and satellite imagery (Fitzgerald and Riordin 2003).

To better understand the hydrologic dynamics of the “shrinking” thermokarst ponds in the Council area, a water balance was conducted during the snow-free seasons of 2001 and 2002 on a wetland complex encompassing two thermokarst ponds. The relative importance of the downward migration of water through the open talik compared to lateral water losses through the marshy channels and evaporative losses at the surface is investigated using the water balance technique. Two nested pairs of deep and shallow wells, one located in each of the two ponds, and one deep well into the talik underneath the marshy area were intended to identify vertical hydraulic gradients. Twenty shallow wells were positioned to characterize the active layer flow regime. Ten soil moisture probes and ten thermistors were installed to collect continuous data describing the active layer in three different pits representing upland tundra, banks, and wetland tundra. Meteorological data were collected at a three-meter tower near Pond 20. Net radiometers were positioned over upland, wetland, and pond surfaces.

The results of this two-summer study indicate that drainage through the open taliks may contribute noticeably to the total water loss rate of the ponds, but the impacts of rainfall events and surficial loss mechanisms on the hydrology of the ponds and the surrounding terrain are critical, capable of accounting for 100% of the observed storage changes. When the pond stage is increased dramatically by large rainfall events, lateral drainage through outlet channels depletes the pond water storage quickly but is typically inactive during dry periods. Evaporation from the open water surface accounts for most but not all of the observed storage changes in the ponds during dry periods. Lateral drainage into nearby wetlands is suspected to contribute to storage changes during dry periods also, but the inability to quantify this small but potentially influential loss mechanism prevents the quantification of drainage through the open talik.

2. Study Site Description

Council is located roughly 120 km northeast of Nome on the Seward Peninsula of Alaska. The small community lies on the northeast edge of a mildly sloped valley roughly 6 km wide. This valley, situated approximately 50 m above sea level, has a regional gradient of 0.5% sloped southward to the Pacific Ocean. The Council area is a unique area for climate change scientists because of the defined transition between tussock tundra and spruce forest in a relatively accessible area that perhaps simulates a slightly warmer and wetter Arctic (Beringer et al. 2003a). The hills on the east side of the valley support dense spruce forest while spruce trees are only sporadically distributed on the hills to the west of the valley, defining the western-most boundary of spruce forest on the Seward Peninsula. The valley consists mostly of tussock tundra (mostly *Eriphorum vaginatum*) and dwarf-shrub tundra (*Vaccinium uliginosum* and *Betula nana*) vegetation with *Sphagnum* spp., lichens (*Cladina mitis* and *Cladina rangiferina*) and feather moss (Beringer et al. 2003a; Lloyd et al. 2003; Thompson et al. 2003). Areas of large woody shrubs and spruce trees occupy creek beds and drainages within the tundra landscape. There are numerous small lakes, ponds, and wetlands throughout the valley, most being concentrated in the low-relief areas of local flood plains.

Long-term weather data is unavailable for Council, but the Nome Municipal Airport has been collecting meteorological data since 1906. The average annual temperature and precipitation as recorded in Nome over the period of record are -3.3˚C and 42.4 cm, respectively (National Climatic Data Center). The Council valley is underlain by discontinuous permafrost ranging from 20 to 60 meters in depth (Yoshikawa and Hinzman 2000 and 2003). The maximum thickness of the seasonally thawed soil layer above the permafrost, known as the active layer, is

typically 50 to 80 cm. The permafrost temperature is greater than –1˚C and thermokarst terrain is common in areas of ice rich permafrost.

Shown in figure 4, the specific site monitored in this study is situated in the open tundra (64˚51.4'N, 163˚41.1'W), about five km south of Council and 500 m south of the intersection of Bear River and the Council Highway. A meteorological station and the Circumpolar Active Layer Monitoring (CALM) grid site are less than three km to the south. The study site, approximately 0.2 km^2, consists of two ponds connected by a network of marshy channels and the upland tundra slopes that drain into the wetland complex. The two ponds are about 50 meters in diameter and are typically one to two meters deep. The upland areas are mildly sloped with a maximum gradient of 2.5%, and the wetland areas are relatively flat with gradients typically less 1%.

The exact boundaries of the small basin are uncertain due to the low-relief topography, but the boundaries between upland and wetland areas are obvious due to the well-defined banks that are typically one to two meters in height and often lined with large woody shrubs and even spruce trees. The differences in vegetation between the upland tundra and wetland tundra areas are considerable and the transition is often sudden; this distinction creates additional means to delineate the upland/wetland boundary. The marshy channels support a wet sedge meadow community containing a variety of sedges (mostly *Eriphorum augustifolium*) and mosses while the upland areas are tussock tundra and low shrubs (Lloyd 2003; Thompson et al. 2003). Figures 5 shows the two ponds and the approximate boundary between the upland and wetland areas. Figure 6 is a photograph of a marshy channel and the banks that descend from the upland slopes.

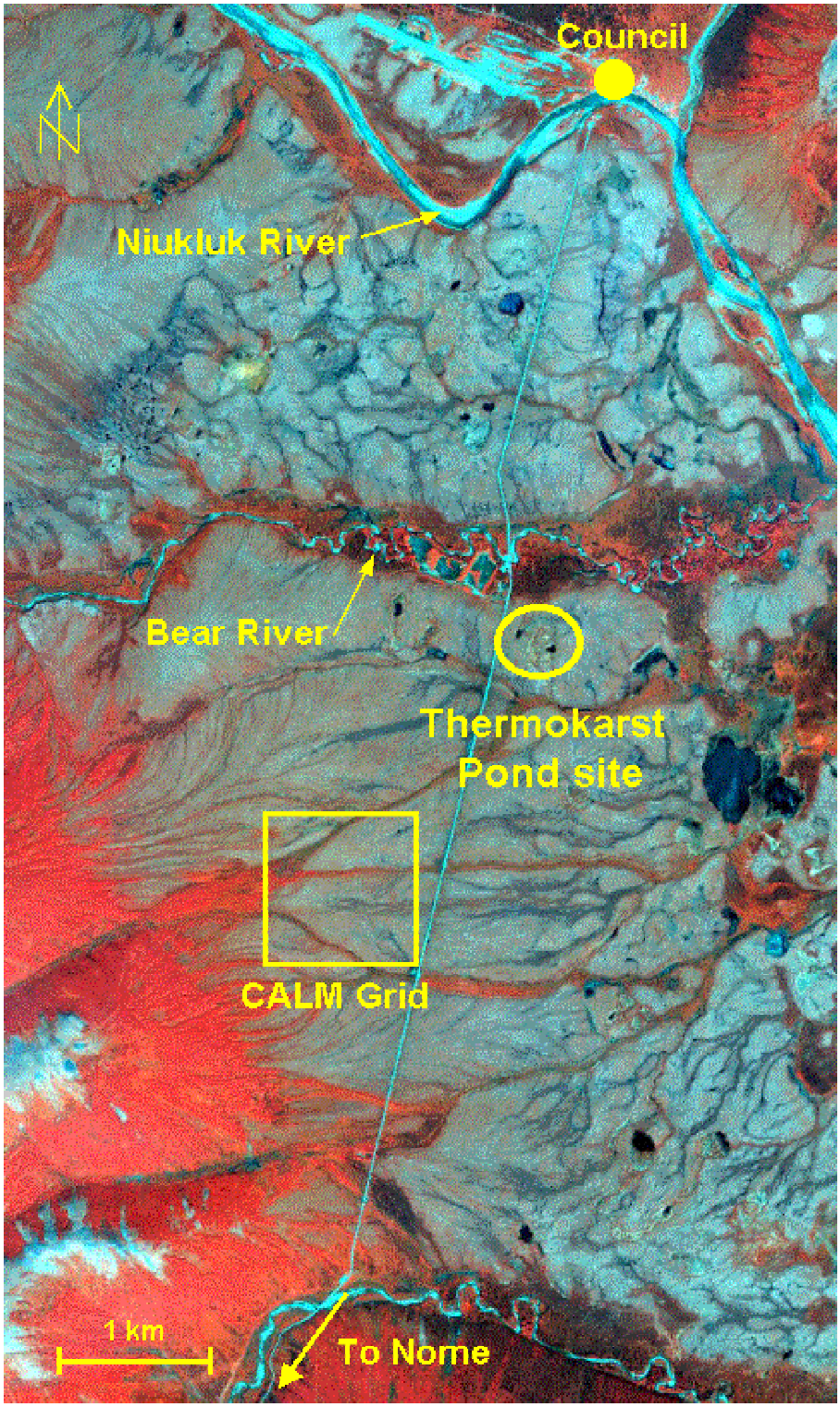

Figure 4. Study area. The “Thermokarst Pond site” is located in the middle of the Council valley, five kilometers south of Council.

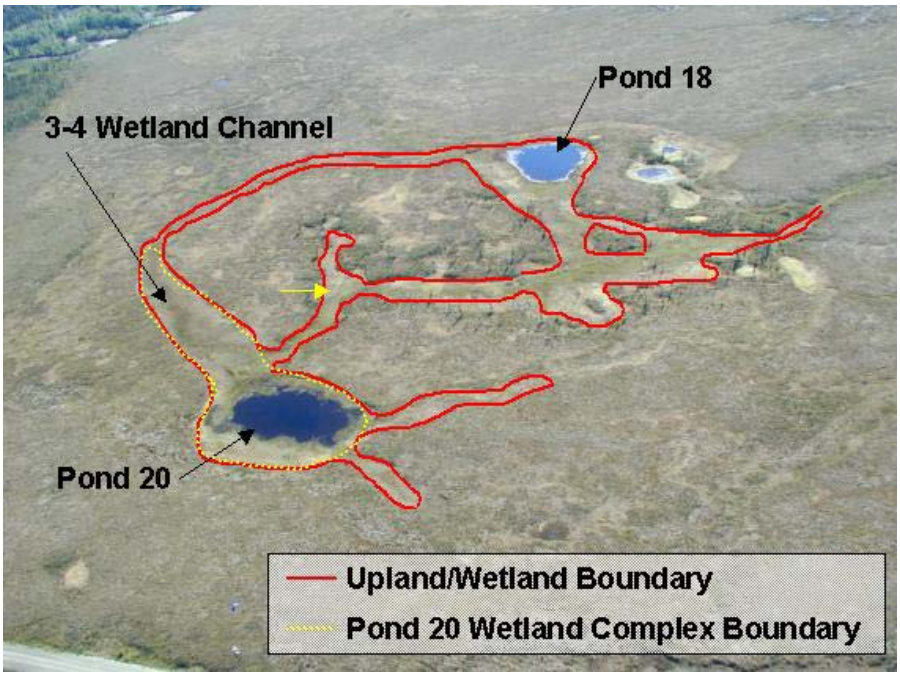

Figure 5. Site boundaries. The watershed boundaries are unknown due to low-relief topography, but the steep banks make the upland/wetland boundary quite obvious. The yellow arrow indicates the location and direction at which the photograph in figure 6 was taken.

Figure 6. Photograph of a marshy channel and banks. This particular area has banks that support spruce trees.

The ponds are located within the subsided wetland terrain. Around the perimeter of the ponds are thick mats of floating vegetation of grassier graminoid species. The horizontal distance from the pond to where the organic mat can still be described as “floating” is variable, ranging from a few meters to as much as 20 m from the edge of Pond 18 near the end of the 2001 summer. The transition from the typical non-floating wetland vegetation to the open water surface of the ponds creates a complex environment where the soil moisture within the vegetation is hydraulically inseparable from the nearby pond. A photograph of Pond 20 and the nearby wetland vegetation taken at low water in mid-August, 2002 is shown in figure 7.

Figure 7. Photograph of Pond 20 and the surrounding wetlands.

The material in the top one-meter of soil at various locations throughout the site was described during the installation of eighteen shallow wells. While there was considerable variability between the individual wells, a typical soil column for the upland areas is a 5 to 15 cm thick organic mat consisting of undecomposed to highly decomposed moss and litters on top of a brown or gray silty clay loam

(Michaelson and Ping 2003). The wetland areas generally have thicker organic mats, averaging 25 cm and ranging up to 50 cm thick.

3. Background

This study cannot be conducted without an understanding of the specific functions and interrelationships of permafrost and wetland hydrology. The relative impermeability of permafrost creates a unique system where only the soil above the permafrost that thaws each year is capable of storing water, influencing soil moisture and vegetation at the surface. The thermal properties of the active layer in turn affect permafrost conditions, regulating a dynamic thermal equilibrium between climatic factors and the cold subsurface. Logically, changes in climate or active layer composition can affect subsurface temperatures, possibly leading to changes in the distribution and thickness of the permafrost that can potentially induce changes at the surface. This dynamic relationship involving permafrost, climatic, and vegetation are all linked with hydrology. The arctic and sub-arctic regions are typically described as arid, and yet wetlands are abundant because of the presence of permafrost. The effect of changing permafrost conditions on the surface is obviously an important factor if the land-climate feedbacks are to be understood.

3.1 Permafrost and Thermokarst

Permafrost is generally defined as soil that is frozen for a period of two years or more (Davis 2001). The temperature at which the soils are “frozen” is slightly variable but is typically defined as 0˚C. The presence of ice in the soil pore space is what makes permafrost so significant to hydrologists; it inhibits groundwater flow by essentially decreasing the hydraulic conductivity of the soil by orders of magnitude (Kane and Stein 1983). By minimizing water migration through the soils to practically nil, permafrost acts as a confining layer, influencing surface water storage and minimizing sub-permafrost and supra-

permafrost ground water interactions (Rouse 2000; Woo and Steer 1982). In this regard, permafrost is necessary for the development of most wetlands in northern latitudes.

Permafrost distribution is related to average annual air temperature on a global scale, but on a local scale, the distribution of permafrost is influenced by local factors that affect the surface energy balance, such as aspect, topography, and vegetation (Osterkamp 1983). Permafrost on the Arctic Coastal Plain is several hundred meters thick, while in regions of discontinuous and sporadic permafrost in central and southern Alaska, permafrost can be as thin as a few centimeters thick. With thinner permafrost in the discontinuous permafrost region, generally occurring in Alaska south of the Brooks Range, the response to climate warming is faster, resulting in the warming and thinning of permafrost at a more dramatic scale than in the continuous permafrost on the North Slope of the Brooks Range (Osterkamp and Romanovsky 1999; Jorgenson et al. 2001; Romanovsky et al. 2002; Fitzgerald and Riordan 2003; Yoshikawa and Hinzman 2003). Every thaw season, beginning at the completion of snowmelt, the frost table recedes from the just below the ground surface until it reaches the permafrost table at the end of the thaw season, typically late in September on the Seward Peninsula. The depth to frozen soils at any given time during the summer is called the thaw depth, and the soil above the permafrost table (the depth of maximum seasonal thaw) is defined as the active layer.

Thermokarsting is the process most simply defined as the ground subsidence resulting from the melting of ice rich permafrost and the subsequent compaction of soil layers (Harry and French 1983; Gallinger 1991). Thermokarsting, described as one of the most important and dynamic processes in northern regions (Black 1969; French 1974), is often the mechanism initiated to return a soil column to thermal equilibrium after a disruption to the thermal regime

resulting from a change in surface conditions (Burn and Smith 1988; Lawson 1986). Changes in surface conditions can be a result of climatic changes, such as long-term temperature or precipitation changes, or anthropogenic disturbances, most commonly resulting in the removal of the surface organic layer (Burn and Smith 1988; Burn 1992). A great number of thermokarst features, including small thermokarst ponds, can be observed beneath and around the Trans-Alaskan oil pipeline (Thomas and Ferrel 1983). Black (1969) and Gallinger (1991) have noted small depressions tens of centimeters deep developing as quickly as one to three years.

With ground subsidence, water may accumulate in the depressed surface, and if the local topography supports it, ponds or lakes may develop (Williams and Smith 1989). Under ponded water in thermokarst depressions, heat conduction and advection is much greater, and the effect of the thermal properties of water instead of air results in a warmer subsurface and deeper thaw at the end of the growing season (Bosikov 1998; Swanson and Rothwell 1986). If the pond does not completely freeze to the bottom in the winter, permafrost degradation occurs thoughout the year with the development and growth of taliks (Burn and Smith 1988; Burn and Smith 1990). Taliks are zones of thawed soil in the vicinity of perennially frozen soil. With gradual downward talik propagation and concurrent upward thaw from the bottom of the permafrost, the talik can potentially “pierce” the permafrost, creating an open talik (Yershov 1998). Brewer (1958) investigated the permafrost on the North Slope of the Alaskan Coastal Plain and found that larger lakes with depths greater than two meters could create taliks as deep as 60 m. If the talik reaches the bottom of the permafrost, the possibility of significant water migration through the open talik is then a factor worthy of consideration (Hopkins 1949 and 1955; Yoshikawa and Hinzman 2003). Figure 8 shows the development of a thermokarst lake in the Central Yukechi area in Siberia and the resulting permafrost degradation over a period of twenty years.

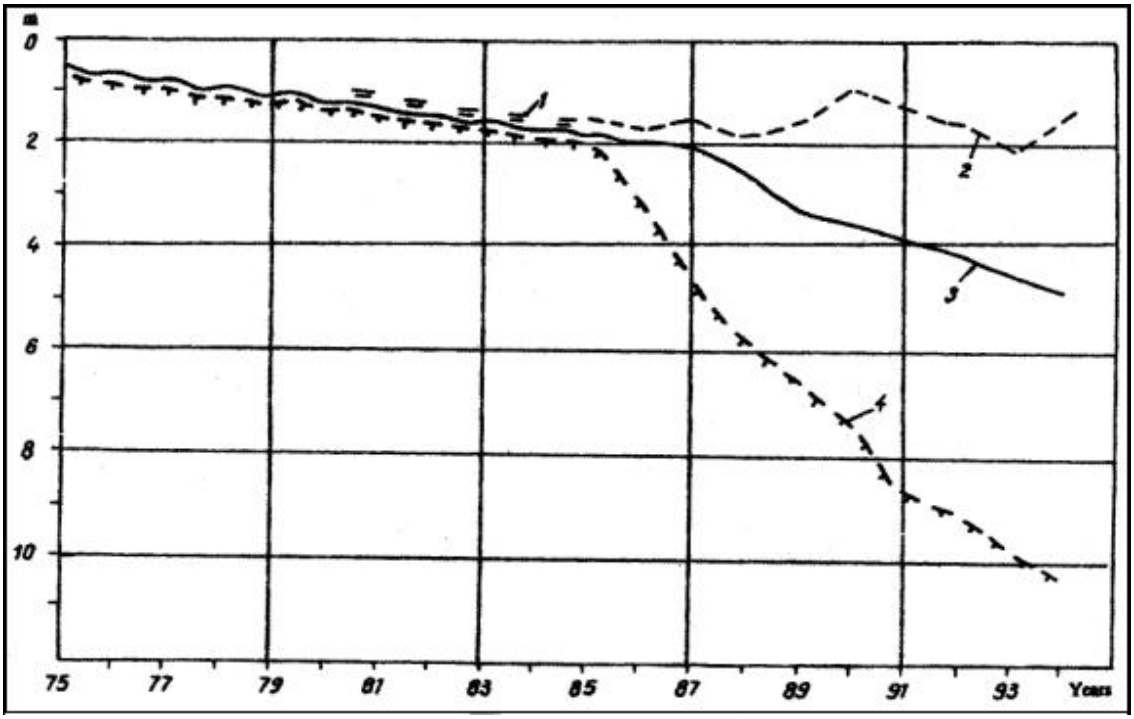

Figure 8. The growth of a thermokarst lake in Central Yukechi, Siberia. 1. water level in inter-polygonal troughs; 2. lake water level; 3. depth of subsidence; and 4. depth of thawed soil beneath lake (Bosikov 1998).

The development and drainage of thermokarst lakes is dependant on site-specific factors, such as bedrock geology, topography, or vegetation (Burn and Smith 1990). The abundant thaw lakes on the Arctic Coastal Plain on the North Slope of the Brooks Range have been the topic of a number of studies, most focusing on the orientation and vegetation patterns (Billings and Peterson 1980; Black 1969). The thaw lake cycle describing the evolution of these lakes was developed by Britton (1957) and expanded upon by Billings and Peterson (1980). The cycle has been predicted to take 2000 to 3000 years to complete. A diagram of the phases in the thaw lake cycle is shown in figure 9.

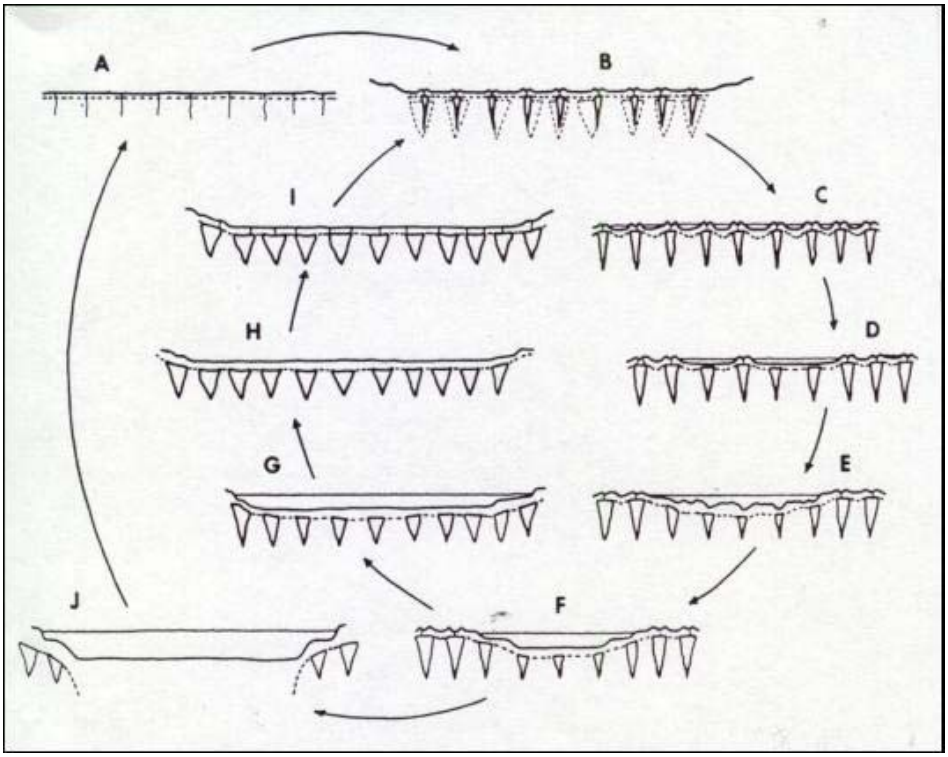

Figure 9. The thaw lake cycle (Billings and Peterson 1980). The thaw lake cycle can simply be described as the melting of ice wedges (B) and the resulting ground subsidence (C) facilitating ponding (D). The effect of the new surface conditions result in more ice-wedge melting and ground subsidence that facilitate water coalescence and the development of a lake (E and F). Depending on the depth of the lake, either a talik is formed or the ice-wedges are reestablished (J or G). The thaw lake cycle does not describe the drainage of the lakes after the development of the large talik, shown on the diagram as J → A, but the drainage from G to H occurs from a bank rupture and "catastrophic" lateral drainage.

Hopkins (1949) described the initiation, development, and eventual drainage of thaw lakes in the Imuruk Lake Area on the Seward Peninsula several years earlier. He suggests that lateral drainage of the ponds occurs from the melting and ground subsidence along ice wedge paths on the downslope side of the ponds and the creation of an outlet channel. This is likely the same mechanism responsible for drainage described in Britton's thaw lake cycle. Hopkins also

theorizes lake drainage resulting from an intersection of the downward migrating talik with a course-grained soil layer or weathered bedrock, leaving what he called “thaw sinks”. While these formations are certainly different than the thermokarst ponds in the Council area, the drainage mechanisms are assumed to be similar. The evolution of a thaw sink is shown in figure 10.

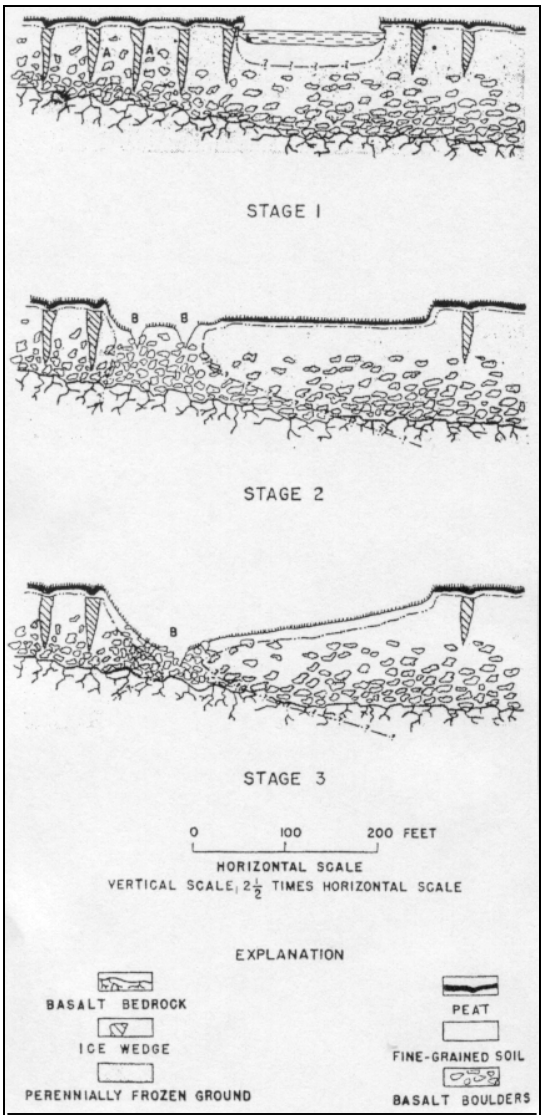

Figure 10. The evolution of a thaw sink in the Imaruk Lake area on the Seward Peninsula (Hopkins 1947). Coarse-grained material or bedrock must be relatively close to the surface for the lakes to rapidly drain.

3.2 Wetland Hydrology

Wetland hydrology in northern latitudes has been largely understudied and is poorly understood despite its spatial abundance (Ford and Bedford 1987; Roulet and Woo 1986a). The vast majority of wetland research in Alaska has been conducted on the Arctic Coastal Plain and the North Slope of the Brooks Range or around Fairbanks; hydrologic research on the Seward Peninsula is sparse. Results from hydrologic studies conducted in the Arctic Coastal Plain of Alaska and Northern Canada are primarily used as references for the hydrologic analysis for the wetland complex in this study.

The basic concept of the water balance is based on the conservation of mass; the changes in water within a system should be balanced by the sum of the water inputs and outputs. Thoroughly conducted and complete water balances are seldom done in northern wetlands (Ford and Bedford 1987; Kane and Hinzman 1988; Kane et al. 1992), but numerous studies can be found incorporating simple water balances in their methods (Kane et al. 1990; Lafleur 1994). The complete form of the summer water balance is as follows:

$$M + P + Q_{in} - Q_{out} - ET - T = \Delta S$$

where M is the contribution from snowmelt; P is precipitation as rainfall; Q_{in} is the surface and subsurface lateral flow into the wetland; Q_{out} is the surface and subsurface lateral flow out of the wetland; ET is evapotranspiration; T is ground water drainage through the open talik, (or negative value for recharge); and ΔS is the change in water storage within the system. The typical units for the components of the water balance are volumetric, but they can be in terms of length (i.e. centimeters or inches) when normalized over an area. The period over which the water balance is conducted determines the active terms in the

water balance. By conducting a summer water balance beginning after the completion of snowmelt, M is dropped from the equation, as is the case with this study. Also, during periods between large precipitation events, Q_{in} and Q_{out} can sometimes be neglected or dismissed as negligible (Roulet and Woo 1986a; Glen and Woo 1997). Some researchers have shown that ΔS is negligible from year to year for their particular study sites (Kane and Hinzman 1988; Lilly et al. 1998). In arctic and subarctic regions, most studies can disregard T because of the presence of continuous ice-rich permafrost (Kane and Hinzman 1988; Woo 1980; Rouse 1998).

Most water balance studies have some residual term that is calculated as the sum of the other water balance components (Roulet 1991; Glen and Woo 1997). The error from the other water balance components is accumulated in the residual term, and as a result, the residual term is only as accurate as the least accurate modeled or measured water balance component. As stated earlier, T is often ignored in northern water balance studies because of the presence of continuous, ice-rich permafrost, allowing for the designation of ET, Q, or ΔS as the residual term, but this is not always the case. Several studies have discussed groundwater recharge to wetlands in interior Alaska and sub-Arctic Canada (Roulet 1991; Ford and Bedford 1987). Kane and Slaughter (1973) identified groundwater recharge to a small lake near Fairbanks, Alaska by the use of nested piezometers. Interactions between suprapermafrost and subpermafrost groundwater are most commonly associated with large thawed regions beneath irregularities at the surface, such as a lake or river in an otherwise tundra landscape (Hopkins 1949 and 1955), however springs are also a common mechanism for hydraulic connection between the subpermafrost groundwater and the surface. Where suprapermafrost and subpermafrost groundwater interactions are potentially significant, T is usually designated as the residual term (Roulet 1990; Ford and Bedford 1987).

Lateral water fluxes can be divided into surface and subsurface flow. Due to the presence of permafrost, subsurface lateral flow is restricted to the shallow active layer. This and the low hydraulic gradients typical of many northern wetlands together often result in negligible subsurface flowrates (Roulet and Woo 1986a). Hydraulic conductivity in the organic layer is often orders of magnitude larger than the underlying mineral soil, and as a result, lateral flow is possible at the organic-mineral interface when the organic layer is saturated or if infiltration rates are beyond the percolation capacity of the mineral soils (Kane and Hinzman 1988). Kane et al. (1978) describes the saturated hydraulic conductivity of organic soils to vary with depth, ranging from about 10 and 100 m/day depending on the degree of decomposition. This range is similar to data published by Hinzman et al. (1991) and Roulet (1990). The unsaturated hydraulic conductivity of organic soils can be greater than that of underlying mineral soils and should be considered in the analysis. Unsaturated hydraulic conductivity can range from $1x10^{-6}$ m/day at very dry conditions to $1x10^{-1}$ m/day near saturated conditions (Hinzman et al. 1991), whereas typical saturated hydraulic conductivity for silts ranges $1x10^{-4}$ to $1x10^{0}$ m/day (Fetter 1994).

Surface flow has been shown to be far more influential than subsurface flow at some sites, but the majority of studies concluding this have included the spring snowmelt event in their analyses (Roulet and Woo 1986b; Roulet and Woo 1988; Kane and Hinzman 1988; Woo 1980). After snowmelt, surface runoff from upland tundra areas can occur only if the rate of rainfall exceeds infiltration rates or if the suprapermafrost groundwater level rises above the surface (Woo and Steer 1982). Surface flow is typically non-existent between periods of significant recharge from rainfall events, and therefore subsurface flow controls lateral water fluxes, but as stated earlier, this term is often dismissed as negligible. Roulet and Woo (1988) suggest that lateral discharge from a wetland site essentially ceases with the drop of the water table below the surface of the organic material.

In between periods of probable surface flow, the water balance of the active layer can often be simplified because the lateral fluxes are assumed negligible, reducing the water balance equation to a combination of vertical fluxes. This assumption has been proven reasonable for several studies conducted in areas of low relief where hydraulic gradients are small (Rovansek 1994; Glen and Woo 1997; Lafleur 1994; Rouse 1998). The water balance for the active layer assuming negligible lateral fluxes is shown below:

$$\Delta S = ET - P$$

Glenn and Woo (1997) observed that, after an extended dry period, a rainy period raised the suprapermafrost water table very near but not to the ground surface, but subsurface flow over the period was less than 1% of the volume of rain that fell. But after an ensuing rainy period, the results of the water balance assuming negligible lateral fluxes deteriorated, indicating a net inflow into the wetland from the upland slopes. Because lateral flow out of the wetlands remained negligible, they were able to calculate the lateral inflow to the wetland as the residual term of the previously simplified water balance equation. Hinzman et al. (1991) described surface organic soils (15 cm thick) being desiccated after extended dry periods, and then producing down-slope runoff after absorbing only 1.5 cm of rain.

4. Data Collection

Data collection for this site was initiated in June of 2001 with the installation of a meteorological station and several shallow and deep wells. Continuous data recorders were immediately installed for the meteorological station and the deep wells, and observations of the soil profile were obtained with the installation of the shallow wells to describe the active layer throughout the site. Additional instruments were installed in August of 2002 and June of 2003.

The meteorological station consists of a three-meter aluminum tower positioned on the tundra about two meters from the east edge of the bank of Pond 20; the tower holds air temperature and relative humidity sensors (Campbell Sci., HMP 45C) at one and three meters above the ground surface as well as a Frischen-type net radiometer (REBS, Q*7.1) positioned 1.5 m above the ground surface. A three-meter aluminum tripod staked to the bottom of Pond 20 about 10 m from the tower holds another net radiometer 1.5 m above the water surface (at high water). Dataloggers (Campbell Sci., CR10X) were used to collect hourly data from these four instruments.

Three nested well pairs were installed at the site in June 2001, one in each pond and one in a relic talik underlying the large marshy area between the two ponds. In both of the ponds, the wells are positioned roughly 1 m beyond the edge of the floating vegetation surrounding the open water. In Pond 20, the deep wells were installed to a depth of 3.34 and 1.06 m below the bottom of the pond. The nested wells in Pond 18 were drilled to 3.69 and 1.59 m. Hobo dataloggers were used to collect continuous data from pressure transducers in each well. Manual water level data were collected twice during the 2001 summer and several times throughout the 2002 summer.

Eighteen shallow wells, each approximately 1.5 m in length, were installed throughout the site to describe the active layer flow regime. The locations of these wells are shown in Figure 11. The position of the water table and the ground surface were measured from the top of the wells upon each site visit during the two field seasons. The position of the frost table was also measured at each well by driving a graduated steel probe into the ground until impeded by the top of the frozen soil. The elevations of all wells relative to each other were surveyed in June 2001, June 2002, and September 2002.

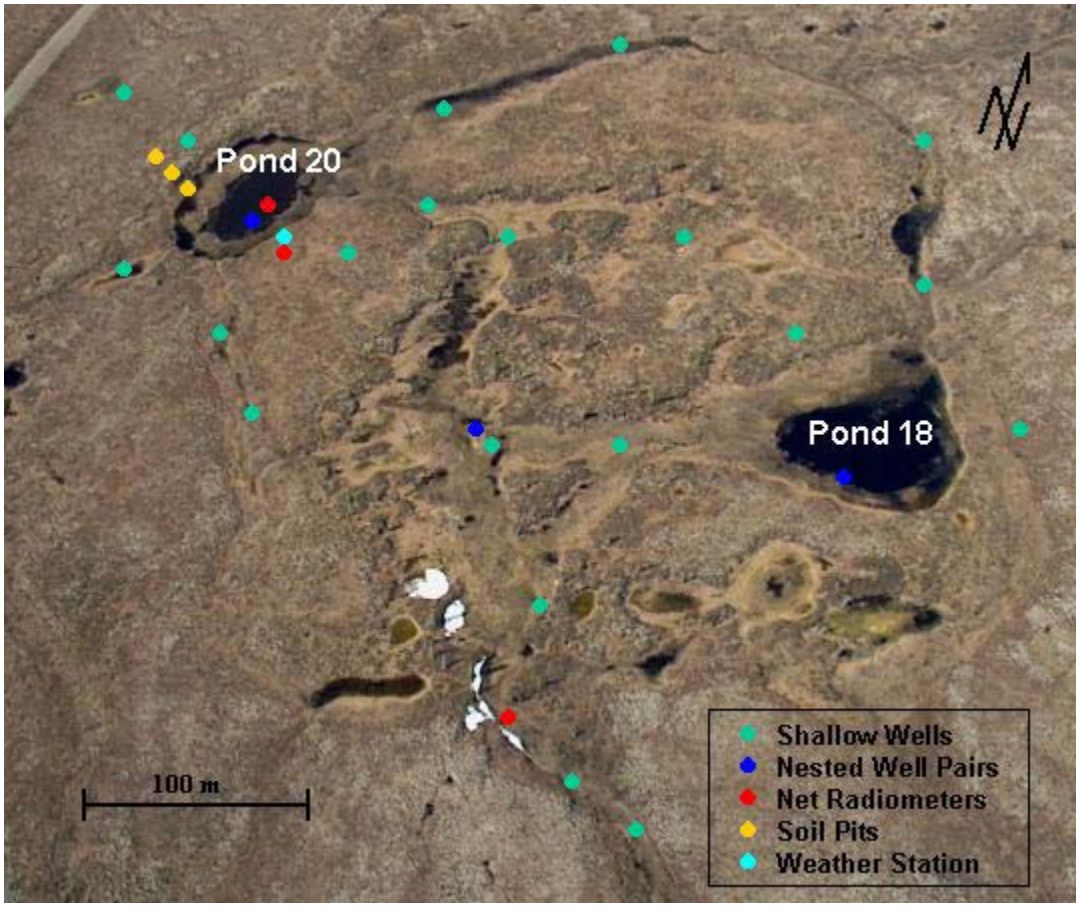

Figure 11. Site instrumentation necessary to conduct a water balance.

Cumulative hourly rainfall, wind speed, and wind direction data collected from a similar meteorological station located three km away at the Council CALM grid were used to supplement the data collected onsite. This station is located in the same valley at a site with similar elevation and topography, with vegetation matching that of the upland tundra areas within the site of this study. Wind speed and direction were collected using a RM Young propeller-type anemometer positioned three meters above the ground surface. Cumulative rainfall was measured with an eight-inch-diameter tipping bucket rain gage utilizing an Alter shield to reduce undercatch resulting from wind. It is suggested that a correction factor be applied to further compensate for wind effects (Yang et al. 1998). The corrected rainfall is calculated from:

$$P_{corrected} = P_{measured}/R$$

where $P_{corrected}$ is the wind corrected precipitation (mm), $P_{measured}$ is the precipitation measured from the Alter shielded gage (mm), and R is the correction factor, calculated by the formula:

$$R = \exp(4.606 - 0.041*W_s^{0.69})$$

where W_s is the wind speed (m/s) at gage height. The wind speed is converted from the 3-meter instrument height to the rain gage height with the following equation:

$$W_s(h) = \ln(h/z_0)/\ln(H/z_0)*W_s\ (H)$$

where $W_s(h)$ is the wind speed at rain gauge height (m), h is the rain gauge height (m), H is the height of the measured wind speed (m), z_0 is the surface roughness (m), estimated at 0.02 for tundra surfaces, and W_s (H) is the wind

speed at measurement height (m/s). The rain gage does not record trace events, which may result in an underestimate of precipitation, and the occurrence of small convective storms only partially covering the Council valley has been witnessed first hand, suggesting the possibility of minor discrepancies in rainfall volume between the two sites.

In August of 2001, ten soil moisture sensors (Campbell Sci., CS615) and ten corresponding temperature sensors (Alpha thermistors) were installed in three different soil pits located on the west edge of Pond 20. The specific locations of the pits were chosen to represent soil conditions for uplands, wetlands, and the banks that divide the two terrain types. These data were collected continuously with another CR10X datalogger with an output interval of three hours. The CS615 probes are used to estimate soil moisture by measuring the dielectric constant of the soils (Campbell Sci. 2001; Stein and Kane 1983).

In June of 2002, two thermistors were installed in Pond 20 to collect temperature data at the pond surface and slightly below the pond surface. A Styrofoam shield was used to keep the upper thermistor at the water surface and to shield the thermistor from direct solar radiation. The lower thermistor was weighted so that it would hang approximately 34 cm below the surface. Four additional thermistors were installed just beneath the ground surface at four different locations between the pond and the soil pits to describe various surface temperatures. The four surfaces were described as dry tundra, sphagnum moss and grass, graminoid, and saturated graminoid, the latter two being on the floating mat. All six of these additional thermistors were added to the CR10X data logger currently used for the soil moisture and thermistors in the three soil pits. An additional net radiometer was installed onto an anchored arm extended over the marshy vegetation in the outlet channel.

5. Analysis Methods

The magnitude and temporal activity of all water transfer mechanisms are explored using the water balance technique. With inputs, outputs, and changes in storage accounted for, ideally the sum of the components will balance; however, even with the most accurately modeled water balance, there will be error associated with some or all of the terms and the system will often not balance exactly. Also, the amount of water lost through open taliks is not quantified directly but is assumed to account for any residual water volume unaccounted for by the other measured terms. The water balance is a versatile method to analyze hydrologic dynamics. It can be conducted over the entire site or over a unit area, such as a column of soil. The water balance can also be conducted over the entire summer or over the period of a few hours. Of all of the spatial and temporal combinations of the water balance, the conditions that correspond to the calculations with the highest level of confidence can best be used to identify the activity of the residual term. Where the system is not balanced, intuitive explanations are provided to describe the hydrology qualitatively.

The site is divided into three general surface types (uplands, wetlands, and ponds) to simplify the complex natural system while still respecting the sizeable differences in the hydrologic behavior of different surfaces. (Physical descriptions of the three surface types are provided in the Study Site Description section). Analysis methods for computations of all components of the water balance are specified for each surface type. By looking individually at the one-dimensional (1D) water balances over each surface, speculation can be given to the quality of the ET modeling as wells as to the validity of the assumption of negligible lateral fluxes.

5.1 Evapotranspiration

Evapotranspiration (ET) from the study site is calculated using the Priestley-Taylor (PT) model (Priestley and Taylor 1972). This method uses the concept of equilibrium evaporation in terms of latent heat (LE) and then relates actual ET to evaporation under equilibrium conditions with the introduction of the empirical coefficient alpha (α):

$$\alpha = LE/LE_{EQ}$$

where LE is the actual latent heat used for evaporation (W/m^2), and LE_{EQ} is the latent heat under equilibrium conditions (W/m^2). LE_{EQ} can be quantified:

$$LE_{EQ} = (S/(S + \gamma))(Q^* - G)$$

where S is the slope of the saturation vapor pressure curve ($Pa/^{\circ}C$), γ is the psychometric constant ($Pa/^{\circ}C$), Q* is the net radiation (W/m^2), and G is the ground heat flux (W/m^2). It has also been shown that $S/(S + \gamma)$ (dimensionless) is adequately described by the linear function of the screen air temperature T_a ($^{\circ}C$) (Stewart and Rouse 1976a):

$$S/(S + \gamma) = 0.406 + 0.011\ T_a$$

Therefore, by combining these three equations, the PT model is reduced to the form:

$$LE = \alpha\ (0.406 + 0.011T_a)(Q^* - G)$$

The alpha term has been shown to vary considerably for different meteorological and surface conditions, resulting in spatial and temporal variability (Engstrom et al. 2002). Typically, alpha is less than one for hot and dry surfaces and always greater than one for surface with unlimited moisture supply (Bello and Smith 1990; Eichinger et al. 1996). An alpha value of 0.95 has been used successfully in the PT model for upland tundra surfaces on the North Slope of the Alaskan Range for summer-long studies (Kane et al. 1990). For wetland soils and lakes, alpha values range from 1.1 to as high as 2.0 with 1.26 being a commonly used value for surfaces with unlimited water supply (Stewart and Rouse 1976b; Rovansek et al. 1996; Mendez et al. 1998).

Because of the sizeable range of reasonable alpha values, it is suggested that another method be used to calculate actual ET in order to calibrate the PT model and apply the correct alpha value for a specific site during specific time periods (Mendez et al. 1998). For this reason, the Bowen Ratio-energy balance method (BREB) is applied to the 2002 season data set in an attempt to approximate the ratio of actual LE to LE_{EQ}. The BREB method uses the available energy term (Q* - G) and the Bowen ratio (B) to calculate the evaporative heat flux (Bowen 1926):

$$LE = (Q^* - G)/(1 - B)$$

where Q* is net radiation (W/m^2), G is the ground heat flux (W/m^2), and B is the Bowen ratio (dimensionless). The Bowen ratio (B) is quantified:

$$B = \gamma(\Delta T/\Delta e)$$

where γ is the psychometric constant (Pa/˚C) and $\Delta T/\Delta e$ is the vertical temperature gradient divided by the vapor pressure gradient (˚C/Pa). γ is calculated:

$$\gamma = (P_a C_{pa})/(0.622\lambda)$$

where P_a is the air pressure (Pa), C_{pa} is the specific heat of air (J/kg/˚C), and λ is the latent heat of vaporization (J/kg), which is calculated from the following linear relationship of surface temperature:

$$\lambda = (2.501*10^6 - 2370T_s)$$

where T_s is the surface temperature (˚C). The vertical temperature and vapor pressure gradients required for Bowen ratio calculations are ideally measured between two heights above the ground surface (Mendez 1997), but with only one tower, only one pair of gradients can be measured between the instruments at 1 and 3 m above the surface. This method leaves no way to distinguish between the three terrain types. For this reason, ΔT and Δe for each terrain type are measured from the respective ground surface to the 3 m sensor located at the tower. This method assumes the air temperature and relative humidity at three meters is the same over the entire site and that the three-meter sensor is within the boundary layer for each surface type.

The vapor pressure of air necessary for Bowen ratio calculations is the product of the saturation vapor pressure and the relative humidity of air:

$$e_a = e_{as} *RH$$

where e_a is the vapor pressure of air (Pa), e_{as} is the saturation vapor pressure (Pa), and RH is the relative humidity of air (fraction). The saturation vapor pressure is calculated with the use of the following two equations (Brutsaert 1982):

$$e_{as} = 101325\exp(13.3185t_R - 1.9760t_R^2 - 0.6445t_R^3 - 0.1299t_R^4)$$

$$t_R = 1 - (373.15/(T_a + 273.15))$$

The vapor pressure of the pond surface may be assumed to be saturated and may be calculated from the pond surface temperature (Stannard and Rosenberry 1991; Bello and Smith 1990). For unsaturated soils, the vapor pressure at or near the surface is the product of the saturation vapor pressure and the relative humidity at the ground surface. The relative humidity at the ground surface is assumed to be equal to the relative humidity within the pore space of the near-surface soils. The relative humidity of the soils is related to the soil water potential by the following equation (Campbell 1985):

$$RH_s = \exp(M_w\psi/RT)$$

RH_s is the relative humidity of the pore space of the soil (fraction), M_w is the mass of a mole of water (kg/mol), ψ is the soil water potential (J/kg), R is the gas constant (8.3143 J/mol*K), and T is the soil temperature (K). The soil water potential of the surface soils is estimated from a measured characteristic curve for surface organic tundra soils published in Hinzman et al. (1998). The characteristic curve is the relationship of extraction pressure (kPa) and volumetric soil water content:

$$\varphi = 100*\exp(12.6127-1.49193\theta+0.0631116\theta^2-0.00138392\theta^3+1.47234*10^{-5}\theta^4-6.02334*10^{-8}\theta^5)$$

where φ is the extraction pressure (kPa) and θ is the soil water content (% by volume). The extraction pressure is converted to soil water potential ψ (J/kg) with the following equation:

$$\psi = -1000*\varphi/\rho_w$$

where ρ_w is the density of water (kg/m^3).

LE calculations require the computation of the ground heat flux G. G is calculated from the vertical temperature gradient in the upper layer of the soil column:

$$G = K*dT/dz$$

where K is the thermal conductivity of the soils (W/m $^\circ$C), dT/dz is the vertical temperature gradient in the soil column ($^\circ$C/m). The assumption that purely conductive heat transfer processes can be used to estimate ground heat flux during the summer when the active layer is thawing has been shown to be reasonable (Glen and Woo, 1997; Boike et al. 1998). Because evaporative processes occur at or near the ground surface, the ground heat flux at depth is less significant; however, to ensure the accurate estimation of G, the vertical temperature gradient is measured for the upper two soil columns: the surface to 5 cm, and then from 5 cm to the next soil moisture/temperature sensor (10 cm for the uplands and 15 cm for the wetlands). With the exception of a few weeks where the soil was still frozen at 15 cm in the lower pit, the G calculations for the upper two soil layers are averaged. This is done to combat the sensitivity of this model to surface temperature, which is a difficult measurement to make accurately.

The thermal conductivity of thawed soils varies with water content and, as a result, is spatially and temporally variable (Swanson and Rothwell 1986; Farouki 1981). Based on the results of Hinzman et al. (1991), the following empirical relationship was developed to account for the varying thermal properties of the near-surface organic soils with changing moisture conditions:

$$K = 0.2065\text{Ln}(\theta) - 0.3781$$

where K is the thermal conductivity (W/m^2), and θ is soil moisture (% by volume). The average soil moisture of a soil layer must be used in the assignment of an appropriate thermal conductivity value for that soil layer. For this reason, a number of assumptions are made about the moisture conditions in the various soil layers based on the available soil moisture data, soil type, and location. Only the two uppermost soil layers in the upland and wetland soil pits are used in the ground heat flux analysis. The soil moisture of the surface-to-5cm layer in the upland soil pit is assumed to be exactly half of the soil moisture at 5 cm during dry periods when evaporative processes certainly desiccate the surface organic soils (Kane et al. 1978); during rainy periods, the soil moisture in the same layer is assumed to be constant at a value equal to the soil moisture at 5 cm. For the 5cm-to-10cm layer in the upland pit, the average moisture conditions are simply the average of the soil moisture at 5 and 10 cm. For the wetland soil pit, the soil moisture at 5 cm remains fairly constant at a value near the specific retention (0.57), and because of the abundance of water in the wetlands and the relative proximity of the water table to the ground surface, it is assumed that the moisture conditions at the surface remain at the specific retention as well. The 5cm-to-15cm soil layer in the lower pit contains a significant amount of silt and cannot be described by the previous equation, which is for organic soils only, so a constant value of 0.7 W/m^2 was chosen as an average of saturated organic and mineral

soils (Hinzman et al. 1991; Swanson and Rothwell 1986). The K values used in this analysis are similar to those published elsewhere in the literature (Farouki 1981; Yoshikawa et al. 2003).

For the ponds, G is a combination of the heat flux into the sediments at the bottom of the pond Q_s and the change in heat storage within the pond S. The calculation of Q_s is the same as the ground heat flux calculation for a column of soil. Unfortunately, the necessary instrumentation to measure temperature gradients in the bottom sediments were not installed; consequentially, Q_s is not calculated for the two ponds in this study. Q_s has been shown to be a very small term and is often neglected (Woo 1980; Roulet and Woo 1986a and b; Stannard and Rosenberry 1991), but other studies suggest that this term is small but significant (Stewart and Rouse 1976b; Mendez et al. 1998). Both scenarios are explored in the results section.

The possibility of advective heat transfers associated with heat inputs from lateral fluxes or from possible open talik drainage are ignored. While these energy fluxes can typically be neglected in some energy budget analyses (Kane et al 1990), it is possible that these less-common energy transfer mechanisms may be significant if a considerable amount of water is moved, which is possible with drainage through an open talik (Lunardini 1998). Additional energy loss through advective heat transfer would result in less available energy for latent and sensible heat fluxes, and consequentially lower ET rates.

The change in heat storage within the pond is calculated with the following equation:

$$S = Cz\Delta T/\Delta t$$

where S is the change in heat storage ($W/m^2/day$), C is the heat capacity of water ($W/m^{\circ}C$), z is the average depth of the pond (m), and $\Delta T/\Delta t$ is the average daily temperature change ($^{\circ}C/day$). The temperature used in this calculation is the average of the surface temperature, the temperature at 34 cm below the surface, and the temperature at the bottom of the pond.

The BREB method requires scrutiny of the data set in order to identify and omit unreasonable and false LE calculations produced from a range of conditions, so the rejection criteria prescribed by Ohmura (1982) is used to ensure that only valid data are incorporated in the analysis. By plotting the actual latent heat calculated from the BREB method (LE_{BREB}) versus the equilibrium latent heat (LE_{eq}), the slope of the best-fit line is approximately equal to an appropriate alpha value for that data set (Stewart and Rouse 1976b; Rouse 1998). While bearing in mind that the alpha-value incorporates a number of factors that will result in temporal and spatial variability (Kane et al. 1990), the result from other studies where the PT model is used will be used as comparison with the alpha values calculated in this study. In particular, data collected from a study in the 2000 summer in the Council area is used as a reference for the results of this study (Beringer et al. 2003a and b). Beringer's study used an eddy flux tower to obtain direct measurements of evapotranspiration over an upland tundra site in the Council valley approximately two km from this study area.

After the relative magnitudes of G and LE are checked and assumed reasonable, LE is converted to a physical depth of evaporated water with the following equation:

$$ET = LE/(\rho_w \lambda)$$

where ET is the water lost due to evapotranspiration (m/s), LE is the evaporative heat flux (W/m^2), ρ_w is the density of water (kg/m^3), and λ is the latent heat of vaporization (J/kg).

5.2 Lateral Fluxes

The subsurface lateral flow through the shallow active layer is calculated using Darcy's Law with the simplified flow field assumptions of the Dupuit-Forchheimer theory. This method has been shown to work well for shallow flow fields with small hydraulic gradients (Freeze and Cherry 1979),

$$Q = K_s h(x) dh/dx$$

Q is the lateral groundwater flowrate (m^3/day), K_s is the saturated hydraulic conductivity (m/day), h is the depth of flow (m), and dh/dx is the hydraulic gradient measured between two wells (m/m). The term (x) represents a unit width, or the width of the channels in case of wetland subsurface flow calculations. Because the typical soil profile encountered at the site is basically a two-layer system of an organic mat on top of mineral soils, and because the hydraulic conductivity of organic materials is typically orders of magnitude greater than that of mineral soils, flow through the organic and mineral soils are calculated separately and then summed. The possibility of notable flow in the unsaturated regions of the organic layer is explored with the application of a conservative unsaturated hydraulic conductivity value and assuming the hydraulic gradient within the unsaturated region is the same as the hydrostatic pressure gradient used for flow calculations of the saturated regions. Based on previous studies, the following values are used to produce conservative estimates of the flowrates in saturated organic material, unsaturated organic material, and mineral soils, respectively: 10^2 m/day, 10^{-1} m/day, 10^{-1} m/day.

Saturation overland flow occurs when storage of the active layer soils is at capacity, or the storage deficit is zero. The storage capacity of the active layer, defined as the total volume of water that a soil column is capable of holding, is a function of porosity and increases throughout the summer along with increasing thaw depth. The storage deficit, defined as the volume of water required to saturate a soil column, is a function of both the storage capacity and the amount of water already in the soil column. Given the storage deficit of the soils and the size of a rainfall event, the likelihood of surface flow can be predicted.

The likelihood of the occurrence of surface flow can be identified using the continuous soil moisture data from 5 cm below the surface. When the storage deficit is zero, the soil moisture will equal the porosity of the soil, but because data are three-hour averages of the soil conditions, large spikes in the data approaching porosity are designated as periods of probable surface flow. Because the magnitude of the surface flow is unknown, the water balance is simply reset at a later time when surface flow has likely ceased.

5.3 Storage

The change in water storage (ΔS) is calculated differently for each of the three surface types (uplands, wetlands, and ponds). Preference is given to methods that utilize continuous data instead of the manual data collected during the sporadic site visits. Additional consideration is given to the areas occupied by floating mats and the areas between the floating mats and the sedge meadows (wetlands), as they occupy a considerable fraction of the total area, especially when focusing on a particular pond. A transect depicting the transition of the general surface types and the method used for calculating changes in storage for each zone is shown in figure 12.

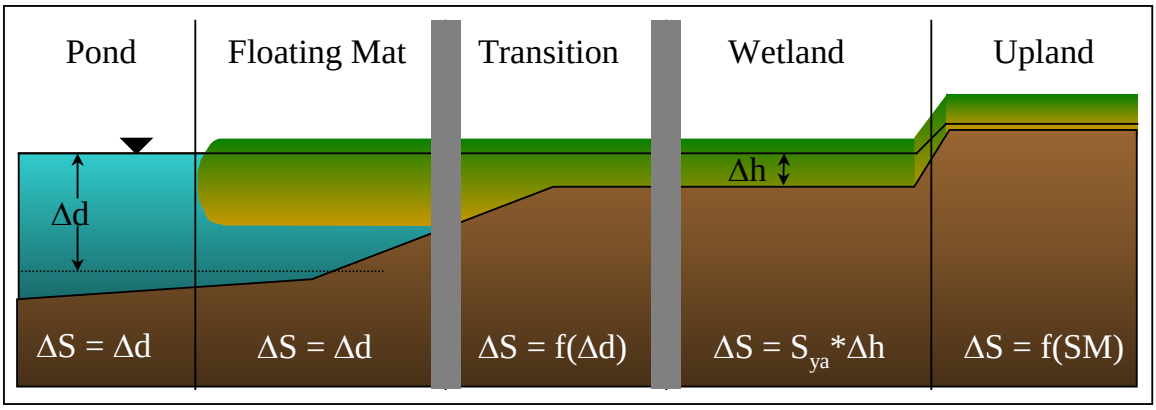

Figure 12. Generalized transect from pond to uplands. The methods used to calculate storage across a generalized transect from a pond to the uplands are a function of either pond water level, well water level, or soil moisture. The exact boundaries of the transition zone are unknown.

For the open water surfaces of the ponds, ΔS within a column of water is equal to the change in water level, Δd. The ΔS for the organic mat around the perimeter of the ponds can be calculated in a similar manner if the material is floating. This implies that soil moisture is constant within the floating mat, even at the surface. If the level of the vegetation surface ceases to change 1:1 with the change in water level, the mat is no longer floating and storage changes within the mat are not equivalent to changes in pond water level (Roulet 1991). This defines the boundary between the floating mat and the transition zone, where the ΔS is not equal to but is still a function of changes in pond water level (see figure 12). This phenomenon is evident in the relationship between Pond 20 water level and soil moisture from 5 cm below the surface in the wetland soil pit shown in figure13. Prior to some critical period in 2002, possibly when the frost table no longer interferes with the hydraulic connectivity between the wetland vegetation and the nearby pond, the soil moisture at 5 cm in the transition zone remains nearly constant at value near the specific retention of the organic mat, but after the critical period, the soil moisture changes with changing Pond 20 water level. The slope of the best-fit line indicates that soil moisture, equivalent in magnitude to

storage within the transition zone, changes 0.014 cm for every 1 cm change in pond water level. The same relationship during the latter half of the 2001 summer shows a similar rate of change (0.015 cm/cm).

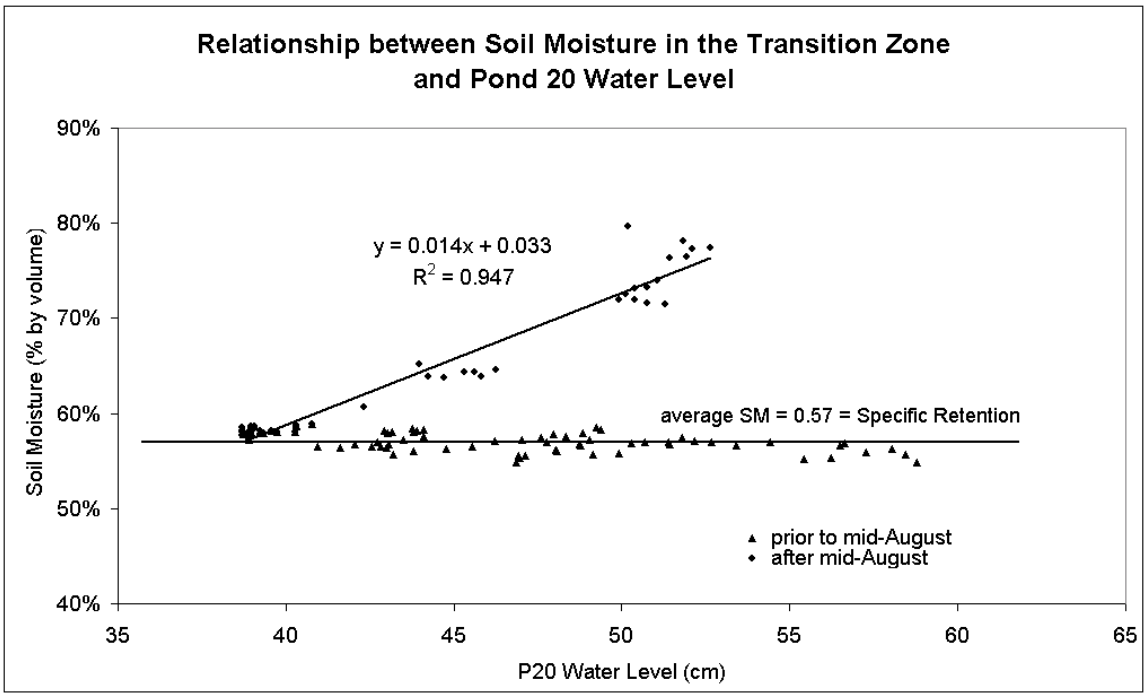

Figure 13. The relationship between 5 cm soil moisture from the wetland pit and Pond 20 water level. Prior to mid-August, soil moisture in the wetland soil pit remained near the specific retention, regardless of pond water level.

The identification of the boundary between the floating mat and the transition zone is problematic because it is not defined by an obvious topographic or vegetative change, plus the location of the boundary is suspected to change along with frost table position and pond water level. The differentiation between floating mat and non-floating vegetation is of critical importance in overall ΔS calculations, plainly evident in the sudden reduction of the influence of pond water level changes by almost 99%. (1:1 for floating soils versus 0.014:1 for the non-floating soils.) This boundary is estimated from aerial photographs taken at extremely high water level, where non-floating material beyond the floating mats

are inundated with water. It is suspected that the actual transition from floating mat to wetland is smoother and asymptotic, with the influence of the pond approaching null with distance away from the pond, but pond water level and frost table dynamics along with topographic heterogeneity render modeling this process very difficult.

For a typical soil column located on the upland tundra slopes, ΔS is equivalent in magnitude to changes in the storage deficit within the soil column. The storage deficit (S_d) of a typical upland tundra soil column is calculated using the continuous soil moisture data from the upper soil pit by simplifying the soil column into layers in which each soil moisture probe represents the average soil moisture within the layer. Storage deficit is then calculated with the following equation:

$$S_d = \Sigma(n_i - \theta_i)*z_i$$

where S_d is the storage deficit (cm), n_i is the porosity (dimensionless), θ_i is the soil moisture (fraction), and z_i is the thickness of each soil layer (cm) (Glenn and Woo 1997). This method is not prescribed to the wetland soils because of the lack of representative soil moisture data.

Water level data from the shallow wells throughout the wetland areas can be used to estimate storage in the wetland soils beyond the transition zone where storage is not assumed to be a function of pond water level. Changes in water levels at the wells can be related to ΔS with the application of an apparent specific yield shown in the following equation:

$$\Delta S = S_{ya}*\Delta h$$

where ΔS is the change in storage within a wetland soil column (cm), S_{ya} is the apparent specific yield (dimensionless), and Δh is the change in water level (cm). The S_{ya} of the thick organic layer that is necessary for storage calculations in the wetland soils is always less than the specific yield, which is calculated

$$S_y = n - S_r$$

where S_y is the specific yield, n is the porosity and S_r is the specific retention (all parameters are dimensionless). The laboratory analysis of the organic mat surrounding the two ponds is summarized in Table I.

Table I. Results of laboratory analysis of organic mat soil samples.

Sample	Porosity	Specific Retention
1	0.866	0.576
2	0.819	0.572
3	0.875	0.547

The porosity values produced from the analysis are similar to published values for organic mats (Kane et al. 1978; Roulet 1991; Wessel and Rouse 1994). The data displayed in Table I indicate a S_y of approximately 0.3. The S_{ya} of 0.1 used by Glen and Woo (1997) and Rovansek (1994) is prescribed for this analysis and satisfies the requirement previously stated.

6. Results and Discussion

Cumulative evapotranspirtation (ET) from the three terrain types were calculated using the Priestley-Taylor (PT) model. The PT model was calibrated to the specific site conditions with aid of the Bowen ratio-energy balance (BREB) method. By plotting the actual latent heat LE calculated from the BREB method (LE_{BREB}) versus the equilibrium latent heat (LE_{EQ}), the slope of the best-fit line is approximately equal to an appropriate alpha value required in the PT model. The conclusions of previous studies specifically identifying the applicability of the BREB method to tundra surfaces support the assumption that the BREB method can produce accurate estimates of actual ET in this application (Wessel and Rouse 1994; Mendez et al. 1998). An important note is the BREB method does not take into account vegetation effects directly but assumes that any evaporative changes due to adaptations of the plants used to maintain minimum moisture requirements are accounted for in the temperature and vapor pressure profiles (Wessel and Rouse 1994).

One-dimensional (1D) water balances were conducted for the upland, wetland, and open water surfaces during the 2001 and 2002 summers. The simplified water balances of the ponds reveal the activity of lateral fluxes both into and out of the pond during periods of heavy rainfall. The accuracy of the ET and ΔS calculations do not allow for the quantification or even the certain identification of drainage through open taliks. Water balances on the wetlands reveal little storage changes, despite large ET – P deficits, indicating obvious lateral inputs, either from the upland slopes or from a nearby pond.

6.1 Site Conditions

The hydrologic conditions at the site were dramatically different during the 2001 and 2002 summers. A number of factors must be considered when comparing the two study seasons, one of which is the severity of the previous winter and the timing of snowmelt. The severity of the winter affects initial ground temperatures and moisture contents, consequentially affecting ground heat flux, frost table dynamics, and storage capacity of the active layer. The timing of spring melt can impact the hydrology by determining when solar radiation can begin depleting water storage through ET. The spring ablation data taken from the tundra slopes in the Council valley during the two winters preceding the field seasons (Sturm 2002) reveal two distinctly different spring melt conditions. The combination of mild air temperatures and a larger snow pack in the 2000-2001 winter resulted in an incomplete freezing of the active layer in many locations throughout the site, especially in the wetland areas where high water contents result in large latent heat sinks. Snowmelt was completed two weeks earlier in 2002 than in 2001, resulting in a two-week “head start” in the drying of the site, thus contributing to lower water levels at the beginning of the field season in June of the 2002.

This study focuses on the snow-free period; therefore, the summer climatic data is more relevant to this study than average annual data. The long-term average monthly temperature and precipitation data, as well as the data from the two field seasons are summarized in tables II and III (Western Regional Climate Center). The data from Nome compared to data collected from the study site reveal a notable climatic difference between the two locations, but are still useful in comparing the individual years with the long-term average. The 2001 summer can generally be described as typical, but the 2002 summer was warmer and dryer than average with an exceptionally dry June and August, followed by a very rainy September.

Table II. Monthly air temperature data (˚C) from Nome and the study site.

	June	July	August	September
LTA*	7.95	10.67	9.88	5.79
2001[1]	7.04	9.08	8.92	5.74
2001[2]	10.88	10.72	9.52	5.53
2002[1]	9.29	11.13	8.78	6.00
2002[2]	11.13	12.26	9.69	5.14

* Long-term Average recorded at Nome (Western Regional Climate Center 1949-2001)

[1] Recorded at Nome

[2] Measured at the study site

Table III. Rainfall data (mm) from Nome and the study site. The 2002 summer was exceptionally dry prior to the very wet September 2002.

	June	July	August	September
LTA*	26.9	56.1	85.3	64.0
2001[1]	29.7	54.6	80.3	18.5
2001[2]	NA	64.8	69.5	26.5
2002[1]	7.6	38.6	15.7	75.4
2002[2]	5.2	44.0	18.3	109.0

* Long-term Average recorded at Nome (Western Regional Climate Center 1949-2001)

[1] Recorded at Nome

[2] Measured at the study site

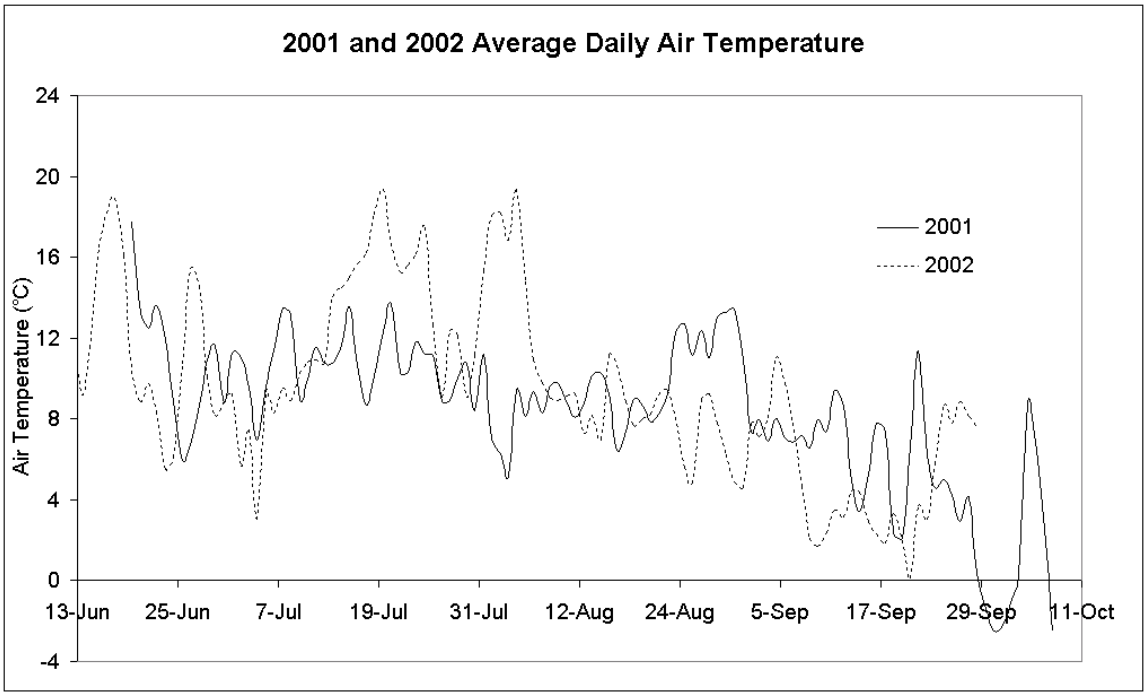

Figure 14. Average daily air temperature. The data reveal a much warmer July in 2002 than 2001.

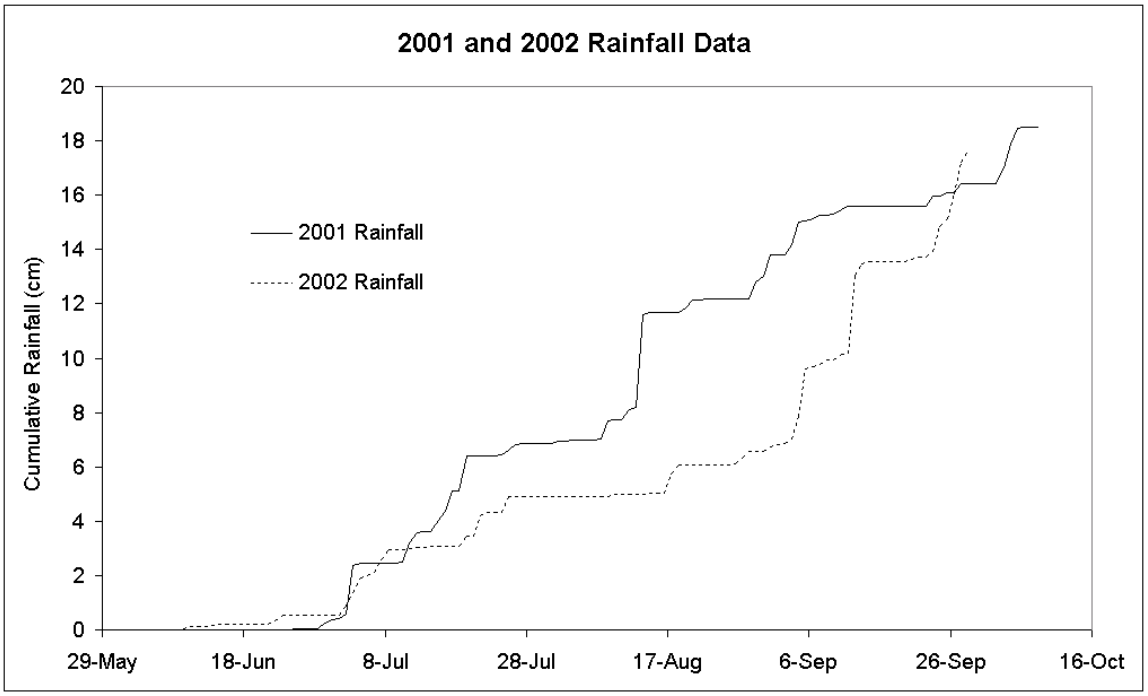

Figure 15. Cumulative rainfall. The cumulative rainfall in 2001 was almost twice that of 2002 in late August, prior to the heavy rains in September 2002.

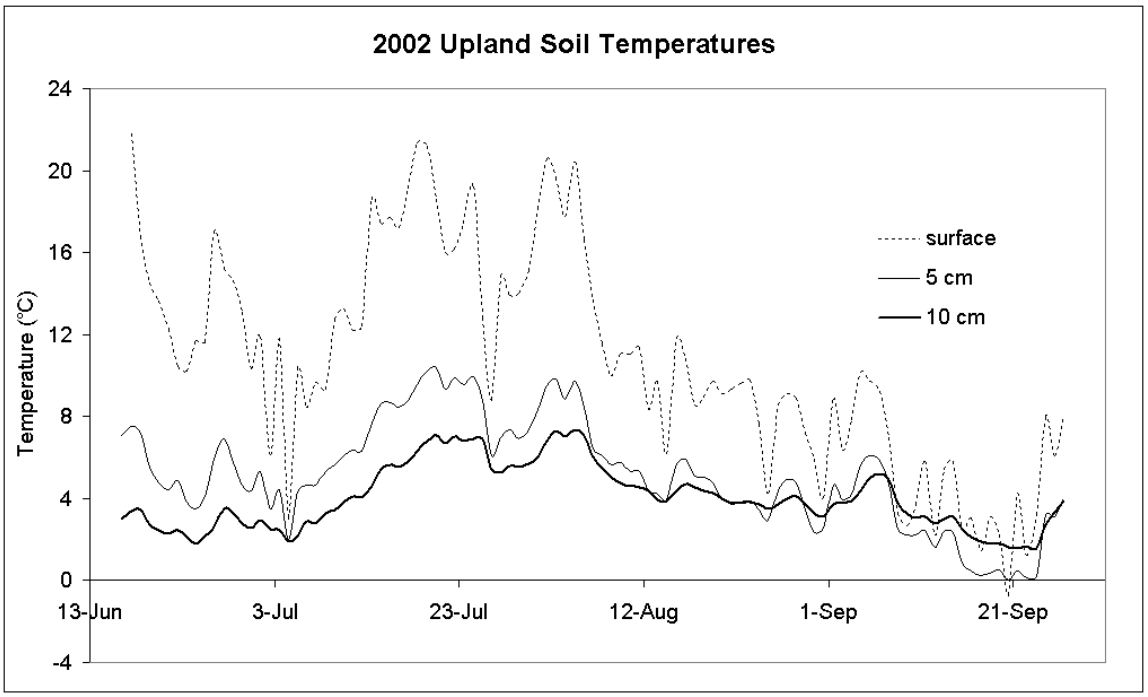

Figure 16. Ground temperatures from the upland soil pit. The data show average daily temperatures exceeding 20˚C.

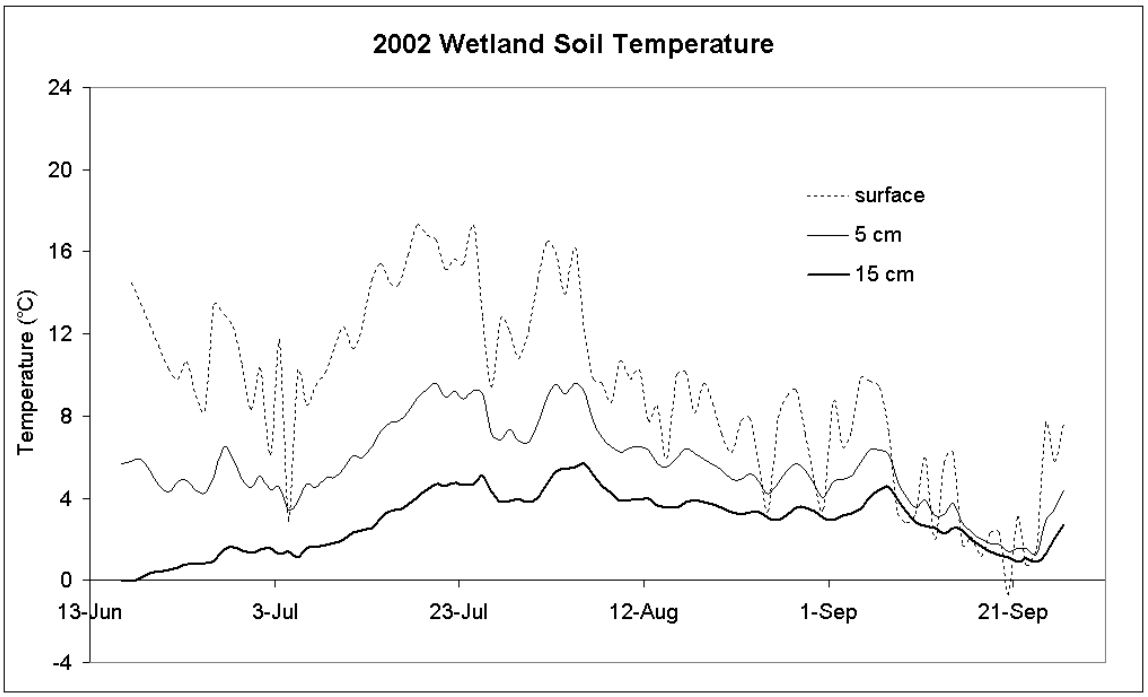

Figure 17. Ground temperatures from the wetland soil pit. Temperatures in the wetlands were slightly cooler than in the uplands.

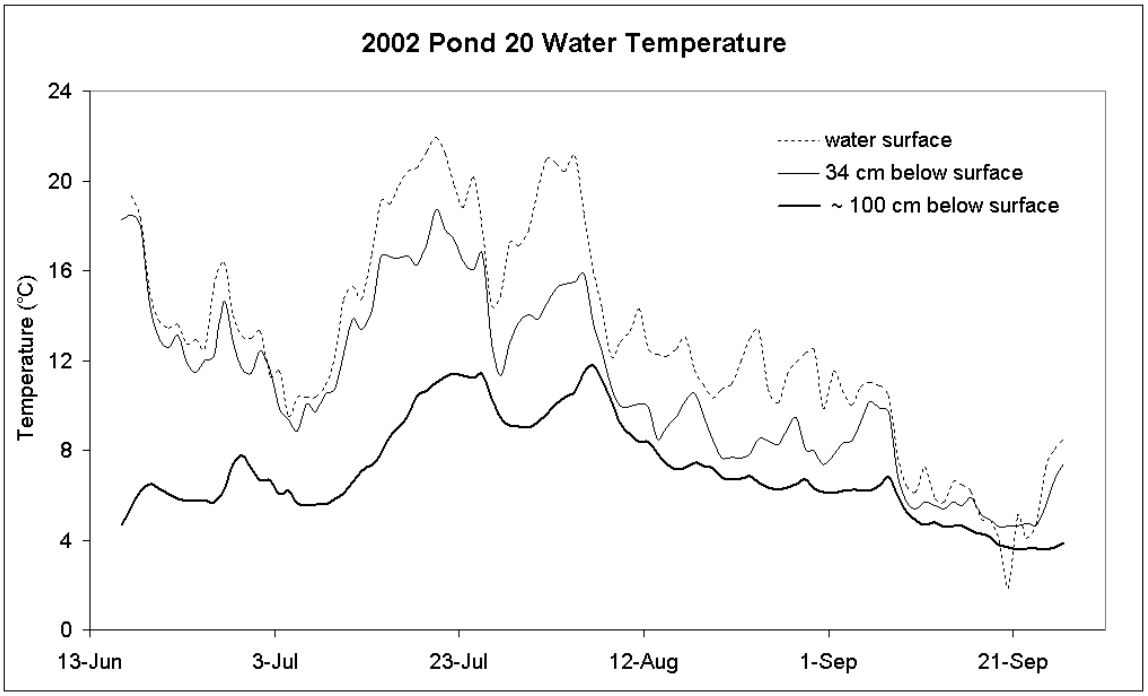

Figure 18. Water temperatures from Pond 20. The data suggest significant thermal stratification, contrary to generalizations about small shallow ponds.

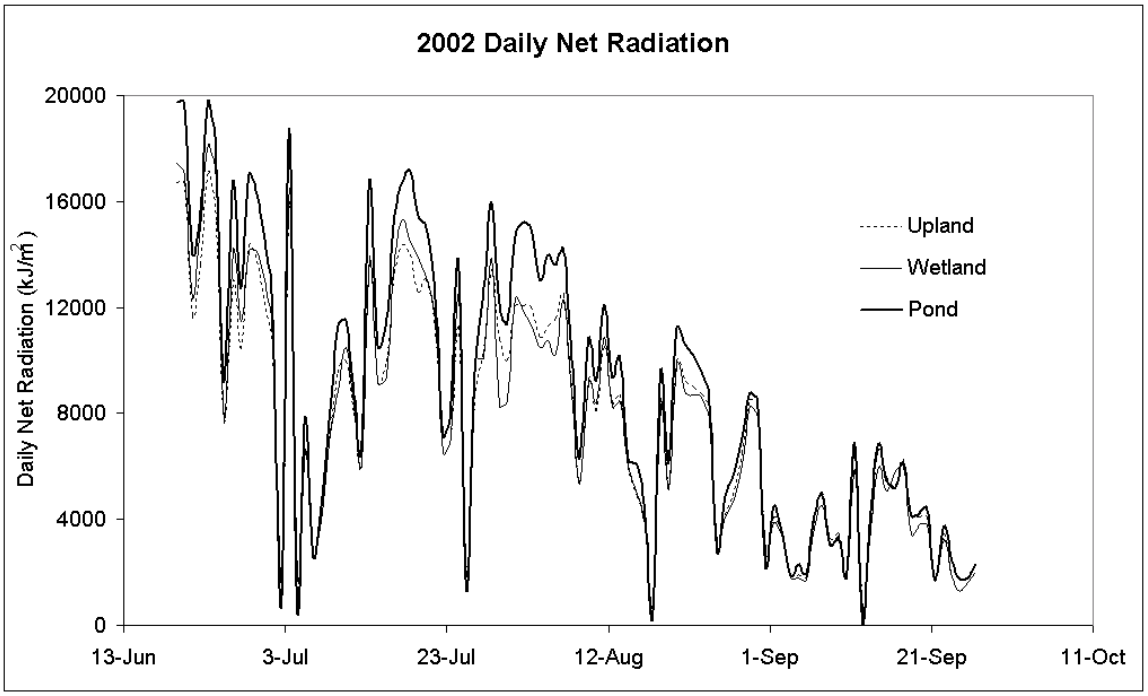

Figure 19. Net radiation from the three surface types. Net radiation from the ponds is greater than the wetlands, which is in turn greater than the uplands.

Figures 16 and 17 show soil temperatures necessary for ground heat flux calculations for the upland and wetland surfaces. The data shown are average daily temperatures, but diurnal temperature data (not shown here) indicate upland surface temperatures exceeding 40˚C on hotter days, while the wetland surface remained cooler, approaching only 30˚C as a maximum. Temperature data from the two lower thermistors in both pits are not shown because they were not used in ground heat flux calculations. Figure 18 shows temperature data obtained from the thermistors in Pond 20. The data indicate thermal stratification, contrary to generalizations about small shallow ponds. Net radiation was consistently greater over the pond than over the uplands and wetlands. The net radiation data or each surface type for the 2002 summer are shown in figure 19.

The pressure transducer in Pond 20 allowed for a continuous water level record of Pond 20 only after a calibration curve was developed relating manual stage measurements to continuous pressure transducer data. The number of points used in the calibration curve are limited by the infrequent site visits; only two manual stages measurements were recorded for the 2001 summer and eight valid measurements were made during the 2002 summer. The pressure transducer shifted on two occasions: one somewhere during the 2001-2002 winter, and the other after a site visit on August 5, 2002, the latter creating a 12-day gap in the continuous water level record. The calibration curve including the adjustments for the pressure transducer shifts is shown in figure 20, and the stage of Pond 20 throughout both summers is shown in figure 21. The pressure transducer data from Pond 18 were bad due to complications with the loggers' power source, and as a result, there are no continuous water level data for Pond 18.

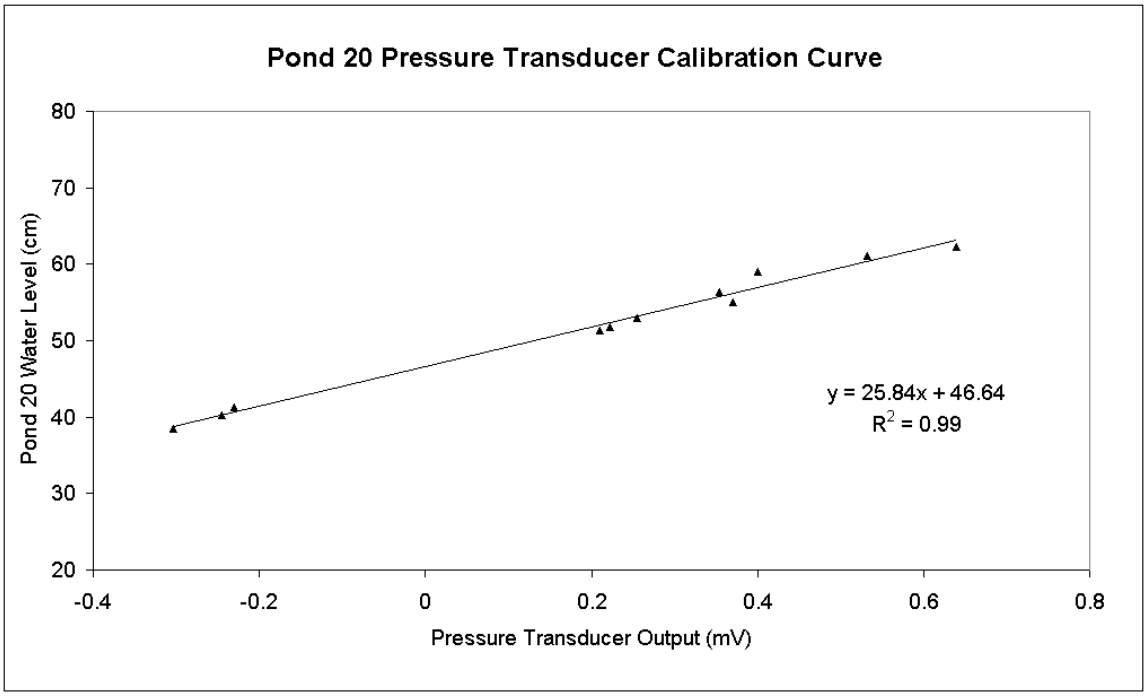

Figure 20. Calibration curve for Pond 20 water level.

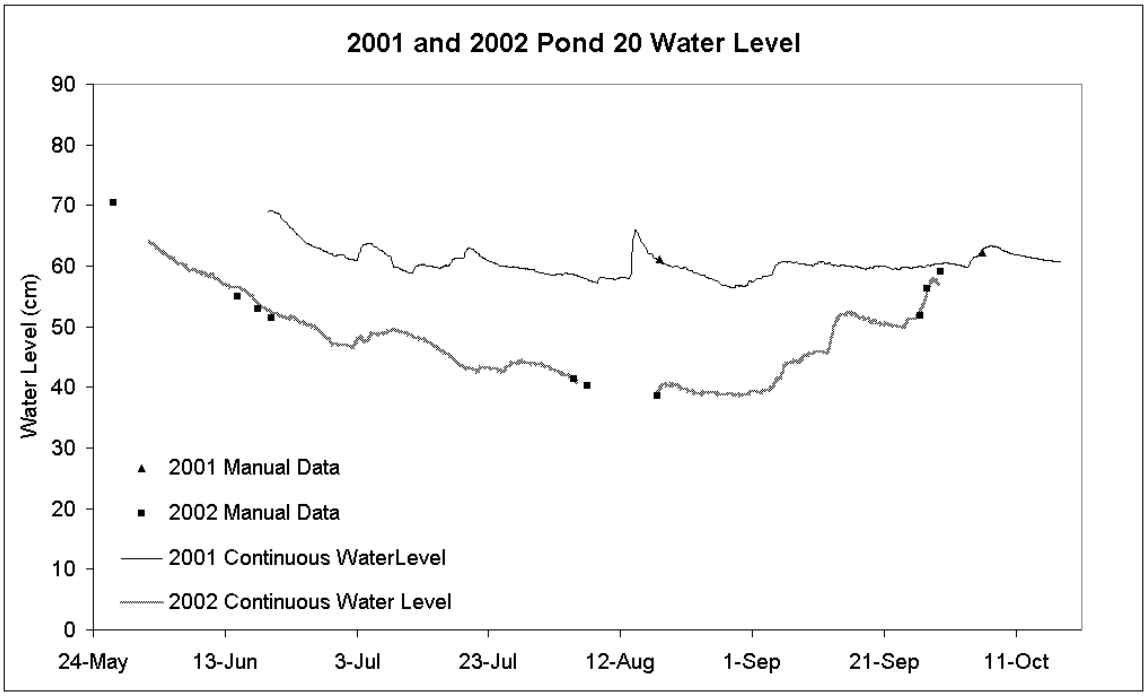

Figure 21. Pond 20 water level. Continuous water level data from Pond 20 show the drastically lower water levels for the majority of the 2002 season.

Manual water level data in the shallow wells were obtained during the four site visits in 2001 and the three site visits in 2002. The behavior of the water table at the different wells was not always consistent; this may be a result of differences in the actual soil profiles or variations in local microtopography. Examples of the latter include such discrepancies as whether the well is located in the center of a marshy channel or closer towards the banks, or perhaps if the well is located on a mossy patch versus a grassier area. A glance at the average water level dynamics in the active layer can be obtained by grouping the wells based on their general location (upland or wetland). Figures 22 and 23 show the average water level and frost table depth with respect to the ground surface for the two surface types for both field seasons.

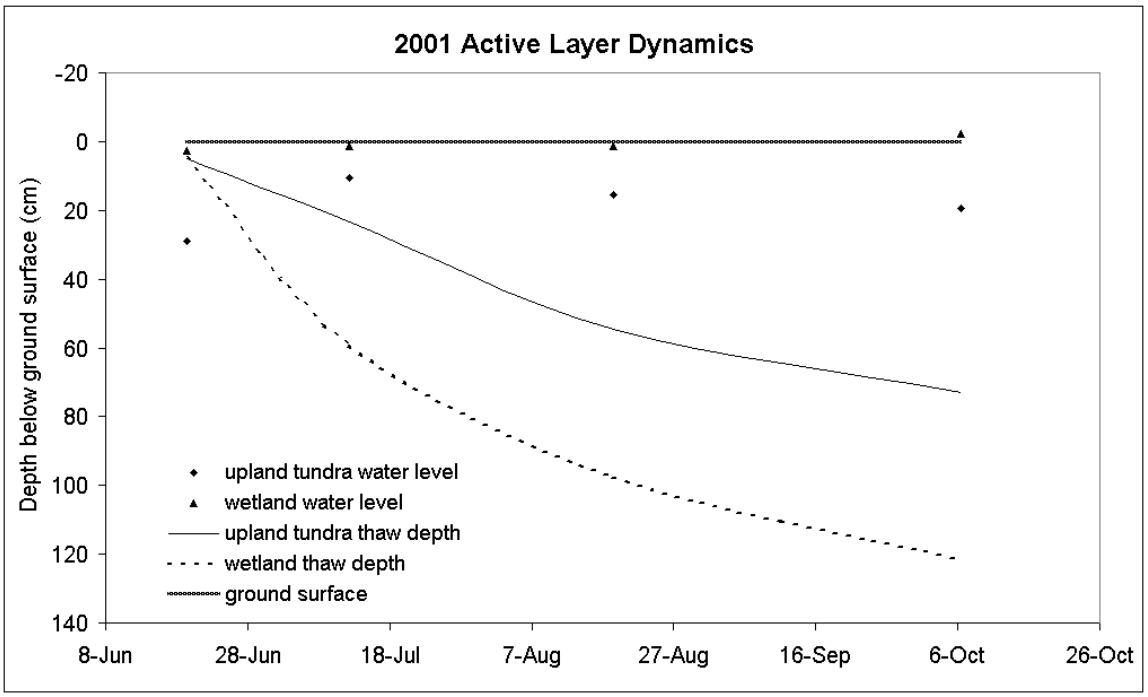

Figure 22. Active layer dynamics for 2001. Water levels were relatively similar upon each site visit in 2001, with the wetland maintaining water levels near the surface and the upland water level remaining below the organic/mineral horizon.

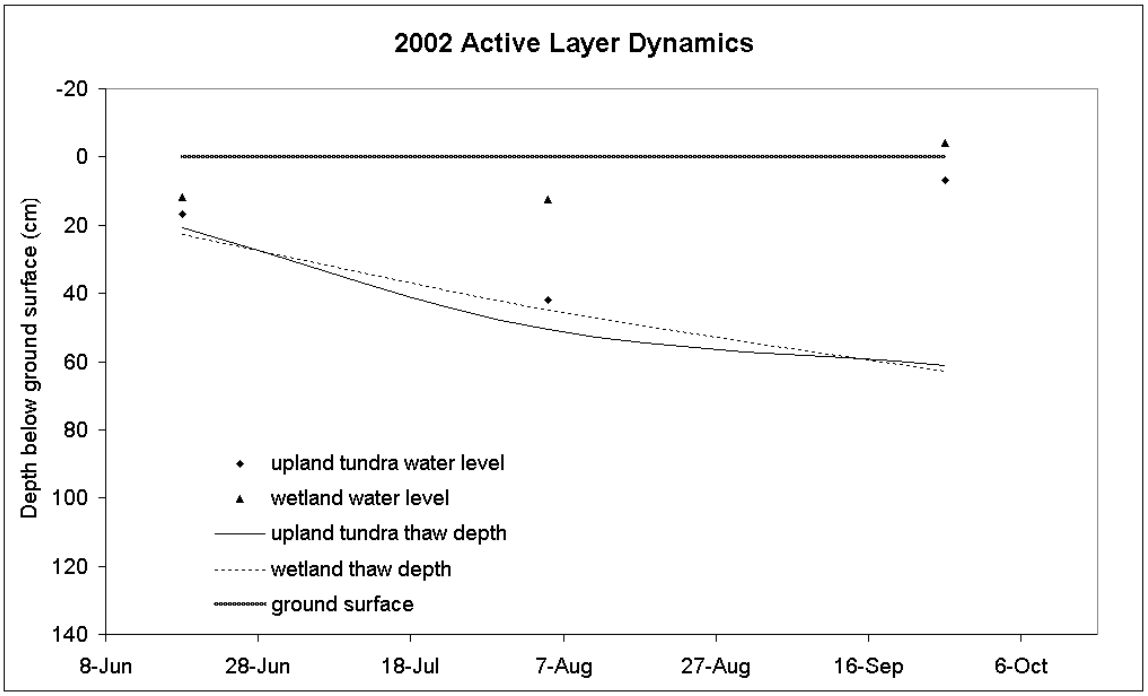

Figure 23. Active layer dynamics for 2002. Water levels in 2002 were consistently lower than water levels in 2001.

In the wetland areas, water remained near the ground surface for the majority of both growing seasons. Many large puddles persisted throughout the growing season in various areas within the wetlands, except for the middle of the anomalously dry 2002 summer where the average water level in the wetland wells was 10 cm below the ground surface. Even at its driest, the vegetation in the wetlands remained quite moist at the surface. After rainy periods, standing water was present throughout the majority of the wetland areas, and standing water could be found in rills and depressions on the upland tundra surfaces. Surface runoff was only observed during the heavy rains in late September 2002 in the narrow channel draining Pond 20 and in the outlet channel that drains the entire site. At both of these locations, the noticeable flow was concentrated in micro-channels of less-dense sedges, often around the perimeter of sphagnum moss patches.

Inside the each of the nested wells in the ponds were pressure transducers connected to Hobo data recorders, but none of them produced useful data as a result of a malfunction with the recorders. For this reason, continuous data describing water levels in these wells throughout the two summers is nonexistent. Only one water level measurement was made for each nested well pair during the 2001 summer. More complications with the nested well pairs arose in early 2003 with the presence of ice slightly below the pond bottom in each well. The ice plugs persisted throughout the summer often interfering or obstructing manual water level measurements.

The manual data collected on October 6, 2001 indicate the absence of a vertical gradient beneath Pond 20, and the presence of a downward vertical gradient beneath Pond 18 of 0.25 m/m from the bottom of the pond to the shallow well located 1.59 m below the pond bottom, and a gradient of 0.086 m/m from the shallow well to the deep well at 3.69 m below the ground surface. In both ponds during 2002, the water level inside the deep wells remained at or below the ice plug, except for after intense rains in late September when the water level in the deep well in Pond 20 rose 31 cm above the ice plug to a depth 89 cm below the surface. This sole emergence of water above the ice plug in the deep well suggest that the ice plugs did not prohibit water movement, and that the actual hydraulic head (evident as the water level in non-pressurized conditions) is below the ice plug throughout the 2002 growing season in both ponds. This would imply that a downward hydraulic gradient was present in the open talik throughout the summer, which was the case for other thermokarst ponds in the area studied by Yoshikawa and Hinzman (2003). In Pond 18, the water level inside the shallow wells also remained below the ice plug, but in Pond 20's shallow well, the water level fluctuated from the ice plug to the Pond water surface. It is possible that the well casing was cracked during the winter, allowing water seepage from above the well screening at the bottom of the well.

6.2 Evapotranspiration

Daily ET is modeled with the PT model after calibration by use of the BREB method. Before ET rates are calculated, the PT model requires an estimate of the amount of heat conducted into the soil (G), and in the case of the ponds, the change in heat storage within the ponds (S). The accurate estimation of G is required to ensure accurate approximations of latent heat fluxes. The ratio of ground heat flux to net radiation (G/Q*) is of considerable importance in the PT model, being almost as influential as the alpha term. Fortunately, the available energy term (Q* - G) has little effect in the LE/LE_{EQ} relationship as described in the methods section; therefore, any error associated with the estimation of G is not compounded in the alpha-determining analyses.

Figure 24 shows the ground heat flux calculations for the upland surfaces compiled in three-hour time intervals. The amplitude of the diurnal oscillations for the upland surfaces is similar to published results, along with the trend of decreasing heat flux with increasing depth (Hinzman et al. 1991). Figure 25 shows the ground heat flux for the wetland surfaces. The diurnal oscillation of G for the wetland surfaces is larger than that of the uplands. McFadden et al. (1998) also found this to be the case in the Alaskan Arctic. The accuracy of thermal conductivity K estimates directly affects G, and without laboratory analysis of the soils at the site, previous studies are the only means of justification. The average K values of 0.32 and 0.41 W/m^2 as applied in the model match well with published results for upland and wetland surface respectively (Hinzman et al. 1991; Hinzman et al. 1998).

Figure 26 shows the changes in heat storage within Pond 20. The large day-to-day changes in heat storage, along with a long-term average approaching zero, precisely matches the description of previous studies. Ground heat flux through

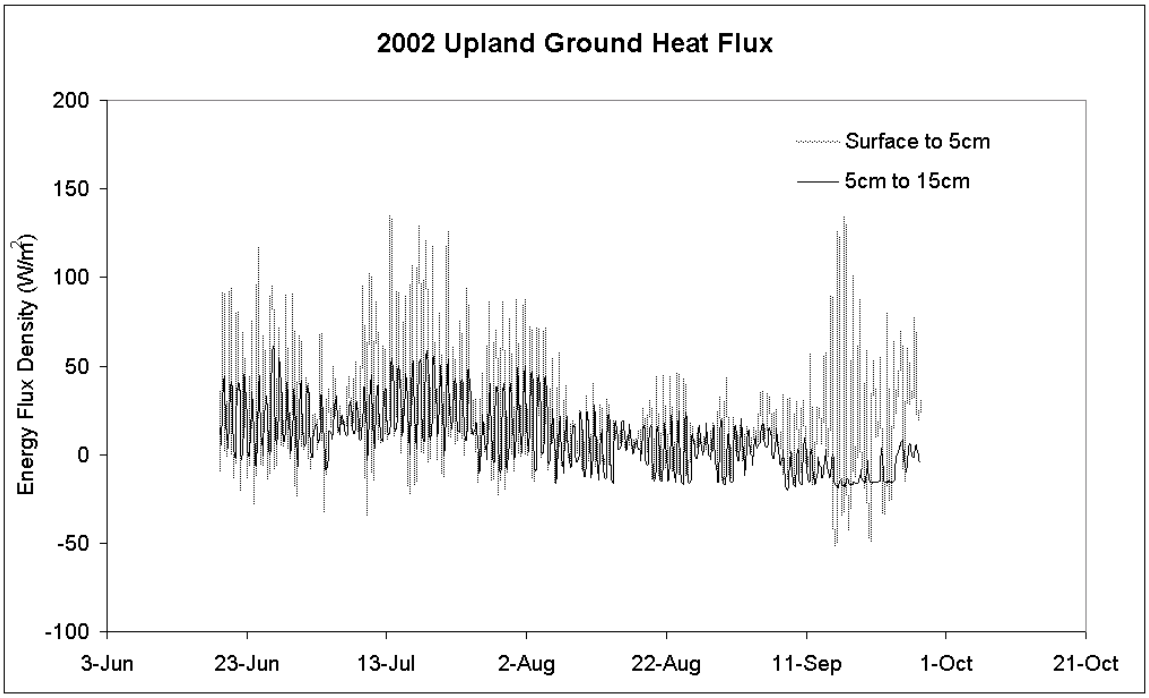

Figure 24. Ground heat flux for upland surfaces.

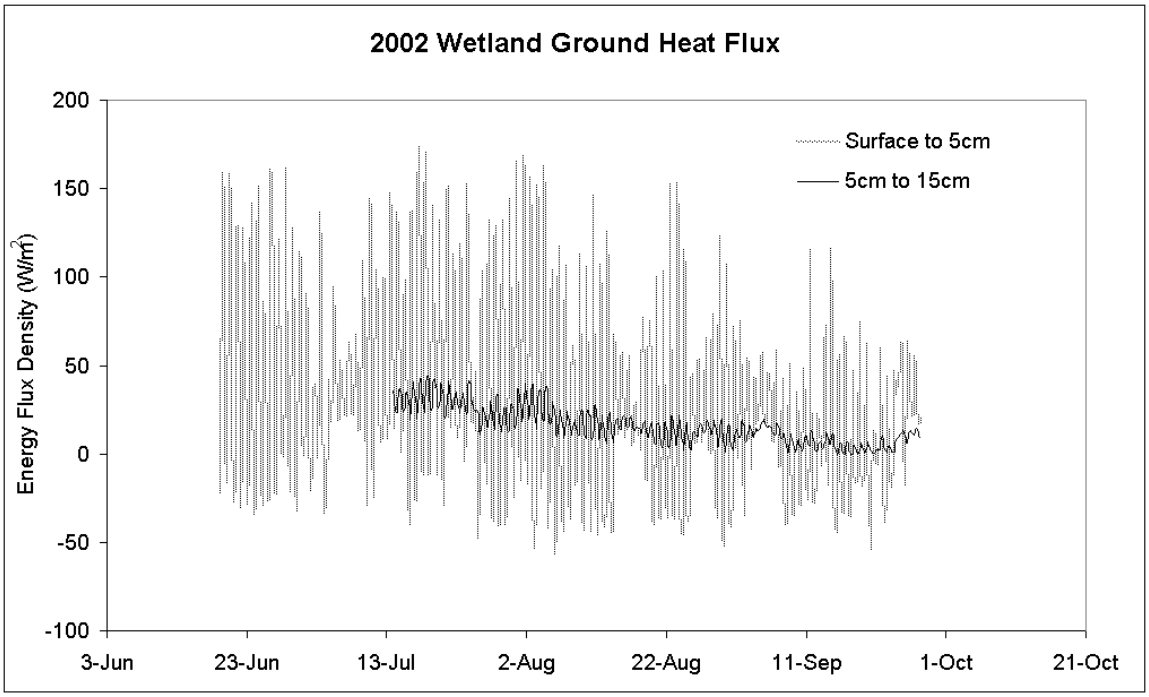

Figure 25. Ground heat flux for wetland surfaces. The data show large diurnal oscillations in the upper soil layer but not in the lower soil layer.

the bottom of the pond was not estimated, and the magnitude of this term is debatable. Mendez (1997) concluded that G_s accounted for 11% of the summer Q* over a pond on the Arctic Coastal Plain of Alaska. Stewart and Rouse (1976b estimated G to account for 25% of Q* in a sub-arctic shallow subarctic lake, essentially all of which was due to G_s. Contrariwise, other sources conclude that G_s is negligible (Woo 1980; Roulet and Woo 1986c; Stannard and Rosenberry 1991). Because G_s was not calculated in this study, the possibility of G accounting for the wide range of 0-25% is investigated.

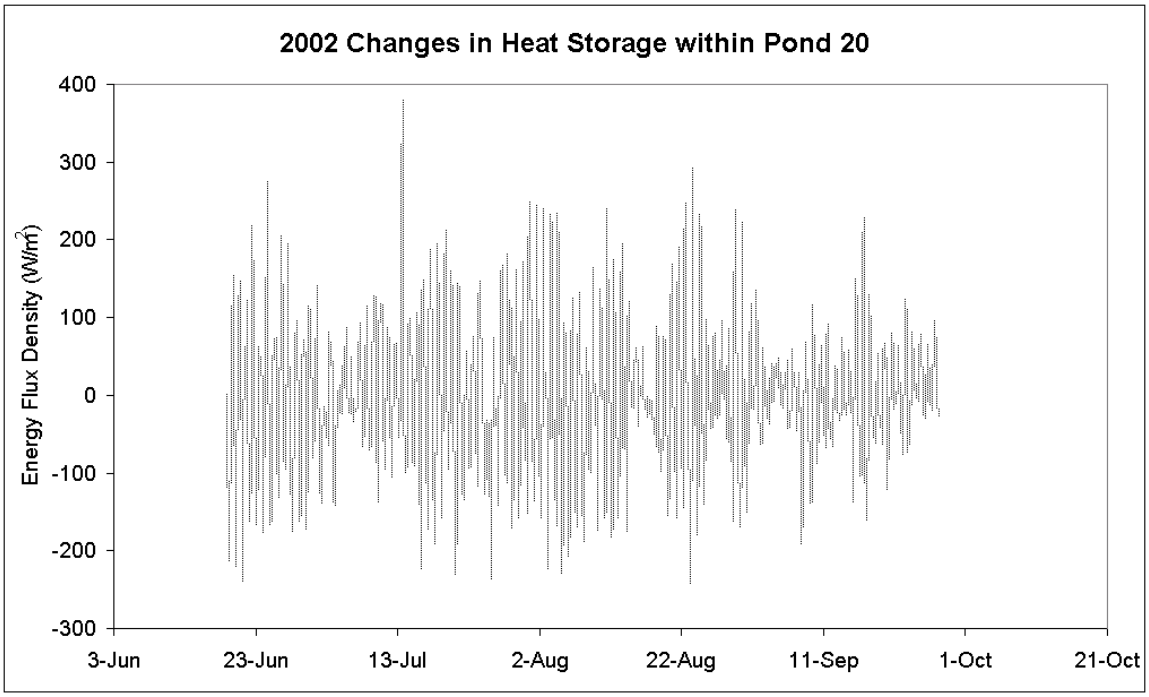

Figure 26. Changes in heat storage within Pond 20. The day-to-day changes in heat storage are large but the cumulative energy approaches zero.

Although temporal and spatial variability prevent the direct comparison of energy fluxes with results from other studies, the energy partitioning can be assumed to be more constant, and therefore the ratios of LE/Q* and G/Q* provide a more useful parameter for comparison (Beringer et al. 2003a). The results of the ground heat flux analysis, presented as fractions of net radiation, are shown in

table IV. During the 2002 summer, ground heat flux averaged 23.8% of the daily net radiation for the upland surfaces, which is on the high end of typical values for similar surfaces. Similar to Rovansek's (1994) estimate of 12%, Beringer et al. (2003a) calculated G to account for 10.4% of daily net radiation for a tussock tundra surface in the Council valley. On the north slope of the Brooks Range, Kane et al (1990) said G accounts for 15% to 17% of summer net radiation on tussock tundra slopes. Mendez (1997) estimated G from upland tundra surfaces at his site on the Arctic Coastal Plain of Alaska to be 25.3% of net radiation.

Table IV. Summary of G as a fraction of net radiation for each surface type.

	Upland	**Wetland**	**Pond**
June	0.213	0.321	-0.014
July	0.315	0.383	0.015
August	0.15	0.241	-0.036
September	0.274	0.252	-0.017
Average	0.238	0.312	-0.01
Confidence in Methods	medium	low	?????
Typical Values	0.10 - 0.25	0.15 - 0.20	0 - 0.25

Ground heat flux from wetland surfaces averaged 31.2% of the net radiation. Mendez estimated wetland ground heat losses to be 16.4% of the net radiation, and McFadden et al. (1998) estimated daily G/Q* for a similar wetland site to approach 15%. At a subarctic sedge fen, Rouse (2000) describes G/Q* decreasing from 37% in May to 14% in September, averaging 20% for the entire snow-free season. Because the magnitude of G as calculated in this analysis is slightly higher than published values, and because of the large difference between the G estimates from the two upper and lower soil layers create a low level of confidence in the magnitude of this G for wetland surfaces.

Bearing in mind that the magnitude of G has very little affect on the alpha-determining analysis, the modeled results previously discussed are used in the following analysis, regardless of discrepancies with the literature. Figure 27 shows the LE_{BREB}, calculated using vapor pressure and temperature gradients from the ground surface to 3 m, versus the LE_{EQ} for the upland tundra surface.

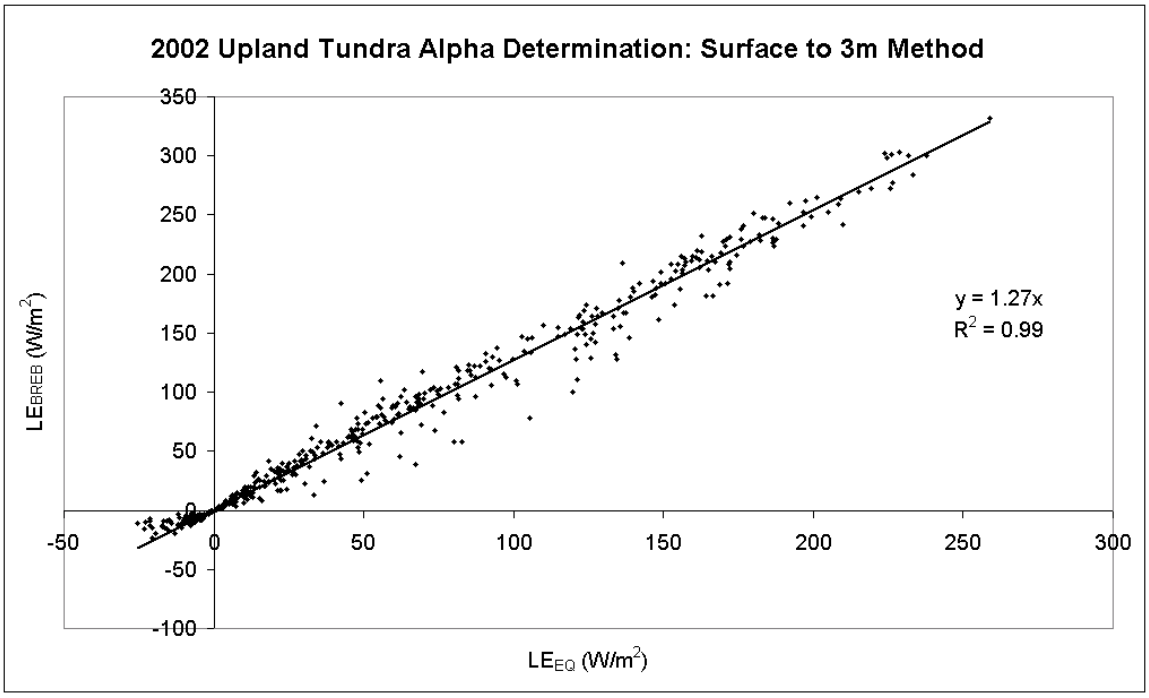

Figure 27. Upland alpha-determining relationship. The slope of the best-fit line suggests an alpha value of 1.27.

The data indicates an alpha value of 1.27. This value is unreasonably high for tundra, practically equivalent to the alpha value of 1.26 almost universally prescribed as the lower limit for surfaces with unlimited water supply (Lafleur et al. 1987; Rouse et al. 1977). This was certainly not the case during the anomalously dry 2002 summer. Published values for tussock tundra are consistently less than 1.0, with 0.95 being a frequently used estimate (Kane et al. 1990). Eichinger et al. (1996) suggest that an alpha value is always less than 1.0 for hot and dry surfaces.

The high alpha value produced in this analysis suggests that the LE_{BREB} was overestimated. A likely cause of this is the use of moisture conditions at 5 cm below the ground surface to describe moisture conditions at the surface. This simplification results in a higher vapor pressure gradient, in turn resulting in a lower Bowen ratio, which signifies higher partitioning of the total energy into latent heat. This is demonstrated by a synthesized reduction of moisture conditions by 50% and the resulting reduction in alpha value from 1.27 to 0.97 (an exercise intended only to support the discussion and not for modeling application).

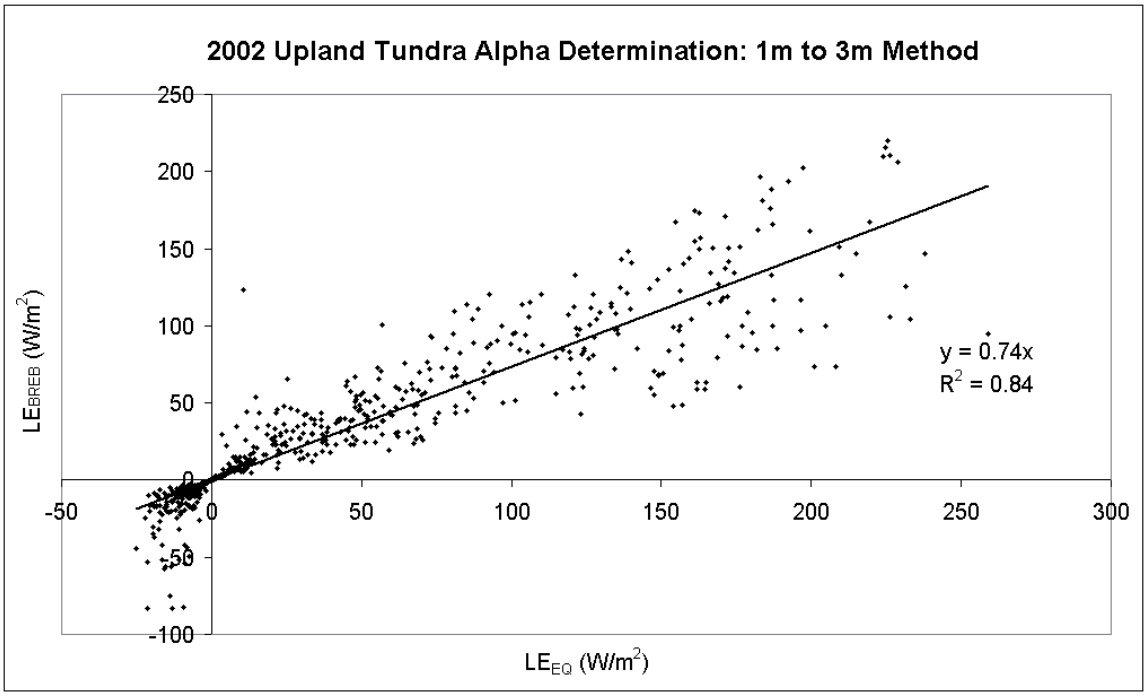

Figure 28. Alpha-determining relationship from 1 m to 3 m. The BREB method from the two heights above the surface produces a lower R^2 value than from the surface-to-3m method, but produces a more reasonable alpha value of 0.74.

Another method to check the alpha value for the upland tundra slope is the BREB method applied at the two heights above the ground surface. Because the tower is located on the uplands but only a few meters from the upland/wetland

boundary, the temperature and moisture gradients measured at the tower may not represent the upland energy fluxes only; they may be a composite of wetland and upland surfaces. Figure 28 shows the comparison of LE_{BREB} estimated using the BREB method from 1 m to 3 m on the tower to the LE_{EQ}. The data indicates an alpha value of 0.74, which is similar to the alpha value of 0.73 used in the PT model fit to the 2000 eddy correlation LE measurements (Beringer et al. 2003b).

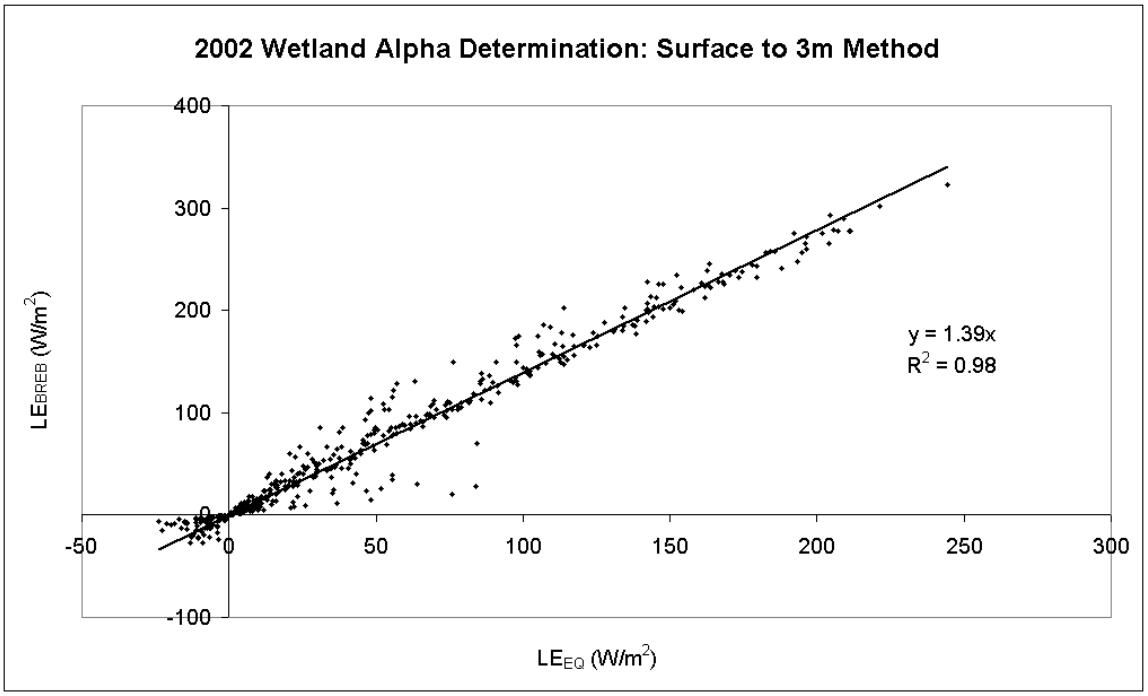

Figure 29. Wetland alpha-determining relationship. The data supports an alpha value of 1.39 for wetlands surfaces.

An alpha value of 1.39 for wetland surface was based on the plot shown in figure 29. This value is completely reasonable. This alpha value is greater than 1.26 often suggested as the lower limit for open water or surfaces with unlimited moisture supply. Rouse (1998) describes seven years of daily ET data from a subarctic sedge fen, similar to the Council site, is best modeled by the PT model with an alpha value of 1.34, the same value used by Quinton and Roulet (1998)

for the subarctic wetland in their study. Roulet and Woo (1986 a and c) described ET for a Northern Canada wetland site to be best described by alpha values of 1.3 and 1.6 for flooded and non-flooded conditions, respectively. Rovansek (1994) used alpha values of 1.6, 1.3, and 1.1 to represent the trend of decreasing evaporation over the coarse of a summer for wetland surfaces on the Arctic Coastal Plain. Mendez et al. (1998) used two alpha values (1.15 and 1.1) for the same purpose at the same site but during different years.

Contrary to the high alpha values and ET rates associated with wetlands, the tendency of wetland vegetation to revert to minimal transpiration rates to conserve water during dry periods is commonly cited (Rouse 1998; Roulet and Woo 1986c). McFadden et al. (1998) calculated an LE/LE_{EQ} value for a wet sedge meadow to be only 0.86 while the tussock tundra surface produced an average LE/LE_{EQ} value of 0.73, which is similar to the results from this and Beringer et al.'s study in the Council valley. The usefulness of the BREB method calculated from the surface to some height above the surface, as opposed to being measured between two heights above the surface, is questionable when such biologic factors are likely quite active and influential. Because of this suspicion, the PT model as applied in the water balance calculations must include a conservative estimate using the results of the 1m-to-3m method for both upland and wetlands surfaces.

For the pond surfaces, an alpha value of 1.49 is indicated in figure 30. Bello and Smith (1990) cite an average "summer" alpha value of 1.35 for a shallow lake in Hudson Bay Lowlands, with daily alpha values ranging from 1.0 to 2.0. They also related alpha to general climatic conditions with alpha equal to 1.80, 1.36, and 1.17 for sunny days, cloudy days, and rain and evenings respectively. Mendez et al. (1998) used an alpha value of 1.5 for small ponds on the Arctic Coastal Plain. Using the water balance method to calibrate the PT model,

Rovansek (1994) calculated alpha values of 1.9 and 2.0 for the ponds during the two years of his study.

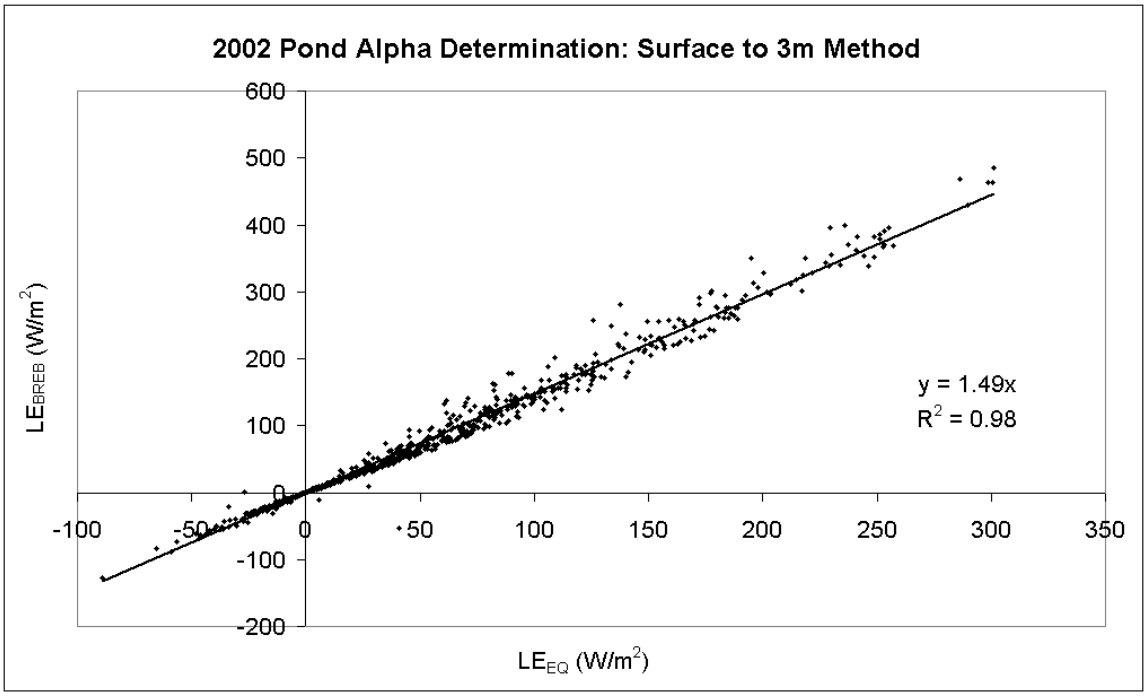

Figure 30. Pond alpha-determining relationship. The data supports an alpha value of 1.49.

The common occurance of alpha values for small lakes to be significantly greater than the standard 1.26 commonly associated with unlimited evaporability is explained by local advective effects from the surrounding relatively hot and dry tundra surfaces (Bello and Smith 1990). Because the BREB method is based on a simplified energy balance where advective heat flux is disregarded (because it is assumed to be negligible), it is possible that the application of these methods, in a situation where local heat advection is possibly significant, could result in inaccurate actual latent heat estimates and, consequentially, a skewed alpha estimate (Guo and Schuepp 1994). However, because the pond alpha value produced in this analysis is quite reasonable, it is assumed that these methods are satisfactory.

Table V summarizes the results of the alpha determining analyses. The table also shows a level of confidence in the methods for each surface type, as well as typical ranges of alpha values for similar surfaces as cited in the literature. Where confidence in the methods is low, minimum and maximum alpha values from the literature are chosen for the proceeding water balance analysis.

Table V. Summary of alpha values chosen for each surface type.

	Upland	**Upland**	**Wetland**	**Pond**
	1m to 3m	Surface to 3m	Surface to 3m	Surface to 3m
alpha	0.74	1.27	1.39	1.49
Confidence in Methods	High	Low	Medium	High
Typical Values	0.73 - 0.96	0.73 - 0.96	1.1 - 1.6	1.26 - 2.0

The final calculations of cumulative ET for the three surfaces are presented as a minimum and maximum, the two corresponding to either to maximum and minimum G/Q* estimates or minimum and maximum alpha estimates or a combination of the two. The chosen parameters are based on a combination of the results of this analysis and the results of published studies. Table VI summarizes the parameters used to calculate the latent heat consumed by ET.

Table VI. Summary of parameters used in the final ET calculations.

	Upland ET		**Wetland ET**		**Pond ET**	
	minimum	maximum	minimum	maximum	minimum	maximum
alpha	0.74	0.95	0.74	1.39	1.49	1.49
G/Q*	23.8%	10%	20%	15%	25%	10%
LE/Q*	29%	45%	38%	62%	59%	71%

Kane et al. (1990) calculated latent heat to consume an average of 39%, 46%, and 65% of the net radiation for three consecutive years, demonstrating the high interannual variability possible for an arctic tundra watershed. Beringer et al. (2003a) estimated the upland tundra in their study in the Council valley to lose 38.7% of daily net radiation to ET. Mendez (1996) estimated LE/Q* to be 23.0%, 45.8%, and 56.5% for uplands, wetlands, and ponds respectively. At a subarctic sedge fen, Rouse (2000) describes sensible heat fluxes as only a minor component of the summer energy budget, allowing LE to consume as much as 52% of Q* in May to 77% in September. Stewart and Rouse (1976b) calculated latent heat to consume 55% of net radiation at a small lake. Wessel and Rouse (1994) estimated the LE/Q* from the wetland in their study to range from 57-66%. The possibility of G/Q* in the pond being zero results in unreasonable LE fluxes; a G/Q* value of 10% is a more reasonable estimate to predict maximum pond ET rates.

Latent heat data are used to calculate daily ET and eventually the cumulative ET used in the water balances. A number of authors have compiled pan-arctic study results exploring the range of ET rates calculated for various arctic and sub-arctic surfaces, as well as for other components of the water balance (Mendez et al. 1998; Kane et al. 1992) but the variable nature of these hydrologic processes limit the usefulness of such broad comparisons (Kane et al. 1990; Lafleur 1994). The cumulative ET of each surface is shown in figure 31, and the daily ET rates calculated for each surface type during the 2002 summer are shown in figures 32 through 34. The ET rates produced in this study are well within the range of typical ET values found in the literature. Several authors observed the trend of decreasing ET rates with the transition from ponds to wetlands to uplands (Lafleur 1990; Mendez et al. 1998) as well as the highest ET rates early in the summer and the trend of decreasing ET as the growing season progresses (Kane et al. 1990; Glen and Woo 1997).

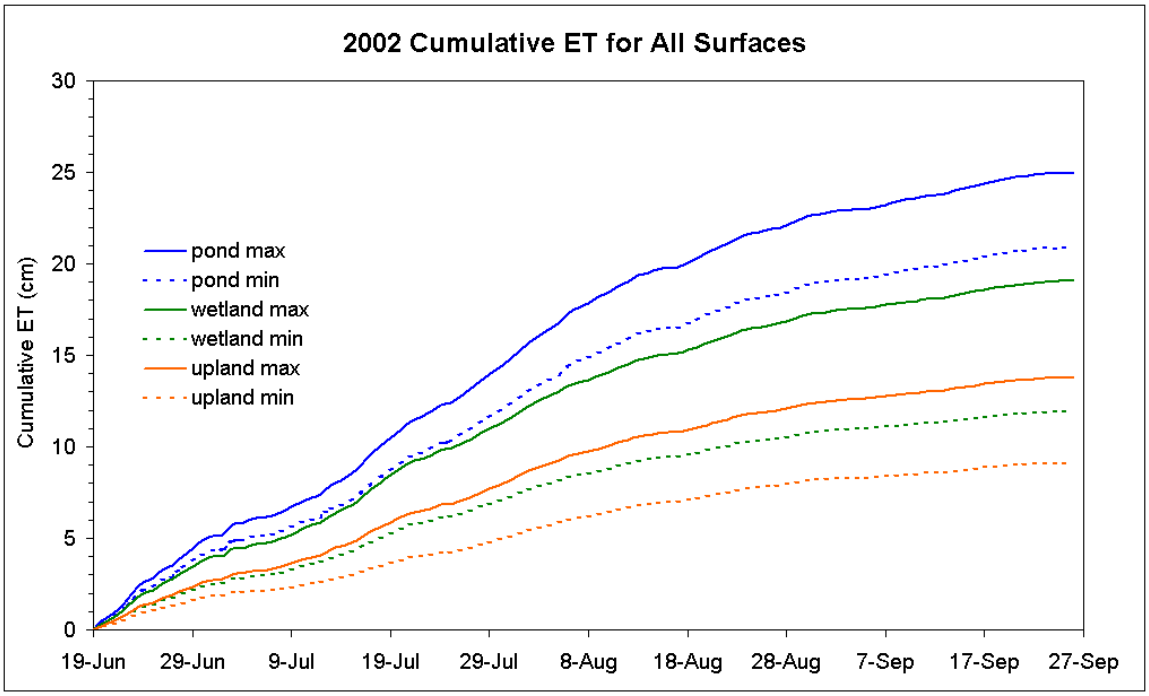

Figure 31. Cumulative minimum and maximum ET for each surface type. The trend of increasing ET from upland to wetland to pond is commonly cited.

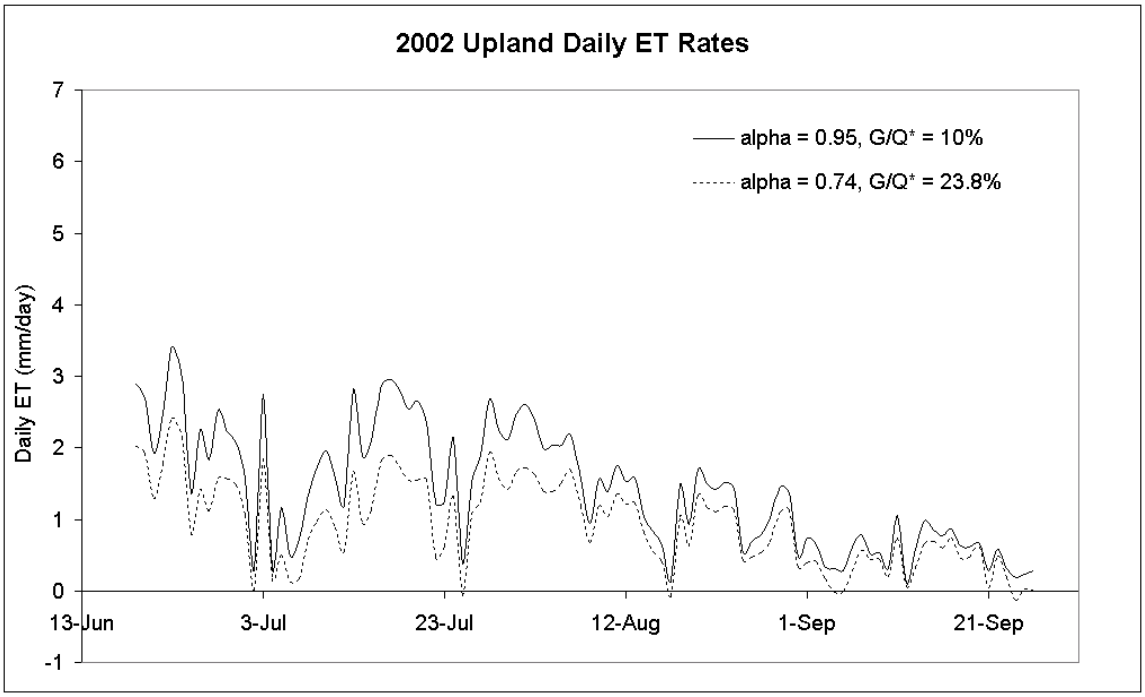

Figure 32. Upland daily ET rates from 2002. ET rates are typically between 1.0 mm/day and 2.5 mm/day.

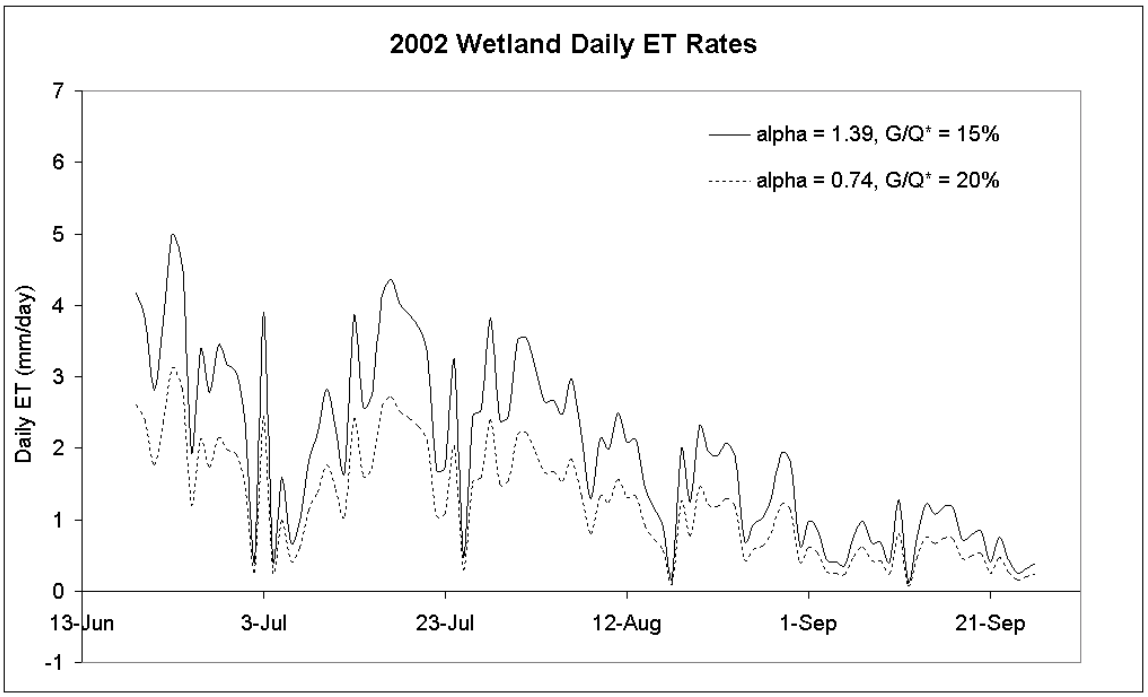

Figure 33. Wetland daily ET rates from 2002.

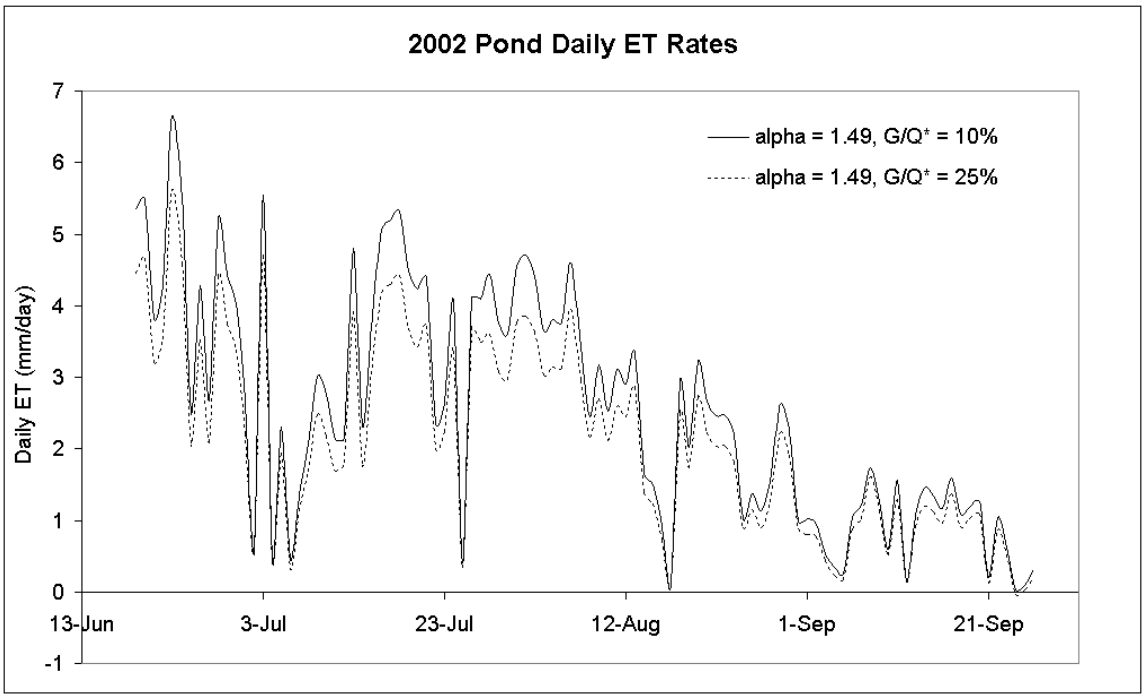

Figure 34. Pond daily ET rates from 2002. ET rates from pond surfaces reach a maximum of greater than 6 mm/day and are typically two or three times larger than the ET rates from the uplands.

6.3 Lateral Fluxes

The survey results revealed a significant margin of error when measuring the relative ground surface and water surface elevations at the wells. This has implications in subsurface flow calculations as well as storage calculations. Discrepancies in measurement consistency were inescapable with the typically saturated ground conditions and spongy peat mat; the soft tundra also created difficulties with keeping the surveying station level. The matter of obtaining accurate ground surface elevations was further complicated by the possibility of a changing ground surface due to the phenomenon of peat swelling and compaction. Changes in the position of the frost table as well as changes in moisture conditions are capable of causing peat mats to swell and compact, causing significant changes in ground surface level (Roulet 1991). These uncertainties create a margin of error of a few centimeters at each well.

The hydraulic gradient in the 3-4 channel away from Pond 20 (see figure 5 on page 10) changed directions on several occasions, indicating a change in flow direction either towards or away from the pond. Rovansek (1994) describes this phenomenon as being a result of the difference in the rates of water table fluctuation in the wetlands as compared to the open water surface. The water level will change more dramatically in the wetlands (approximately at a rate equal to the inverse of the specific yield) and therefore has the potential to fluctuate in a range spanning the water level of the ponds, consequentially reversing the hydraulic gradient. The gradient of the channel was typically towards the pond after significant rainfall events and away from the pond during dryer conditions; the magnitude of the gradient varied between -0.002 and +0.002.

Subsurface flow was calculated for all of the major wetland channels as well as for the upland tundra slope north and west of Pond 20. On the upland tundra

slope, subsurface flowrates varied from zero when water levels in the soil columns were at or near the frost table to 0.11 m^3/day per unit width during near-saturation conditions during the heavy rains of September 2002. If this flux is applied to the upland slopes that drain into the Pond 20 wetland complex, it translates to approximately 30 m^3/day. This flowrate normalized over the wetland complex area is equivalent to 5.5 mm/day, which is similar in magnitude to pond and wetland ET rates. Typical subsurface flowrates from the uplands are roughly a quarter of the maximum calculated rate. Note that these values were calculated between wells 1 and 2, which represent the area of maximum slope for the upland tundra areas; therefore, this is a conservative estimate of the largest possible input from upland slopes during very wet conditions. Subsurface flow in the wetland channels was milder, conveying as much as 2.7 m^3/day and averaging 0.66 m^3/day. When normalized over the entire basin area, this maximum flowrate near the outlet channel is hardly noticeable, at 0.1 mm/day. The maximum discharges into and away from Pond 20 via subsurface flow in the large 3-4 wetland channel were equivalent to 0.7 mm/day and 0.1 mm/day respectively.

While these maximum calculated discharges may contribute a noticeable amount of water to the ponds, they were calculated during periods when surface flow was probable, reducing the subsurface estimates to a fraction of the total lateral flow. Surface flow was observed during the high rains late in September 2002 and was gauged manually using the area-velocity method with a Marsh-McBirney Flo-mate. The number of discharge measurements is not sufficient to generate a hydrograph, which would be useful in estimating certain parameters such as exact basin area and time of concentration, but the magnitude of the surface flowrates relative to the magnitude of subsurface flows is useful in the water balance calculations. Surface flowrates, reaching approximately 850 m^3/day, were more than two orders of magnitude larger than the largest subsurface

flowrate calculated for the wetland channels. This maximum discharge converted to a 1D loss rate over the entire wetland area is approximately 34 mm/day, which is much larger than typical ET rates.

Estimating surface flow is a difficult task when considering the paths that surface flow actually takes through the upland tundra and the marshy channels. When surface flow was observed, it was concentrated in rills and depressions in the upland tundra slopes. In the marshy channels, surface flow was only evident in smaller, irregular channels within the larger, topographically defined channels. Also, small puddles were common at the site, often present for the duration of the summer at some wells and throughout the wetland areas. So measured water above the ground surface at a given well did not necessarily indicate the occurrence of surface flow, and conversely, the absence of water above the ground surface could not ensure the absence of surface flow. The water balance calculations will not include any surface runoff component because the magnitude of this component for individual events is unknown. When the storage deficit of the soils is near zero, it is assumed that surface runoff is probably occurring to some degree.

6.4 Water Balances for the 2002 Field Season

The one-dimensional (1D) water balance applied to a column of soil can be used to both evaluate the assumption of negligible lateral fluxes as well as assess the proficiency of the ET and ΔS estimates. If lateral fluxes are negligible or temporarily inactive, the continuous ET minus rainfall (ET – P) should match the modeled or measured ΔS. Conversely, if the curves do not match, lateral fluxes can be assumed, especially if the incongruity coincides with rainfall events. Figure 35 on the following page shows the 1D water balance for upland soils. The storage of upland soils is described using the soil moisture from the upland soil pit and is fairly balanced with the modeled ET losses combined with inputs

from rainfall events (ET – P), thus supporting the conclusion that the assumption of negligible lateral fluxes is valid for the upland slopes for the 2002 summer prior to the event on September 12. The possibility of lateral flow during the series of smaller events in early July is also worthy of consideration. The 1D model does not appear to work well for the two-week period in late June for reasons unknown. The offset created by this cumulative inaccuracy hides the quality of the model for the remainder of the summer, prior to the heavy rains in September. The ΔS estimates from the manual data match those calculated from soil moisture data well; the error bars indicate the minimum and maximum storage change experienced in any one well.

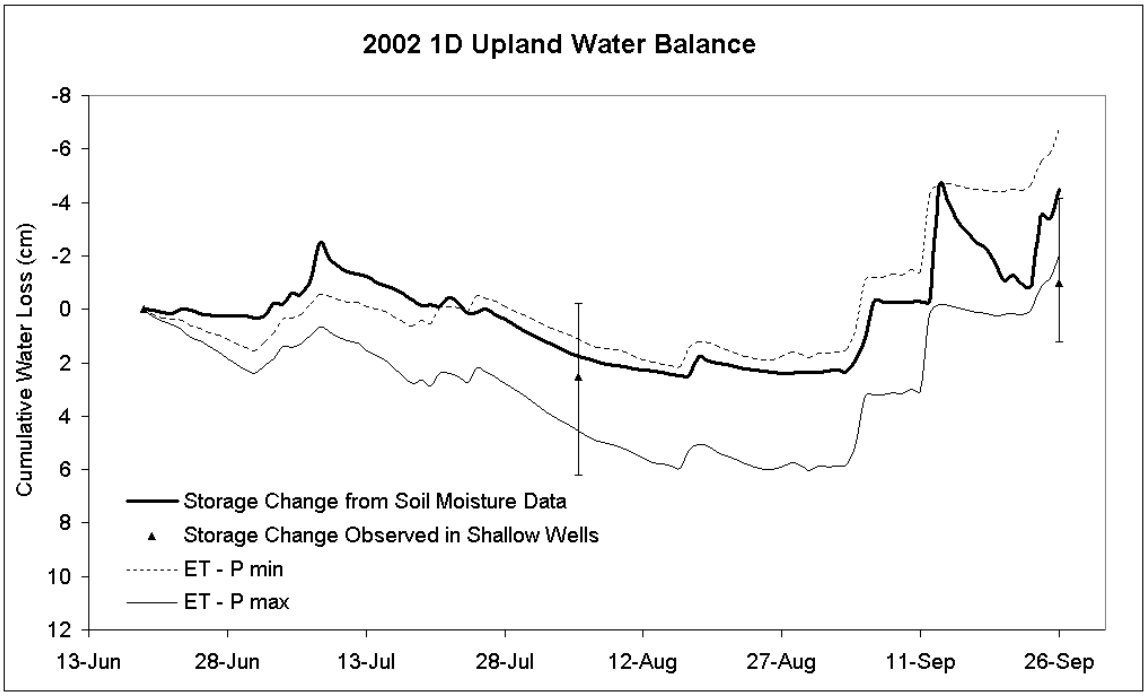

Figure 35. Upland 1D water balance for 2002. The data show that the system is fairly balanced without including lateral flux estimates, justifying the assumption of negligible lateral fluxes for the majority of the summer. Noticable lateral flow (both surface and subsurface flow) probably occurred after the series of smaller rainfall events in early July and certainly occurred after the large event on September 13.

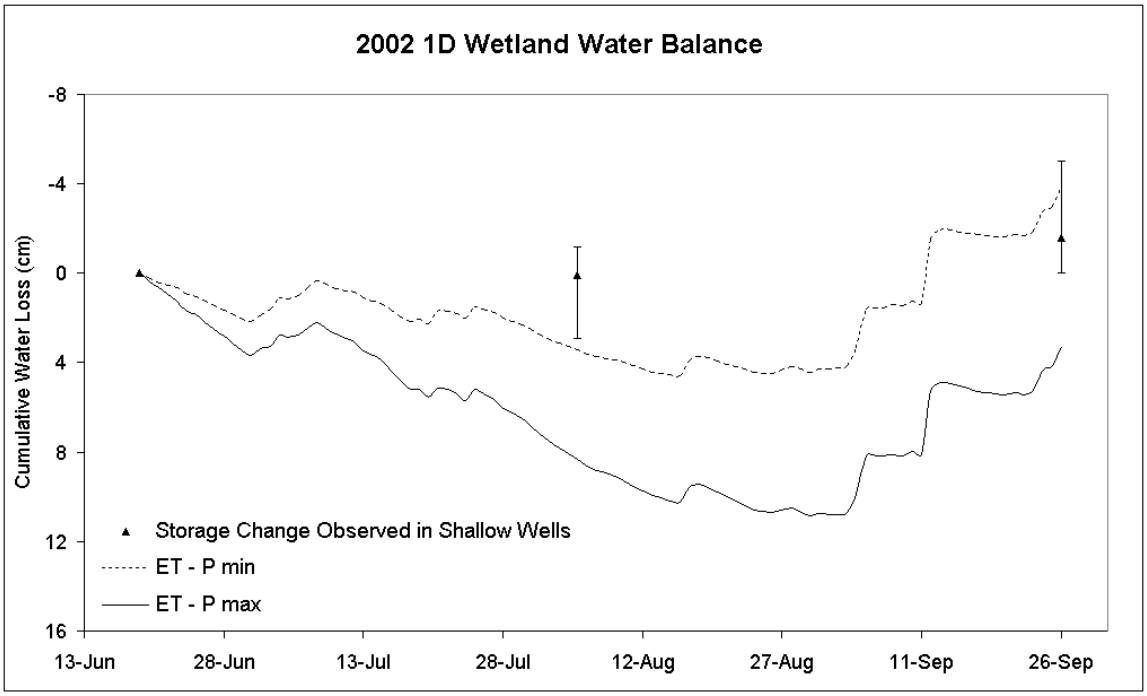

Figure 36. Wetland 1D water balance for 2002. The cumulative ET – P deficit of the warm, dry 2002 summer did not match the small storage changes measured in the wetland wells. This suggests that the assumption of negligible lateral fluxes is inappropriate for the wetlands.

Figure 36 shows the 1D water balance on the wetland tundra surfaces, with only three manual storage data points. Immediately, one recognizes that the storage changes are small and do not support the large prescribed ET – P deficit. The minimum ET estimates are certainly on the low-end of published ET rates to combat the difficult-to-model xerophytic adaptations of the wetland vegetation, so the overestimation of ET is probably not a reasonable explanation for the differences between the observed storage changes and the expected water deficit. This 1D water balance indicates that the assumption of negligible lateral fluxes, even against substantial ET – P deficits, does not hold true for the wetlands surfaces. This may be a result of lateral flow from the pond to the wetland vegetation during dry periods in order to maintain some minimum moisture content within the thick organic mat. Although the hydraulic gradients

calculated from the Pond 20 to the nearby 3-4 channel occasionally indicate water movement from the ponds to the wetlands, the flowrates calculated from the Darcy equation are not large enough to balance the system. It is possible that the wetlands received a considerable input from the uplands during the series of small events in early July where the upland water balance suggests that lateral drainage occurred.

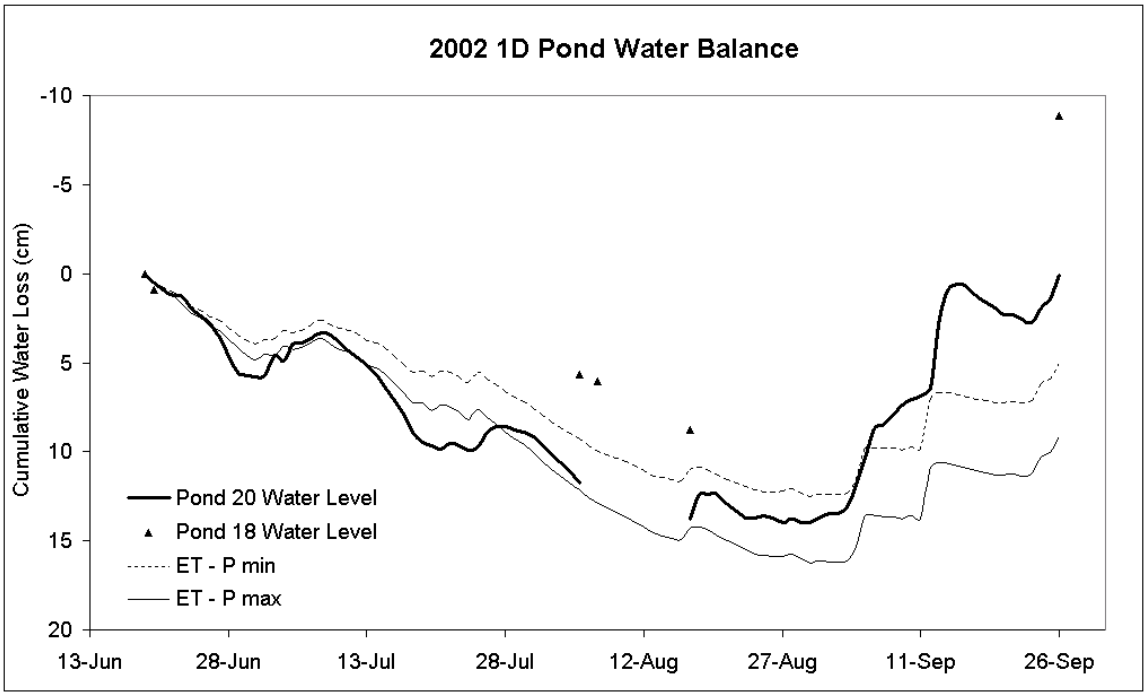

Figure 37. Pond 1D water balance for 2002. Rates of storage change in Pond 20 (the slope of the Pond 20 water level curve) typically exceed the modeled water loss from ET (the downward slope of the ET – P lines) and inputs from rain (the upward slope of the ET – P lines) during both dry periods and rainy periods respectively.

A 1D water balance applied to Pond 20, shown in figure 37, suggests the occurrence of lateral fluxes, apparent by the incongruities in slope of the storage and ET – P estimates during several periods. The changes in storage exceeding the simple ET – P models coincide with substantial recharge events, which

suggest that the pond is receiving water from either the upland slopes surrounding it or the wetland channels adjacent to it. Also, after an extended dry period in July, the pond appeared to lose water at a rate greater than the ET – P model predictions, indicating the activity of an additional loss mechanism, either lateral drainage through the channels or possibly vertical drainage through the open talik. In August, the system appears to be balanced. The ΔS of Pond 20 during the high rains in September is greater than the volume of rainfall, reinforcing the assumption that the pond receives lateral recharge from the surrounding terrain. The rapid storage change the day after the large event on September 13 indicate rapid lateral drainage, probably as a result of high pond stage. This is near the time when the high surface discharges in the outlet channel were measured.

With only a few measurements of storage, the response of Pond 18 to individual rainfall events cannot be known; however, the measured water level changes between site visits suggest that Pond 18 and Pond 20 behave differently. The storage change from June to August as measured in Pond 18 is approximately half of that measured in Pond 20. It is possible that water draining from Pond 20 at high stages recharges Pond 18. The hydraulic gradients measured throughout the wetlands support this conclusion, although the magnitudes of the subsurface flow calculations through these channels were not large enough to support the observed lack of storage change in Pond 18 alone. Another explanation could stem from the fact that Pond 18 is adjacent to a much larger wetland area than the 3-4 channel near Pond 20, and theoretically would require more water to support the high ET rates and to maintain the minimum moisture requirements of the wetland plants.

To avoid the troublesome unquantified lateral fluxes from the ponds to the adjacent wetlands, and vice versa, a water balance is conducted on the Pond 20

wetland complex including the 3-4 wetland channel (see figure 5 on page 10). The likelihood of noticeable lateral fluxes from the surrounding upland slopes associated with rainfall events is not included in the water balance but is conceptually described in the following paragraph. ET from the transition zone is assumed to be equal to that of the wetlands, and the floating mat is assumed to evaporate water at a rate equal to the average of pond and wetland ET. Discrepancies in the estimated and actual boundary between the floating mat and transition zone could potentially create considerable error; therefore, minimum and maximum storage estimates are created by using two extreme estimates of the boundary. The ΔS estimates are presented as only three data points because of the necessary incorporation of the limited data set of the wetland storage. The 1D water balance for the Pond 20 wetland complex including the 3-4 channel is shown in figure 38.

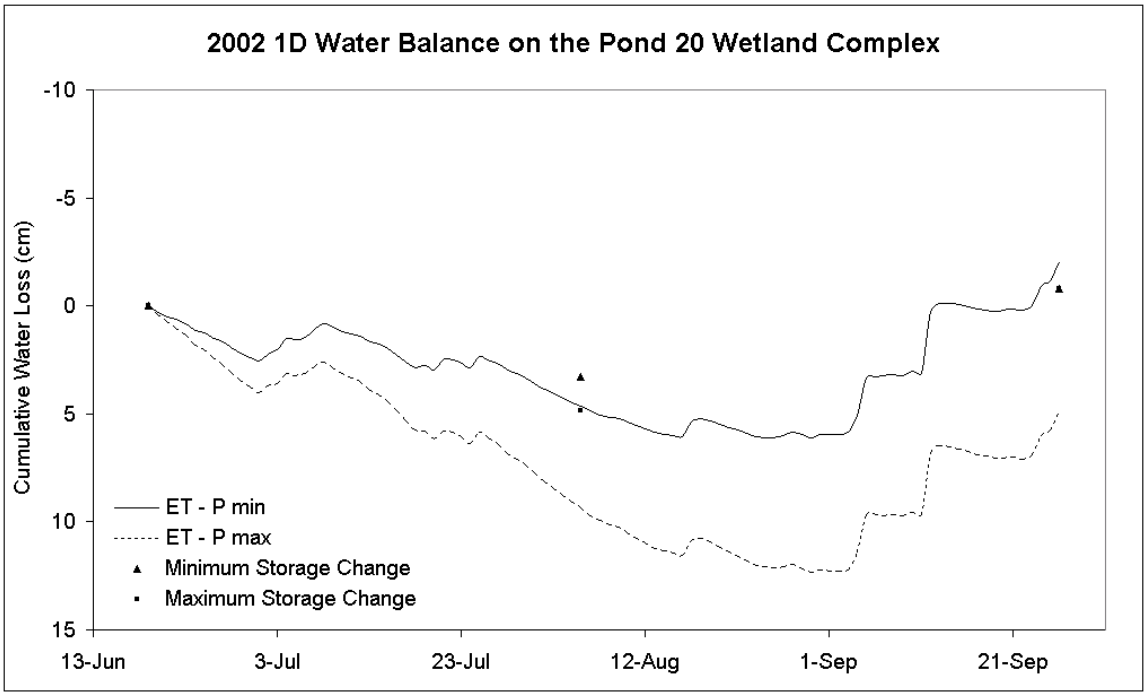

Figure 38. Pond 20 complex 1D water balance for 2002. This water balance is a more accurate model than either the wetland or pond surfaces alone.

The 1D water balance of the Pond 20 wetland complex reveals an almost-balanced system if the minimum ET estimate is used. Considering occasional subsurface lateral fluxes from the upland slopes of up to 5 mm/day for a few days after sizeable rainfall events would increase the wetland storage substantially, thereby minimizing the storage change observed from June to August, the system could potentially be balanced using the maximum ET estimate as well. Unfortunately, the methods used to describe the active layer flow regime in this study are not accurate enough to quantify the lateral fluxes exactly. The flowrates through the open talik as estimated by Yoshikawa and Hinzman (2003) for Pond 20 are from 0.28 m^3/day to 1.3 m^3/day. These flowrates applied to the entire Pond 20 wetland complex are equivalent to 0.04 mm/day and 0.2 mm/day respectively, which are easily within the bounds of accuracy for this water balance.

A water balance for the entire site is not conducted because the ΔS and ET estimates for the uplands would dominate the vertical components of the water balance (because of an unknown but certainly large percentage of the total area of the watershed is uplands), reducing the potential impact of the loss mechanism created by the presence of open taliks underneath the ponds. Also, without the cumulative water volume lost though the outlet channel, the importance of T relative to lateral drainage would be purely speculative.

6.5 Water Balances for the 2001 Field Season

Some necessary data for the 2001 summer water balance calculations were not collected. These data include net radiation for wetlands and ponds, all surface temperature data, soil temperatures necessary for ground heat flux calculations, and soil moisture data, which is necessary for continuous storage estimates and Bowen ratios calculations. Without surface temperature and soil moisture data,

only the 1m-to-3m BREB method can be used to estimate actual LE in the alpha-determining analyses. With only an alpha calculation for uplands, the alpha applied to wetlands and ponds during the 2001 season are based on the relative evaporability of upland surfaces as compared to the 2002 results. The ground heat flux, essential for both BREB and PT model calculations, is assumed to consume the same fraction of net radiation (G/Q*) as in the 2002 season, despite the serious differences in active layer dynamics between the two summers. The necessary net radiation data are reconstructed by using the 2002 net radiation data to calculate average ratios of $Q^*_{pond}/Q^*_{uplands}$ and $Q^*_{wetland}/Q^*_{uplands}$ for each summer month and applying it to the $Q^*_{uplands}$ data collected during the 2001 summer. Both ponds and wetland ratios decreased with the progression of the summer, with the pond ratio slightly higher than the wetland ratio. The reconstructed net radiation data are shown in figure 39.

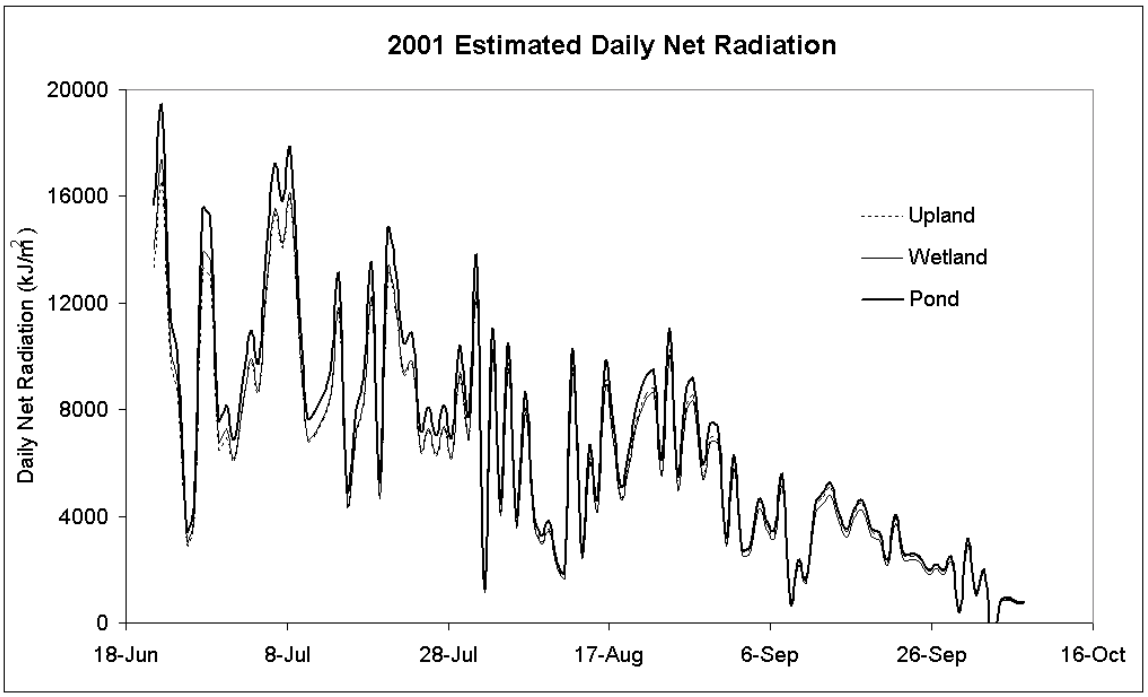

Figure 39. Estimated 2001 net radiation. The relative magnitudes of net radiation from the three surface types in 2002 were used to recreate wetland and pond net radiation from the measured 2001 upland net radiation data.

The 1m-to-3m alpha-determining analysis applied to the 2001 summer data set, shown in figure 40, yields an alpha of 0.75, very close to the 0.74 calculated for the 2002 summer. Because the estimated alpha values are so similar, the same alpha values applied to the 2002 PT models are applied to the 2001 data sets. Because of the consistently larger thaw depth in 2001, the ground heat flux may be less than that of the 2002 season, creating an underestimate of ET in the 2001 water balances. Regardless, the same parameters used in the 2002 analysis are used to create minimum and maximum estimates of ET for 2001 season.

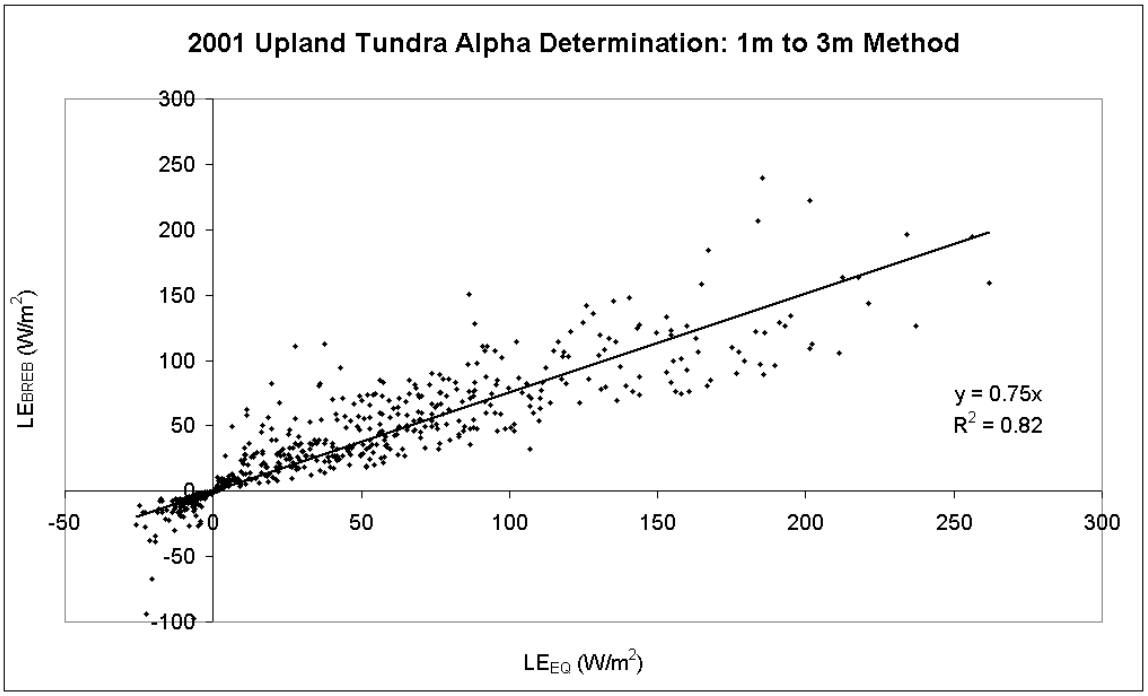

Figure 40. Alpha-determining relationship from 1 m to 3 m for 2001. Estimation of alpha using the 1m-to-3m BREB method produces a similar alpha value (0.75) to that of 2002 (0.74).

The cumulative ET for upland surface for the 2001 summer is modeled using the alpha value of 0.75 suggested in figure 40. Figure 41 shows a 1D water balance on the upland slopes for the 2001 summer. The continuous storage change from

soil moisture data does not start until after the installation of the instruments in August, but it appears to slightly exceed ET - P, indicating an underestimate of ET or perhaps lateral drainage. It is probable that the large event on August 13, which is responsible for the large shift in the ET - P curves, completely saturated the upland soils, yielding considerable subsurface drainage for several days.

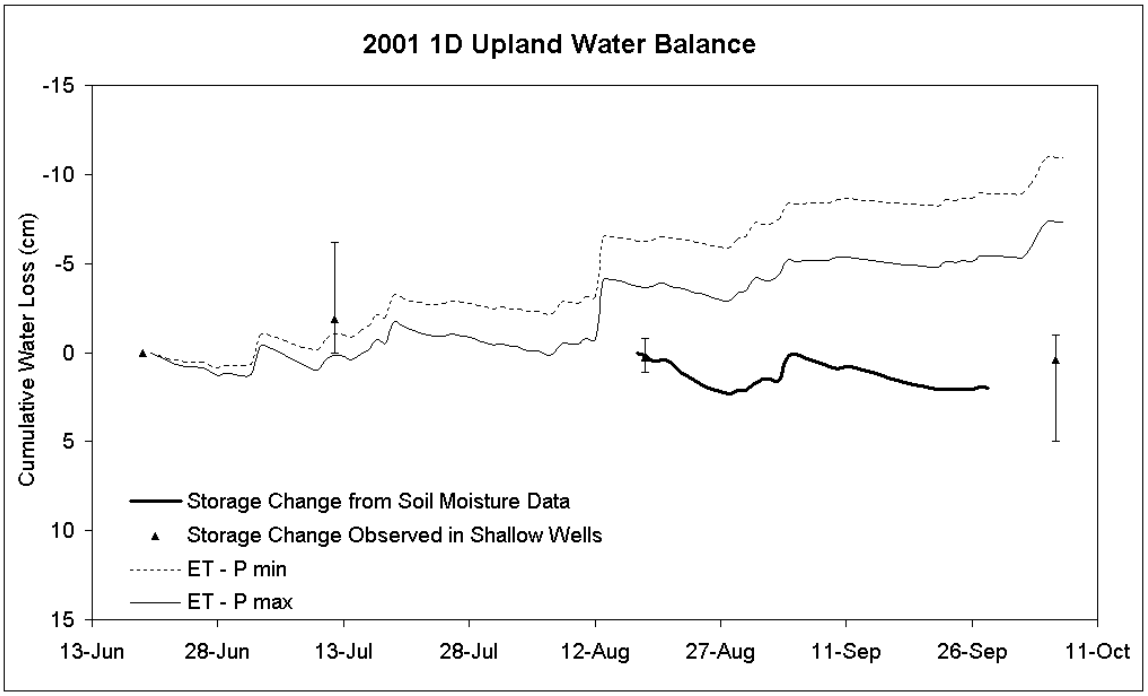

Figure 41. Upland 1D water balance for 2001.

Figure 42 shows a similar trend of little storage changes within the wetland soils; however, this 2001 water balance reveals an ET – P trend that is capable of explaining this phenomenon, falsely justifying the assumption of negligible lateral fluxes; the seemingly continuous proximity of the water table to the ground surface in the wetlands suggest that even mild recharge events could potentially create surface flow within the wetlands, resulting in lateral fluxes to the ponds.

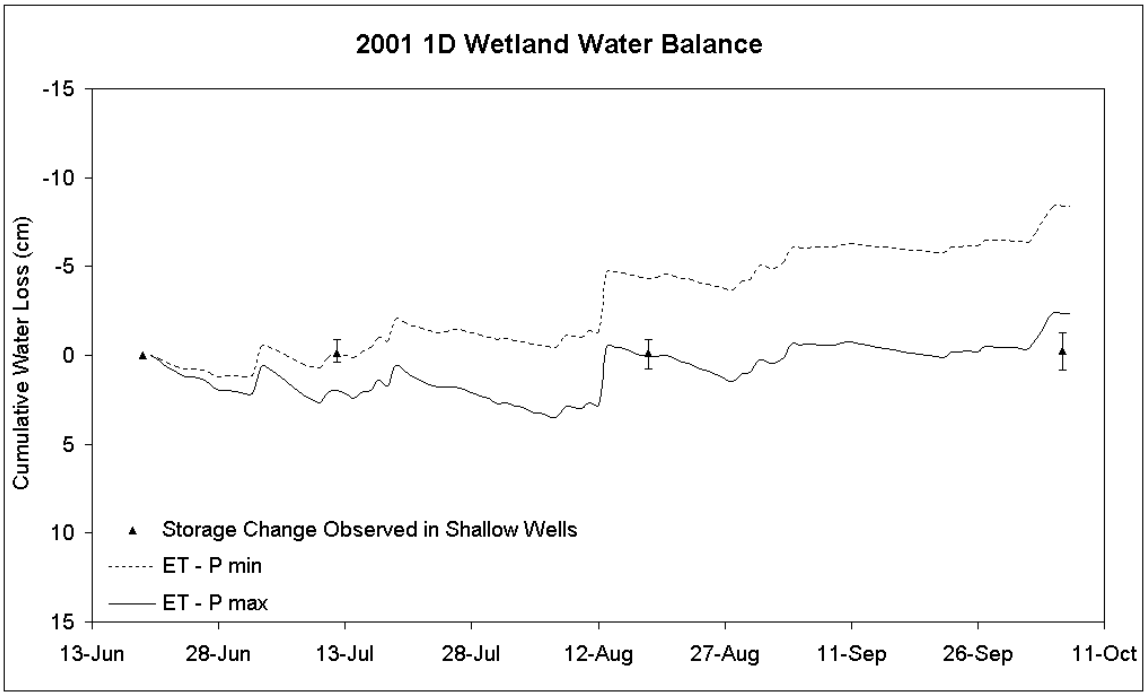

Figure 42. Wetland 1D water balance for 2001. The rainfall in 2001 prevented the accumulation of a large ET – P deficit, consequentially matching the little storage changes observed at the wetland wells.

The 1D water balance of Pond 20 in 2001, shown in figure 43, reveals similar behavior to that of the 2002 pond water balance. During periods of recharge, the pond appears to be responding to lateral inputs from surrounding surfaces, and then the water level drops faster than can be explained by ET estimates, indicating channel drainage. During periods of little rainfall, the system appears to be balanced with ET as the only loss mechanism. Bearing in mind that 2001 was wetter than 2002 with wetland water levels closer to the surface, it is possible that the balanced 1D system between recharge events justifies the assumption of negligible lateral fluxes from the pond to the already saturated wetlands. It is also possible that the lateral fluxes into the pond are balanced by open talik drainage. The increase in storage measured in Pond 18 (shown on the graph as a negative storage change) as compared to Pond 20 suggests that Pond 18 receives lateral drainage from a larger area than Pond 20.

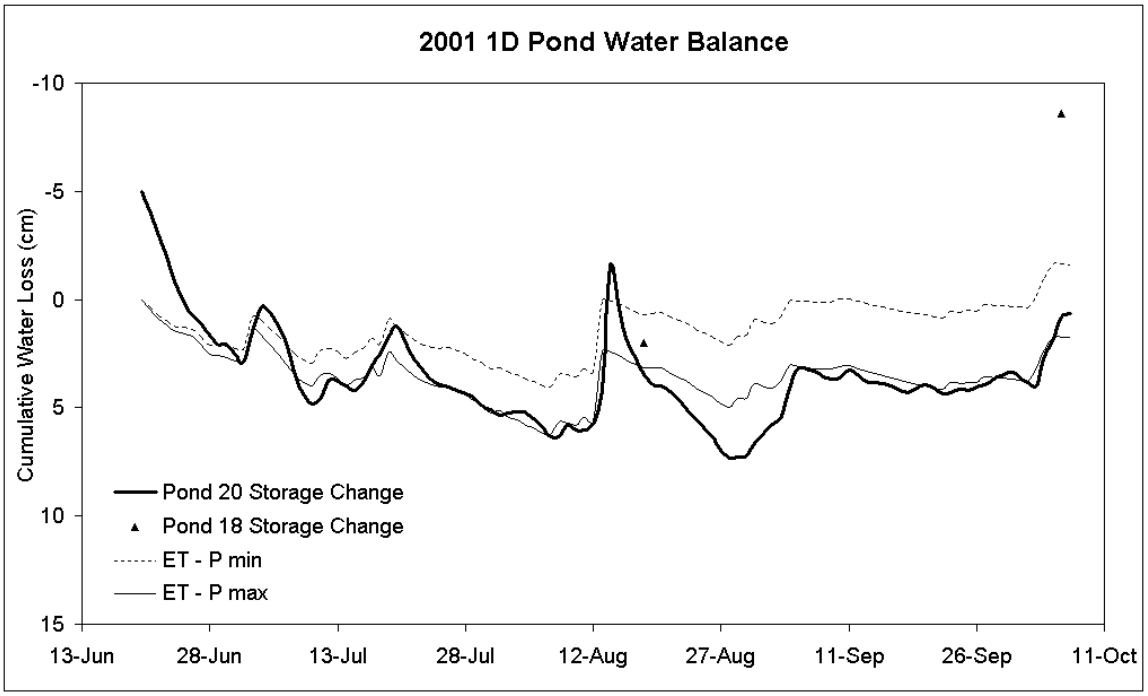

Figure 43. Pond 1D water balance for 2001. The large storage change during the sizeable rainfall event in mid-August followed by a large storage change is explained by lateral drainage of the upland and/or wetland areas during the event and the subsequent channel drainage resulting from a high pond stage.

6.6 Additional Findings

In the alpha-determining analysis discussed above, alpha is essentially reduced to a function of air temperature and relative humidity at some height above the ground surface, surface temperature, and near-surface soil moisture. Because the air temperature and relative humidity data used in the analysis are from the same sensor on the three-meter tower for each of the three surface types, the surface temperature and near-surface moisture data are the only parameters remaining to differentiate between the different surface types. While the pond surface obviously remains saturated, the wetness of the upland and wetland surfaces is assumed to be described by soil moisture data collected at 5 cm below the surface at the corresponding soil pits. The soil moisture is converted

to a relative humidity of the soil pore space, which is used to calculate the vapor pressure at the surface, a necessary component of the Bowen ratio (see section 5.1). The soil moisture data for the upland and wetland surfaces along with the associated relative humidity of the soils are shown in figure 44.

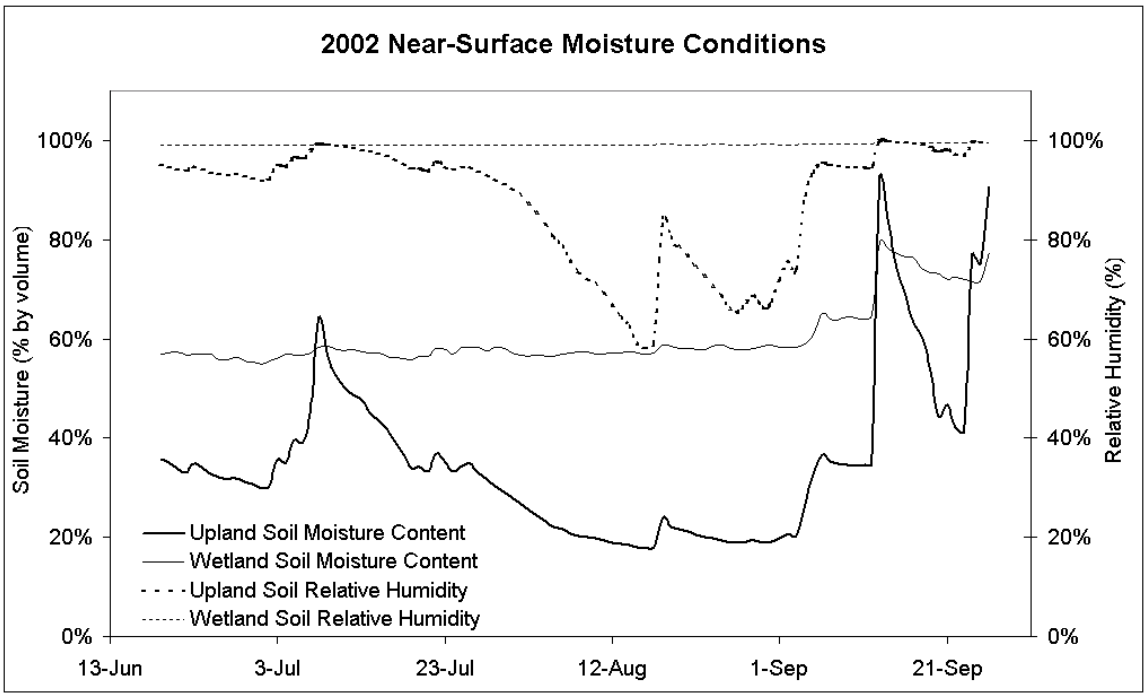

Figure 44. Near-surface moisture conditions of the upland and wetland soils. Measure moisture conditions produce consistently high relative humidity in the soil (>90%) so long as the soil moisture remains above roughly 30%. The relative humidity of the wetland surface soils is near saturation (>99%) for the duration of the 2002 summer.

The data indicates that the pore spaces of the upland near-surface soils are desiccated only slightly, remaining above 90% saturated for the summer, except for the month of August where the relative humidity drops to as low as 58% and averages 72% over the dry period. The pore spaces of the wetland near-surface soils remain essentially saturated (>99%) for the entire season.

Because the BREB calculations for wetland surfaces thus far use data that imply essentially unlimited moisture conditions at the surface, the surface temperature is the only remaining parameter that can affect the estimation of alpha. Because three different sets of surface temperature data exist for various surface conditions within the wetlands, it follows that three different alpha values can be generated, each representing only slightly different vegetation types and wetness. The effect of varying surface temperatures on the alpha value is explored by conducting the alpha-determining analysis with each set of temperature data. The diurnal temperature trends of the wetland thermistors, along with upland and pond surface temperatures, are shown in figure 45.

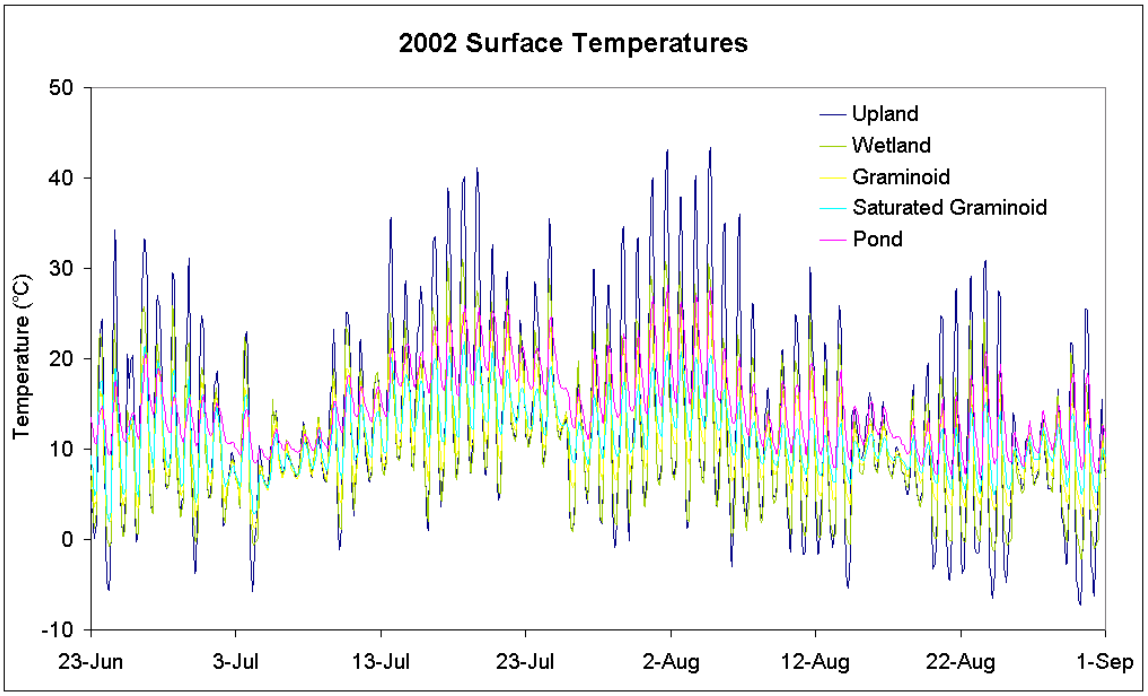

Figure 45. Surface temperatures data from all surfaces. The five surface thermistors compiled in three-hour intervals show larger diurnal variation in the drier soils.

While the soil moisture at the surface is unknown, the amplitude of the diurnal temperature oscillations from the surface do somewhat reflect surface moisture

conditions with drier surfaces responding faster and more dramatically to changes in air temperature than the wetter surfaces. Because most of the latent heat is consumed during daytime hours, the daytime temperatures are more influential in the alpha determining analysis. If moisture conditions are assumed constant, as is the case within the wetlands, the higher daytime temperatures of the drier surfaces produce larger Bowen ratios, lower actual LE estimates, and consequentially lower alpha values. The change in alpha value is noteworthy, as is indicated by the relationships in figure 46.

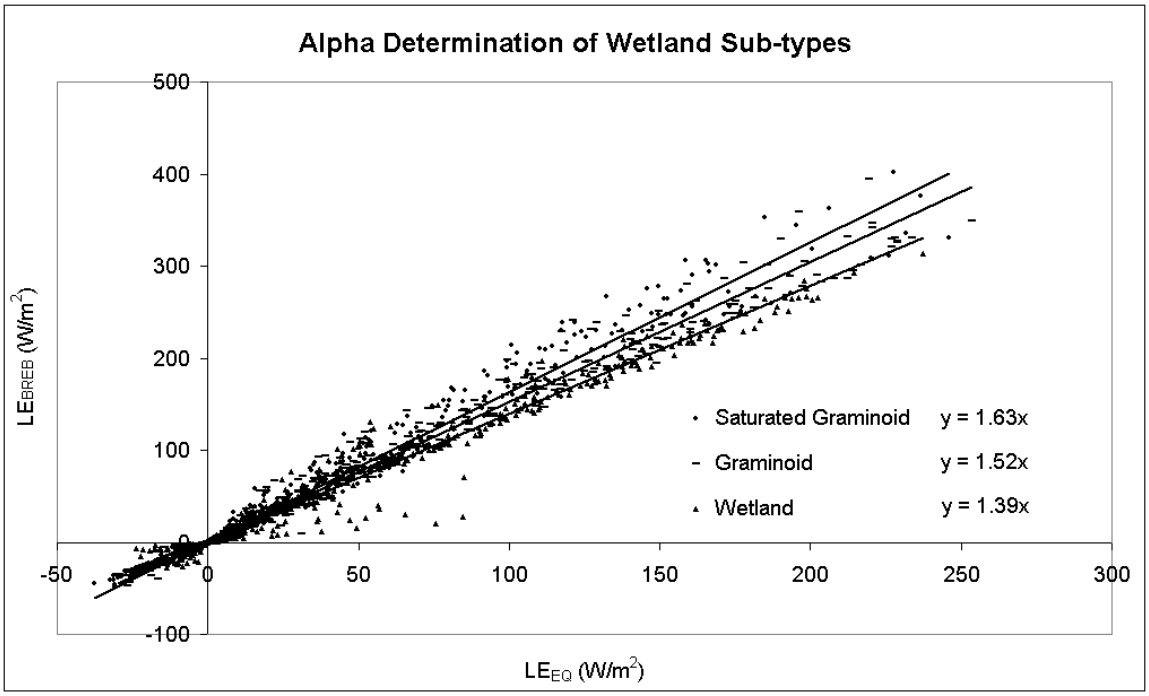

Figure 46. Alpha-determining relationship for three slightly different surfaces within the wetland areas. Alpha values range from 1.39 to 1.63 with the wettest surface producing the highest alpha and the driest surface producing the smallest alpha.

From the wetland alpha of 1.39 applied to the water balance calculations, alpha increases with increasing wetness conditions, with alpha equal to 1.52 and 1.63 for graminoid vegetation and floating mat puddles respectively. Because alpha is

supposedly a parameter used to describe the “evaporability” of surfaces, it follows that wetter surface would have higher alpha values. Roulet and Woo (1986 a and c) however described ET for a Northern Canada wetland site to be best described by alpha values of 1.3 for flooded conditions and 1.6 for non-flooded conditions. This analysis demonstrates the influence of surface temperature from similar surfaces on alpha using the BREB method from the surface to calibrate the PT model. This emphasizes the importance of accurate surface temperature measurements.

7. Conclusions

Use of the BREB method from the surface to some height above the surface to calibrate the PT model by estimating the ratio of actual to equilibrium latent heat appears to produces reasonable alpha values for both pond and wetland surfaces. It is assumed that this method would work equally well for upland surfaces if surface soil moisture data were available. The closeness of the 1m-to-3m alpha-determining analysis results for the two field seasons, along with the results from Beringer et al (2003b), suggest the alpha value of the upland tundra surfaces in the Council area is near 0.74 for both wet and dry summers, which is notably less than the alpha values reported for similar surfaces in other areas of Alaska.

One-dimensional water balances of upland and wetland soils were used to identify the activity of lateral fluxes. The Priestley-Taylor model with an alpha value of 0.74 appeared to estimate ET from upland surfaces well for the majority of the two summers. ET is solely responsible for depleting storage in the upland soils between significant rainfall events; only when the storage of the upland soils is raised to near-saturated conditions are lateral fluxes noticeably active. The wetlands behaved differently than the uplands, showing minimal storage changes regardless of climatic conditions suggest. The tendency of the wetlands to maintain storage levels near the capacity of the soils despite the large ET-P deficit during the dry 2002 summer suggests that a substantial volume of water is transported to the wetlands from the ponds.

The one-dimensional water balances conducted on the ponds revealed the frequent activity of lateral fluxes. Pond 20 receives water via lateral fluxes during even moderate rainfall events, and because large storage deficits were

never observed in the wetland soils, not even during the large cumulative ET – P deficit in August of the exceptionally dry 2002 summer, it is suspected that vast majority water input into the ponds via lateral flux is from the wetlands only. Lateral fluxes out of the pond via an outlet channel appear to occur only when the stage is greater than some threshold value. It seems a worthy consideration that a decrease in this threshold value, probably related to the relative elevation of an outlet channel to the pond, is a mechanism contributing to pond drainage. This is one of the two drainage mechanisms described by Hopkins (1949).

The pond water balance also revealed that ET could not explain the observed storage changes within the pond during dry periods, indicating activity of another loss mechanism. However, this water loss rate cannot necessarily be attributed to drainage through an open talik, mostly because of the unexplained recharge in the wetland areas. The water balance of the pond including the wetland areas surrounding it produced better results than analyzing the open water surface alone, suggesting the presence of significant lateral fluxes between the ponds and the surrounding wetlands. This is reinforced by the measurement of hydraulic gradients in the wetlands both towards and away from the ponds. The magnitude of water loss through the open talik cannot be deduced using the water balance method without the accurate quantification of these lateral fluxes between the wetlands and the ponds.

An underlying conclusion is that precipitation is a very important component of the hydrologic dynamics of both the ponds and the surrounding terrain. Rainfall events have a direct effect on water storage in near-surface soils and an often-magnified effect on pond water levels, with single events capable of recharging several weeks of accumulated water loss due to the combined effect of all loss mechanisms. Rainfall events also influence the activity of lateral fluxes; they are necessary precursors for periods of noticeable lateral flow from uplands slopes.

A dry period resulting from lack of rainfall, such as during the middle of the 2002 summer, will allow for consistently lower water levels, potentially facilitating peat growth around the perimeter of the ponds.

The results of this study do not allow complete attribution of pond shrinkage to drainage through open taliks. Peat growth and the potential change in elevation or degree of subsidence of an outlet channel are capable of contributing to the appearance of pond shrinkage, and should not be discounted as possible causes for pond drainage. The subtle hydraulic connection between the ponds and adjacent wetlands should not be underestimated when investigating hydrologic dynamics of thermokarst ponds as well.

References

Bello R, Smith JD (1990) The effect of weather variability on the energy balance of a lake in the Hudson Bay Lowlands, Canada. *Arctic and Alpine Research* **22**: 98-107.

Beringer J, Chapin III FS, Copass CD, McGuire AD (2003a) Partitioning of surface energy exchanges along a forest-tundra vegetation transition: the importance of canopy structure. *Boundary Layer Meteorology*, (Submitted).

Beringer J, Chapin III FS, Copass CD (2003b) *Climate and Flux Data from Alaska Sites, 1998-2000*. Boulder, CO: National Snow and Ice Data Center/World Data Center for Glaciology. Digital Media.

Billings WD, Peterson KM (1980) Vegetational change and ice-wedge polygons through the thaw-lake cycle in Arctic Alaska. *Arctic and Alpine Research* **12**: 413-432.

Black RF (1969) Thaw depressions and thaw lakes: a review. *Biuletyn Peryglacjalny* **19**: 131-150.

Boike J, Roth K, Overduin PP (1998) Thermal and hydrologic dynamics of the active layer at continuous permafrost site (Taymyr peninsula, Siberia). *Water Resources Research* **34**: 355-363.

Bosikov NP (1998) Wetness variability and dynamics of thermokarst processes in Central Yakutia. In: Lewkowicz AG and Allard M (eds.), *Permafrost*

Seventh International Conference Proceedings, Yellowknife NWT, Canada, June 23-27, 1998: 71-74.

Bowen IS (1926) The ratio of heat losses by conduction and evaporation from any water surface. *Physics Review* **27**: 779-787.

Brewer MC (1958) Some results of geothermal investigations of permafrost in Northern Alaska. *Transactions, American Geophysical Union* **39**(1): 19-26.

Britton ME (1957) Vegetation of the arctic tundra. *In* Hansen HP (ed.) *Arctic Biology*. (2nd edition, 1967.) Oregon State University Press, 26-72.

Brutsaert W (1982) *Evaporation into the Atmosphere: Theory, History, and Applications*. D. Reidel Publishing Co., Boston, MA, 299 pp.

Burn CR, Smith MW (1988) Thermokarst lakes at Mayo, Yukon Territory, Canada. *Proc. Fifth International Conference on Permafrost, Trondheim*, Norway, Tapir: 700-705.

Burn CR, Smith MW (1990) Development of thermokarst lakes during the Holocene at sites near Mayo, Yukon Territory. *Permafrost and Periglacial Processes* **1**(2): 161-176.

Burn CR (1992) Canadian landform examples – 24: Thermokarst lakes. *The Canadian Geographer* **36**: 81-85.

Campbell GS (1985) Soil Physics With Basic: Transport Models for Soil-Plant Systems. Dev. In Soil Sci. 14, Elsevier Sci., NY, 150 pp.

Campbell Scientific, Inc (2001) CS615 Water Content Reflectometer User Guide. 17 pp.

Davis TN (2001) *Permafrost, A Guide to Frozen Ground in Transition*. University of Alaska Press, 351 pp.

Engstrom RN, Hope AS, Stow DA, Vourlitis GL, Oechel WC (2002) Priestley-Taylor alpha coefficient: variability and relationship to NDVI in arctic tundra landscapes. *Journal of the American Water Resources Association* **38**(6): 1647-1660.

Eichinger WE, Parlange MB, Stricker H (1996) On the concept of equilibrium evaporation and the value of the Priestely-Taylor coefficient. *Water Resources Research* **32**: 161-164.

Farouki OT (1981) *Thermal Properties of Soils*. CRREL Monograph 81-1, United States Army Corps of Engineers, Cold Regions Research and Engineering Laboratory, Hanover, NJ, USA, 137 pp.

Fetter CW (1994) *Applied Hydrogeology*. Third Edition. Prentice-Hall Inc. Upper Saddle River, New Jersey, 691 pp.

Fitzgerald D, Riordan BA (2003) Permafrost and ponds: remote sensing and GIS used to monitor Alaska wetlands and the landscape level. *Agroborealis* **35**(1): 30-35.

Ford J, Bedford BL (1987) The hydrology of Alaskan wetlands, U.S.A.: a review. *Arctic and Alpine Research* **19**(3): 209-229.

Freeze RA, Cherry JA (1979) *Groundwater*. Prentice-Hall, Inc. Englewood Cliffs, New Jersey, 604 pp.

French HM (1974) Active thermokarst processes, Eastern Banks Island, Western Canadian Arctic. *Canadian Journal of Earth Sciences* **11**: 785-794.

Gallinger BJ (1991) *Permafrost degradation and thermokarst processes associated with human-induced disturbances*. M.S. thesis. Fort Norman, N.W.T. University of Alberta, Edmond, Alberta.

Glen MS, Woo M-K (1997) Spring and summer hydrology of a valley-bottom wetland, Ellesmere Island, Northwest Territories, Canada. *Wetlands* **17**: 321-329.

Guo Y, Schuepp PH (1994) On surface energy balance over the northern wetlands - the effects of small-scale temperature and wetness heterogeneity. *Journal of Geophysical Research* **99**: 1601-1612.

Harry DG, French HM (1983) The orientation and evolution of thaw lakes, Southwest Banks Island, Canadian Arctic. *Permafrost Fourth International Conference Proceedings*, Fairbanks, Alaska. Washington D.C., National Academy Press: 456-461.

Hinzman LD, Kane DL, Gieck RE, Everett KR (1991) Hydrologic and thermal properties of the active layer in the Alaskan Arctic. *Cold Regions Science and Technology* **19**: 95-110.

Hinzman LD, Goering DJ, Kane DL (1998) A distributed thermal model for calculating soil temperature profiles and depth of thaw in permafrost regions. *Journal of Geophysical Research* **102**(D22): 28,975-28,911.

Hopkins DM (1949) Thaw lakes and thaw sinks in the Imuruk Lake Area, Seward Peninsula, Alaska. *The Journal of Geology* **57**: 119-131.

Hopkins DM (1955) *Permafrost and Groundwater in Alaska*. Geological Survey Professional Paper 264-F. U.S. Government Printing Office, Washington.

Jorgenson MT, Racine CH, Walters JC, Osterkamp TE (2001) Permafrost degradation and ecological changes associated with warming climate in central Alaska. *Climate Change* **48**: 551-579.

Kane DL, Slaughter CW (1973) Recharge of a central Alaska lake by subpermafrost groundwater. In: *Permafrost: North America Contribution to the Second International Conference, Yakutsk, 1973*. Washington, D.C., National Academy of Sciences, 458-462.

Kane DL, Seifert RD, Taylor GS (1978) *Hydrologic Properties of Subarctic Organic Soils*. Institute of Water Resources Report No. IWR-88, 44 pp.

Kane DL, Stein J (1983) Water movement into seasonally frozen soils. *Water Resources Research* **19**(6): 1547-1557.

Kane DL, Hinzman LD (1988) Permafrost hydrology of a small arctic watershed. K.Senneset (ed.) *Proc. Fifth International Conference on Permafrost, Trondheim*, Norway, Tapir: 590-595.

Kane DL, Gieck RE, Hinzman LD (1990) Evapotranspiration from a small Alaskan Arctic watershed. *Nordic Hydrology* **21**: 252-272.

Kane DL, Hinzman LD, Woo MK, Everett KR (1992) Arctic hydrology and climate change. *Arctic Ecosystems in a Changing Climate*, Academic Press, 35-57.

Lafleur PM, Rouse WR, Hardill SG (1987) Components of the surface radiation balance of subarctic wetland terrain units during the snow-free season. *Arctic and Alpine Research* **19**: 53-63.

Lafleur PM (1990) Evapotranspiration from sedge-dominated wetland surfaces. *Aquatic Botany* **37**: 341-353.

Lafleur PM (1994) Annual variability in summer evapotranspiration and water balances at a subarctic forest site. *Nordic Hydrology* **25**: 331-344.

Lawson DE (1986) Response of permafrost terrain to disturbances: a synthesis of observations from northern Alaska, U.S.A. *Arctic and Alpine Research* **18**: 1-17.

Lilly EK, Kane DL, Hinzman LD, Gieck RE (1998) Annual water balance for three nested watersheds on the North Slope of the Alaska. In: Lewkowicz AG and Allard M (eds.), *Permafrost Seventh International Conference Proceedings,* Yellowknife NWT, Canada, June 23-27, 1998: 669-674.

Lloyd AH, Yoshikawa K, Fastie CL, Hinzman LD, Fraver MR (2003) Effects of permafrost degradation on woody vegetation at arctic treeline on the Seward Peninsula, Alaska. *Permafrost and Periglacial Processes* **14**: 93-101.

Lunardini VJ (1998) Effect of convective heat transfer on thawing of frozen soils. In: Lewkowicz AG and Allard M (eds.), *Permafrost Seventh International Conference Proceedings,* Yellowknife NWT, Canada, June 23-27, 1998: 689-695.

McFadden JP, Chapin III FS, and Hollinger DY (1998) Subgrid-scale variability in the surface energy balance of arctic tundra. *Journal of Geophysical Research* **103**(D22): 28,947-28,961.

Mendez J (1997) *Evapotranspiration from a wetland complex on the Arctic Coastal Plain of Alaska*. M.S. thesis, University of Alaska Fairbanks, 189 pp.

Mendez J, Hinzman LD, Kane DL (1998) Evapotranspiration from a wetland complex on the Arctic Coastal Plain of Alaska. *Nordic Hydrology* **29**: 303-330.

Michaelson GJ, Ping CL (2003) Soil organic carbon and CO_2 respiration at subzero temperature in soils of Arctic Alaska. *Journal of Geophysical Research* **108**(D2), 8164, doi:10.1029/2001JD000920, 2002.

Mitsch WJ, Gosselink JG (1993) *Wetlands*, second edition. Van Nostrand Reinhold Publishing, 722 pp.

National Climatic Data Center, http://www.ncdc.noaa.gov.

Ohmura A (1982) Objective criteria for rejecting data from Bowen ratio flux calculations. *Journal of Applied Meteorology* **21**: 595-598.

Osterkamp TE (1983) Response of Alaskan permafrost to climate. *Permafrost Fourth International Conference Proceedings*, Fairbanks, Alaska. Washington D.C., National Academy Press: 145-152.

Osterkamp TE, Romanovsky VE (1999) Evidence for warming and thawing of discontinuous permafrost in Alaska. *Permafrost and Periglacial Processes* **10**: 17-37.

Priestley CHB, Taylor RJ (1972) *On the assessment of surface heat flux and evaporation using large-scale parameters*. Monthly Weather Review **100**: 81-92.

Quinton WL, Roulet NT (1998) Spring and summer runoff hydrology of a sub-arctic patterned wetland. *Arctic and Alpine Research* **30**(3): 285-294.

Racine CH, Jorgenson MT, Walters JC (1998) Thermokarst vegetation in lowland birch forest on the Tanana Flats, Interior Alaska, U.S.A. In: Lewkowicz AG and Allard M (eds.), *Permafrost Seventh International Conference Proceedings,* Yellowknife NWT, Canada, June 23-27, 1998: 689-695.

Romanovsky V, Burgess M, Smith S, Yoshikawa K, Brown J (2002) Permafrost temperature records: indicators of climate change. *EOS*, Transactions, American Geophysical Union **83**(50): 589-594.

Roulet NT, Woo M-K (1986a) Hydrology of a wetland in the continuous permafrost region. *Journal of Hydrology* **89**: 73-91.

Roulet NT, Woo M-K (1986b) Low Arctic wetland hydrology. *Canadian Water Resources Journal* **11**: 69-75.

Roulet NT, Woo M-K (1986c) Wetland and lake evaporation in the low arctic. *Arctic and Alpine Research* **18**: 195-200.

Roulet NT, Woo M-K (1988) Runoff generation in a low Arctic drainage basin. *Journal of Hydrology* **101**: 213-226.

Roulet NT (1990) Hydrology of a headwater basin wetland: groundwater discharge and wetland maintenance. *Hydrological Processes* **4**: 387-400.

Roulet NT (1991) Surface level and water table fluctuations in a subarctic fen. *Arctic and Alpine Research* **23**: 303-310.

Rouse WR, Mills PF, Stewart RB (1977) Evaporation in high latitudes. *Water Resources Research* **13**: 909-914.

Rouse WR (1998) A water balance model for a subarctic sedge and its application to climate change. *Climatic Change* **38**: 207-234.

Rouse WR (2000) The energy and water balance of high-latitude wetlands: controls and extrapolation. *Global Change Biology* **6**: 59-68.

Rovansek RJ (1994) *The hydrology and jurisdictional status of a wetland complex on the Alaskan Arctic Coastal Plain*. M.S. thesis, University of Alaska Fairbanks, 139 pp.

Rovansek RJ, Hinzman LD, Kane DL (1996) Hydrology of a tundra wetland complex on the Alaskan Arctic Coastal Plain, USA. *Arctic and Alpine Research* **28**(3): 311-317.

Stannard DI, Rosenberry DO (1991) A comparison of short-term measurements of lake evaporation using eddy correlation and energy budget methods. *Journal of Hydrology* **122**: 12-22.

Stein J, Kane DL (1983) Monitoring of the unfrozen water content of soil and snow using time domain reflectometry. *Water Resources Research* **19**: 1573-1584.

Stewart RB, Rouse WR (1976a) Simple models for calculating evaporation from dry and wet tundra surfaces. *Arctic and Alpine Research* **8**: 263-274.

Stewart RB, Rouse WR (1976b) A simple method for determining the evaporation from shallow lakes and ponds. *Water Resources Research* **12**: 623-628.

Sturm M (Fall 2002) written communication. Geophysical scientist; US Army Corps of Engineers, Engineer Research and Development Center, Cold Regions Research and Engineering Laboratory.

Swanson L, Rothwell RL (1986) Thawing of ground frost on a drained and undrained boreal wetlands site. In: Kane DL (ed), Cold Regions Hydrology Symposium, American Water Resources Association, Proceedings.

Thomas HP, Ferrell JE (1983) Thermokarst features associated with buried sections of the Trans-Alaskan Pipeline. *Permafrost Fourth International Conference Proceedings*, Fairbanks, Alaska. Washington D.C., National Academy Press: 1245-1250.

Thompson C, Beringer J, Chapin III FS, McGuire AD (2003) Relationship of structural complexity to land-surface energy exchange along a vegetation gradient from arctic tundra to boreal forest. *Journal of Vegetation Science*, (Submitted).

Wessel DA, Rouse WR (1994) Modeling evaporation from wetland tundra. *Boundary-Layer Meteorology* **68**: 109-130.

Western Regional Climate Center, http://www.wrcc.dri.edu.

Williams PJ, Smith MW (1989) *The Frozen Earth: Fundamentals of Geocryology*, Cambridge University Press, 306 pp.

Woo M-K (1980) Hydrology of a small lake in the Canadian high arctic. *Arctic and Alpine Research* **12**: 227-235.

Woo M-K, Steer P (1982) Occurrence of surface flow on arctic slopes, southwestern Cornwallis Island. *Canadian Journal of Earth Sciences* **19**: 2368-2377.

Yang D, Goodison BE, Metcalfe JR, Golubev VS, Bates R, Pangburn T, Hanson CL (1998) Accuracy of NWS 8" standard nonrecording precipitation gauge: results and application of WMO intercomparison. *Journal of Atmospheric and Ocean Technology* **15**: 54-68.

Yershov ED (1998) *General Geocryology*. University Press, Cambridge, ed: Peter J. Williams, Carleton University, Ottawa, Canada, 580 pp

Yoshikawa K, Hinzman LD (2000) Geophysical investigation to determine the affects of discontinuous permafrost on hydrologic processes on the Seward Peninsula. *Arctic Systems Science Land- Atmosphere- Ice Interactions workshop, Seattle, Washington*. February 23-26, 2000. pp110.

Yoshikawa K, Hinzman LD (2003) Shrinking thermokarst ponds and groundwater dynamics in discontinuous permafrost near Council, Alaska. *Permafrost and Periglacial Processes* **14**: 151-160.

Yoshikawa K, Bolton WR, Romanovsky VE, Fukada M, Hinzman LD (2003) Impacts of wildfire on the permafrost in the boreal forests of Interior Alaska. *Journal of Geophysical Research* **108**(D1), 8148: FFR 4 – 1-14.